THESIS FOR THE DEGREE OF DOCTOR OF PHILOSOPHY (PHD)

Cadaverine and lithocholic acid, metabolites of the microbiome reduce breast cancer aggressiveness

Tünde Kovács

UNIVERSITY OF DEBRECEN
DOCTORAL SCHOOL OF MOLECULAR MEDICINE

DEBRECEN, 2019

THESIS FOR THE DEGREE OF DOCTOR OF PHILOSOPHY (PHD)

Cadaverine and lithocholic acid, metabolites of the microbiome reduce breast cancer aggressiveness

by Tünde Kovács

Supervisor: Dr. Péter Bay

UNIVERSITY OF DEBRECEN
DOCTORAL SCHOOL OF MOLECULAR MEDICINE

DEBRECEN, 2019

TABLE OF CONTENTS

1. ABBREVATIONS 4
2. INTRODUCTION 7
   2.1. The microbiome in disease 7
   2.2. Microbes in tumor metabolism 7
3. REVIEW OF THE LITERATURE 9
   3.1. The importance of BC research 9
   3.2. BC classification shames 10
   3.3. Hallmarks of cancer 11
   3.4. The tumor microenvironment 13
   3.5. Epithelial to Mesenchymal Transition 16
      3.5.1. EMT and metastasis 17
      3.5.2. EMT and breast cancer stem cells (BCSCs) 18
      3.5.3. Molecular events of EMT in BC 19
   3.6. The human microbiome 20
      3.6.1. The human gut microbiota 20
      3.6.2. Connection between gut microbiome and BC 22
   3.7. Polyamines and the role of cadaverine 23
   3.8. Bile salt biotransformation and LCA 26
4. OBJECTIVES 29
5. MATHERIALS AND METHODS 30
   5.1. Chemicals 30
   5.2. Cell culture 30
   5.3. Sulphorhodamine B assay 30
   5.4. Colony formation assay 31
   5.5. Detection of cell death 31
      5.5.1. Propidium iodide (PI) uptake 31
      5.5.2. Apoptosis detection using Annexin-V-FITC staining 31
   5.6. Electric cell-substrate impedance sensing (ECIS) 31
   5.7. Scratch assay 32
   5.8. Invasion assay 32
   5.9. Immuncytochemistry 33
      5.9.1. Assessment of changes in actin morphology 33

5.9.2. Assessment of MMP9 expression levels 33
5.10. Measuring “stem cell-ness” 34
5.10.1. Seahorse metabolic flux analysis 34
5.10.2. Aldefluor assay 34
5.11. Determination of lipid peroxidation 35
5.12. Transfections 35
5.13. mRNA isolation and RT-qPCR 35
5.14. Fecal protein sample preparation 36
5.15. SDS-PAGE and Western blotting 36
5.15.1. Validating of E. coli LdcC antibody 37
5.16. Animal studies 37
5.16.1. Tumor injection 37
5.16.2. LCA treatment 38
5.16.3. Cadaverine treatment 38
5.16.4. Infiltration score, tumor mass and TIL calculation 39
5.17. Human studies 40
5.17.1. Fecal DNA samples from NCI (Cohort 1.) 40
5.17.2. Fecal samples from BC patients (Cohort 2.) 41
5.17.3. Human serum samples (Cohort 3.) 42
5.18. Database screening 42
5.19. Statistical analysis 42
6. RESULTS 43
6.1. Cadaverine reduces BC aggressiveness 43
6.1.1. Cadaverine treatment reduces metastasis formation in 4T1-grafted mice 43
6.1.2. Cadaverine administration does not impair BC proliferation 44
6.2. Cadaverine revert EMT and suppress invasion ability 47
6.2.1. Cadaverine exert its beneficial effects through TAARs 53
6.2.2. Cadaverine biosynthesis is suppressed in BC 57
6.3. LCA decrease the aggressiveness of BC in vivo 61
6.3.1. LCA attenuates the aggressiveness of BC in mice 61
6.3.2. LCA Biosynthesis is suppressed in early phases of human BC 61
7. DISCUSSION 66
7.1. The effects of cadaverine in BC 66
7.2. The effects of LCA in BC 70
8. SUMMARY 71
9. ÖSSZEFOGLALÁS 73

10. REFERENCES 75
11. PUBLICATION LIST (APPROVED BY THE KENÉZY LIFE SCIENCE LIBRARY)..... 83
12. KEYWORDS 85
13. ACKNOWLEDGEMENT 86
14. APPENDIX 87

1. ABBREVATIONS

Akt	protein kinase B
ALDH	aldehyde dehydrogenase
BA	bile acid
bai	bile acid-inducible
BC	breast cancer
BCSC	breast cancer stem cell
BRCA1/2	breast cancer type 1/2
BSH	bile salt hydrolase
CA	cholic acid
CadA	acid-inducible lysine decarboxylase
CadB	lysine/cadaverine antiporter
cadBA	cadBA operon
CadC	cadaverine regulating membrane protein / transcription activator
CAEC	cancer-associated endothelial cell
CAF	cancer-associated fibroblast
CAR	constitutive androstane receptor
CDCA	chenodeoxycholic acid
CDH-1	E-cadherin
CDH-2	N-cadherin
CSC	cancer stem cell
DCA	deoxycholic acid
DCIS	ductal carcinoma in situ
E.coli	*Escherichia coli*
ECAR	extracellular acidification rate
ECIS	electric cell-impedance sensing
ECM	extracellular matrix
EGF	epidermal growth factor
EGFR	epidermal growth factor receptor
EMT	epithelial-mesenchymal transition / epithelial-to-mesenchymal trasition

ER/Esr	estrogen receptor
Erbb2 / HER2	tyrosine kinase-type cell surface receptor HER2
FgfBp	fibroblast growth factor binding protein
FOXC	forkhead-related transcription factor
FXR	farnesoid X receptor
GI	gastrointestinal
GPCR	G-protein coupled receptor
HSDH	hydroxysteroid dehydrogenase
IC	immune inflammatory cell
IGF-1	insulin-like growth factor-1
IgfBp	insulin like growth factor binding protein
KLF8	kruppel like factor 8 / zinc finger protein 741
Krt	keratin
LCA	lithocholic acid
LCIS	lobular carcinoma in situ
LDC	lysine decarboxylase
LdcC	constitutive lysine decarboxylase
LXR	liver X receptor
MAPK	mitogen-activated protein kinase
MET	mesenchymal-epithelial transition / mesenchymal-to-epithelial transition
MMP	matrix metalloproteinase
mTOR	mammalian target of rapamycin
OCR	oxygen consumption rate
OXPHOS	oxidative phosphorylation
PR	progesterone receptor
PXR	pregnane X receptor
SCFA	short chain fatty acid
SNAI	snail family transcriptional repressor
Spp	secreted phosphoprotein
TAAR	trace amine-associated receptor
TGF-β	transforming growth factor beta
TGR5	G-protein coupled bile acid receptor 1

TIL	tumor infiltrating lymphocyte
TP53	tumor suppressor P53
TWIST	twist basic helix-loop-helix transcription factor
UDCA	ursodeoxycholic acid
VDR	vitamin D receptor
VEGF-A	vascular endothelial growth factor-A
VIM	vimentin
Wnt	wingless-type family
ZEB1/2	transcription factor-8

2. INTRODUCTION

The human body harbors various kinds of symbiotic, commensal and pathogenic bacteria called the microbiota that lives on the body surface and the cavities of the human body. Its collective genome referred as the metagenome. The intestinal microbiome plays a crucial role in immune response, behavior, cardiovascular functions, metabolic pathways, neurologic signaling, regulate endocrine functions and protect against pathogen overgrowth [2].

2.1. The microbiome in disease

Given the diverse functional repertoire of the microbiome, it is not surprising, that they are associated with a broad range of diseases, even those, that were previously not connected with bacteria [3-6]. Recent studies highlight that changes in the composition or proportion of the microbiome and certain bacterial metabolites affect a large set of pathophysiological processes, from metabolic disorders to psychiatric diseases [7-10].

Microbial dysbiosis is often reflected as a loss of diversity [11]. However, the number of directly tumorigenic bacteria is extremely low (some 10 bacterial species), dysbiosis is associated with cancers of the skin [12], colon [4], urinary tract [13], cervix [14], lung [15], lymphoma [16, 17], prostate [13] and breast [11, 18-23]. It is still unclear whether imbalances of gut microbial communities are a consequence or a cause of chronic diseases, but it seems more likely that it capable of influencing the progression of these diseases [4].

2.2. Microbes in tumor metabolism

Although, most cancers mentioned above, affect organs that are in direct contact with microbes, recent data suggest that bacteria can affect organs in compartments distant to the microbiome through microbial metabolites. Metabolites, produced by the microbiome, can be absorbed and hence enter the circulation and exert their biological effect at distant sites in the body. Alterations of the microbiome are connected to metabolic diseases (e.g. type II. diabetes, obesity) [24] that are risk factors of certain types of cancers, among them, breast cancer (BC) [20, 25], further suggesting the role of bacterial metabolites.

Deconjugated estrogen-derivatives [18, 19], lipopolysaccharide [26], secondary bile acids (BAs) [27-31] and short chain fatty acids (SCFAs) [32] were suggested to participate in

regulating cancer cell proliferation or transformation, the molecular mechanism through which the bacterial metabolites expound their effect are largely unknown.

Numerous bacterial metabolites have been identified as the microbes' own metabolites (e.g. SCFA) or modified products of the host (e.g. secondary BAs and amino acid derivatives). In some cases, both the host and the microbiota can produce certain metabolites (e.g. biologically active amines). These biologically active metabolites can modulate gene expression or signal transduction pathways of cancer cells. My dissertation investigates the causal link between changes in the microbiome, the consequent changes in the microbiome-derived metabolome and BC.

3. REVIEW OF THE LITERATURE

3.1. The importance of BC research

BC is the third most common disease worldwide. Nowadays BC is the major cancer type of women and the fifth cause of death worldwide [33]. Between 2008 and 2012 the incidence of BC enhanced by 20%, and mortality by 14% [34]. Moreover, the incidence of BC increases with 0.5-1% in every year, its occurrence shows geographical and economic distribution. Rates are generally high in Western Europe, North America and Asia, intermediate in Central Europe, Latin America and the Caribbean, and low in most of Africa and Oceania [35] as also presented on Figure 1.

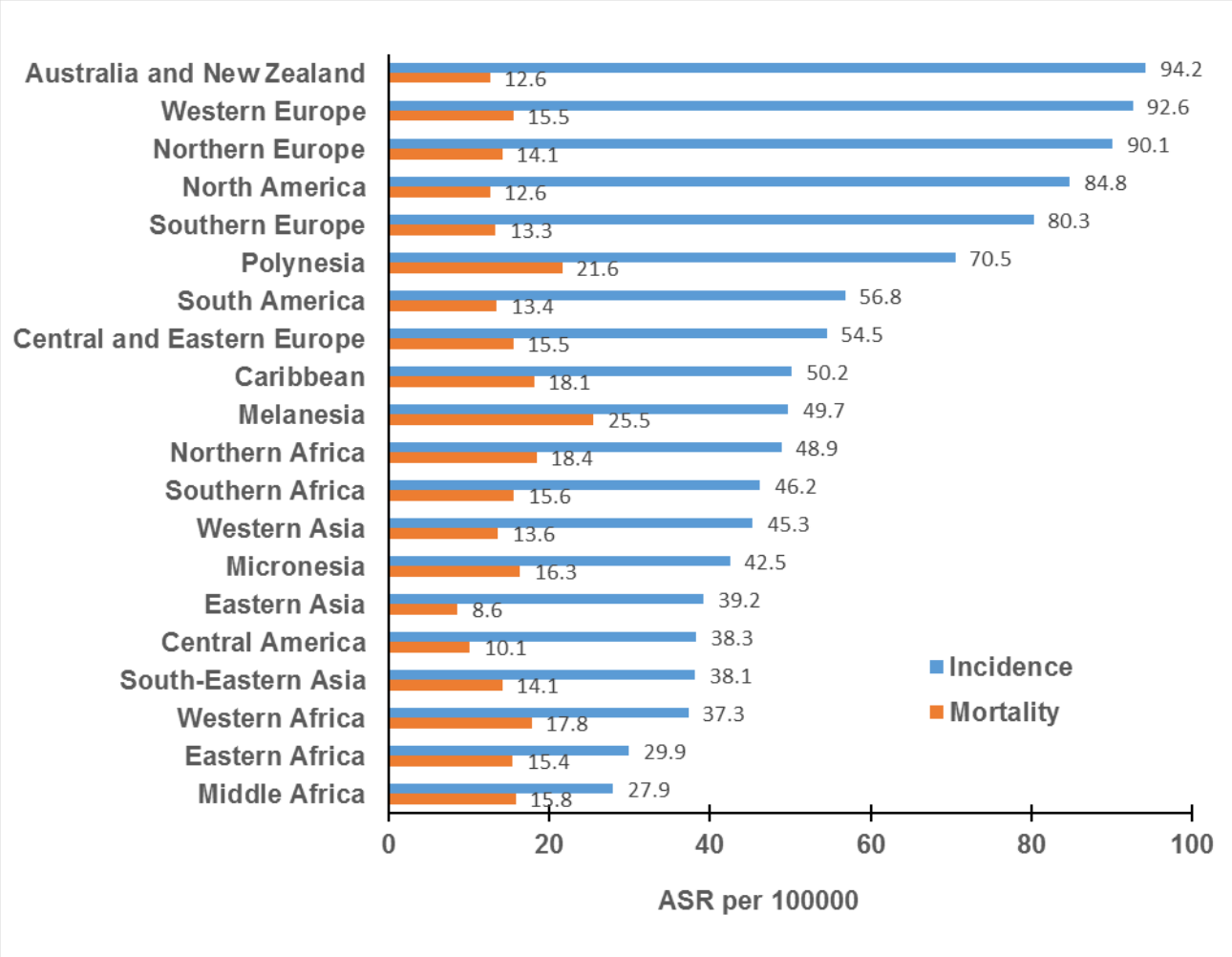

Figure 1. Breast cancer statistics in 2018. Bar chart of the age-adjusted breast cancer incidence and mortality (per 100000 persons) in 2018 among females within all ages, worldwide according to the Global Cancer Observatory (https://gco.iarc.fr/).

From 1990, despite of increased incidence, epidemiological data shows better survival rate. Improved survival is on one hand due to the development of surgical-, medical-, radiation therapy and the extended knowledge of molecular genetics and cancer screening methods. The origin of almost 70 % of all BC cases remain unclear, still according to various studies, the principal identified risk factors are sex, age (higher risk between age 35 and 65) and inheritance [36]. Genetic, epigenetic and environmental determinants are well-established risk factors, such as inherited loss of breast cancer type 1/2 (BRCA1/2) gene, high Insulin-like Growth Factor-1 (IGF-1) expression, the existence of *in situ* carcinomas, high fat diet, alcohol and radiation. Main risk factors are life exposure to hormones, associated with hormonal contraceptives, hormone therapy, puberty, pregnancy and menopause [33]. In contrast early (<age 18) child-birth, breast feeding, regular physical activity, avoiding harmful passions and consuming fiber rich food reduces the risk of developing BC [36].

According to the new paradigm, cancer is a complex, systemic disease, where a plurality of physiological and genomic alterations occur incessantly in the tumor mass [37].

3.2. BC classification shames

BC is a heterogenous disease, that is reflected in the available classification systems, including histopathological type, Nottingham grade, TNM stage and receptor status.

Histopathologically, we determine carcinoma *in situ*, that refers to neoplastic proliferation of malignant epithelial cells within the mammary ductal system (ductal carcinoma in situ, DCIS) or is limited to the lobules by the basement membrane (lobular carcinoma in situ, LCIS), with no evidence of invasion into the surrounding tissues. In contrast, invasive carcinoma (“infiltrating” carcinoma) has penetrated through the basement membrane and have the potential to invade into the circulatory system (infiltrating ductal and lobular carcinoma), thus reach distant sites and lymph nodes.

Nottingham Grading of BC focuses on the appearance of cancer cells compared to normal breast tissue. Grade 1 (low-grade) includes well-differentiated cancer cells that slightly infiltrate the stroma, the nuclei are uniform with little or no evidence of mitotic activity. In grade 2 (intermediate-grade), the tumor is moderately differentiated, the cells have glandular infiltration and some nuclear pleomorphism with moderate mitotic rate. Grade 3 (high-grade) refers to poorly differentiated tumors, the tumor mass consists of solid nests of neoplastic cells, show marked nuclear atypia and significant mitotic activity [38].

The *TNM classification* (T-tumor, N-node, M-metastases) is based on the size of tumor, where it originally started in the body, and the metastatic location. Stage 0 means a

precancerous or marked condition (DCIS or LCIS), while from stage 1 to stage 3 the tumor size and lymph node infiltration increases, without any metastases. Stage 4 denote metastatic BC with poor prognosis and overall survival [39].

Receptor status is critical in BC treatment as it determines the suitability and efficacy of adjuvant treatments. Estrogen receptor positive (ER^+) cells depend on estrogen for their growth and proliferation, thus they can be treated with medication that decrease the level or the effect of estrogen. They generally have better prognosis, while triple-negative BC (ER^-, PR^-, $HER2^-$) lacking targeted treatments and has a very poor outcome [40]. Molecular subtypes of BC - based on receptor status - are:

- Luminal A: ER^+, PR^+, $HER2^-$, low Ki67
- Luminal B ($HER2^-$): ER^+, PR^-, $HER2^-$, high Ki67
- Luminal B ($HER2^+$): ER^+, PR^+, $HER2^+$, low/high Ki67
- $HER2^+$/$ERBB2^+$: ER^- or PR^-, $HER2^+$
- Basal-like (triple-negative): ER^-, PR^-, $HER2^-$. Often harbors BRCA1 mutation

3.3. Hallmarks of cancer

Cancerous and normal cells differ in several features from each other. Tumor cells are more than insular masses of proliferating cells, instead, they are complex tissues, composed of multiple distinct cell types, that need to communicate and interact with one another [1].

Normal tissues carefully control the production of growth-promoting signals, to maintain normal tissue homeostasis, architecture and function, however, cancer cell obtain the capability to *sustain proliferative signaling* in a lot of ways: genome mutations can constitutively activate signaling pathways responsible for proliferation (e.g. mutations in MAPK-pathway [41] or in Akt-pathway [42, 43]), defects in negative-feedback (e.g. mTOR activation [44]) mechanism can attenuate proliferative signaling.

Tumor cells are able to *evade the effect of growth suppressors.* The two principal tumor suppressor - that can limit growth and proliferation – are retinoblastoma and TP53 proteins. Cells with loss-of function mutations or with defects in these pathways are missing the services of a critical gatekeeper of cell-cycle progression, enabling continuous tumor growth [45, 46].

Cancer cells evolve numerous strategies to *limit or evade apoptosis*. Most common is the loss-of-function mutation of TP53, but alternative solutions are increasing the expression of antiapoptotic regulators or survival signals, or downregulating proapoptotic factors [1].

Most normal cells are capable of passing through a limited number of successful cell divisions, while cancer cells have *unlimited replicative potential*. They can maintain optimal telomeric DNA length by upregulating the expression level of telomerase enzyme – that is responsible for extending telomeric DNA - thus counter progressive telomere erosion [1].

Like normal cells, tumors require resources in the form of nutrients and oxygen, and need to deplenish metabolic wastes. In the case of tumor cells, *angiogenesis* addresses these needs by generating tumor-associated vascular network. Angiogenesis is induced early during the multistage development of invasive cancers and reserved throughout its life. Growth factors (Vascular Endothelial Growth Factor-A, VEGF-A), pericytes and bone marrow-derived cells contribute in this process [47].

When a tumor mass is big enough, they start to migrate to other parts of the body. While cancer cells *actively forming metastasis,* as well as, *local invasions*, they develop typical alterations in their shape, their attachment to other cells and to the extracellular matrix (ECM). The best characterized alteration so far is the loss of E-cadherin (CDH-1), a key cell to cell adhesion molecule. Enhanced expression of CDH-1 was determined as an antagonist of both invasion and metastasis [48, 49]. In contrast, N-cadherin (CDH-2) - normally expressed in mesenchymal cells and migrating neurons – is often upregulated in several invasive tumor cells, leading to increased migration [48].

Some papers suggest that other four hallmarks of cancer are involved in the pathogenesis of most cancers. Cancer cells often enhance the rate of mutation through increased sensitivity of mutagenic agents. This *genomic instability and mutability* donate genetic alterations to tumor cells that drive tumor progression and accommodation [50, 51].

Scientific papers show, that *tumor-promoting inflammation* can contribute to multiple cancer hallmarks by supplying molecules to the tumor microenvironment (growth, survival, proangiogenic factors, ECM-modifying enzymes, epithelial-mesenchymal transition (EMT) inducing signals) [52-54].

Otto Warburg first observed, that cancer cells *reprogram their energy metabolism,* so energy production via glycolysis can be the main energy source, even in the presence of oxygen. This process called “aerobic glycolysis” [55]. Moreover, solid tumors are investigated to *avoid the detection of the immune system* or capable to limit immunological killing, thereby, evading tumor cell destruction by the ever-alert monitoring immune system [1] (Figure 2).

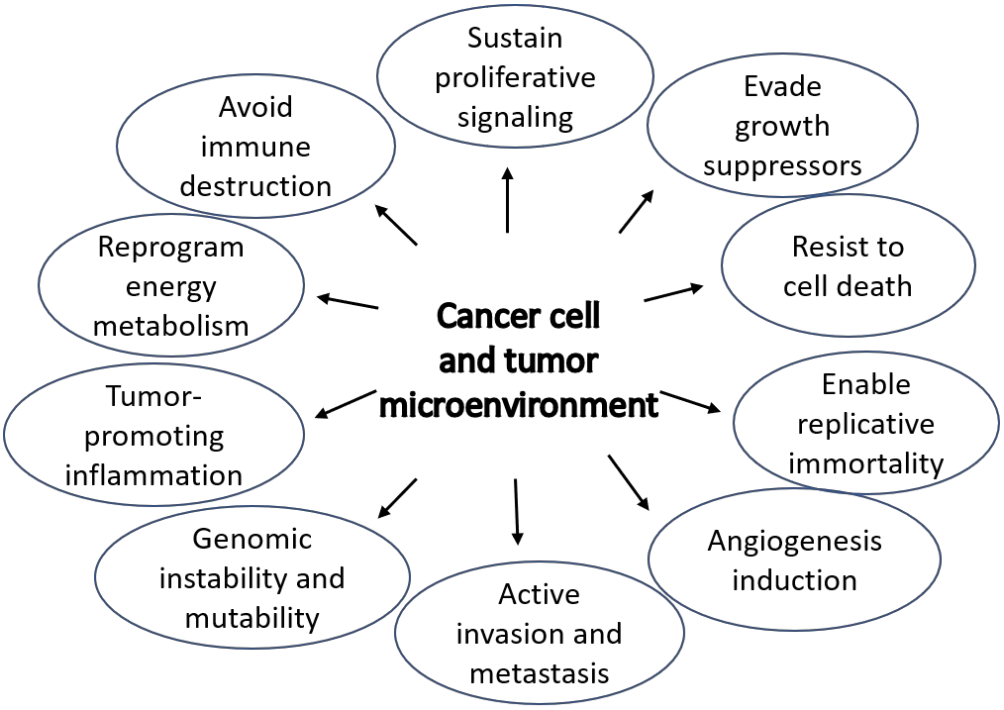

Figure 2. Hallmarks of cancer. The illustration encompasses the capabilities of cancer cells to sustain uncontrolled proliferation (often referred as cancer hallmarks). Each of them contribute to growth, survival and spreading of tumor cells. Figure reproduced from [1].

3.4. The tumor microenvironment

In the past few decades, scientists highlighted, that tumors are not made up of homogenous cancer cells. Tumors have been recognized as organs, whose complexity may exceed that of normal healthy tissues. Thus, the biology of tumors can be examined by studying the cell types within the tumor and the tumor microenvironment together [1].

"Most solid tumors (solid masses of tissue) have a distinct structure that mimics that of normal tissues and comprises two distinct but interdependent compartments: the parenchyma (cancer cells and cancer stem cells(CSCs)) and the stroma (that the parenchyma cells induce and in which they are dispersed)" [56]. The most common cell types of tumor stroma are: cancer-associated fibroblasts (CAFs), pericytes, cancer-associated endothelial cells (CAECs), immune inflammatory cells (ICs) and stroma stem and progenitor cells (Figure 3). Parenchyma contains tumor cells that actively proliferate and seed new tumors, while stroma cells are not malignant *per se*, their role is supporting cancer growth.

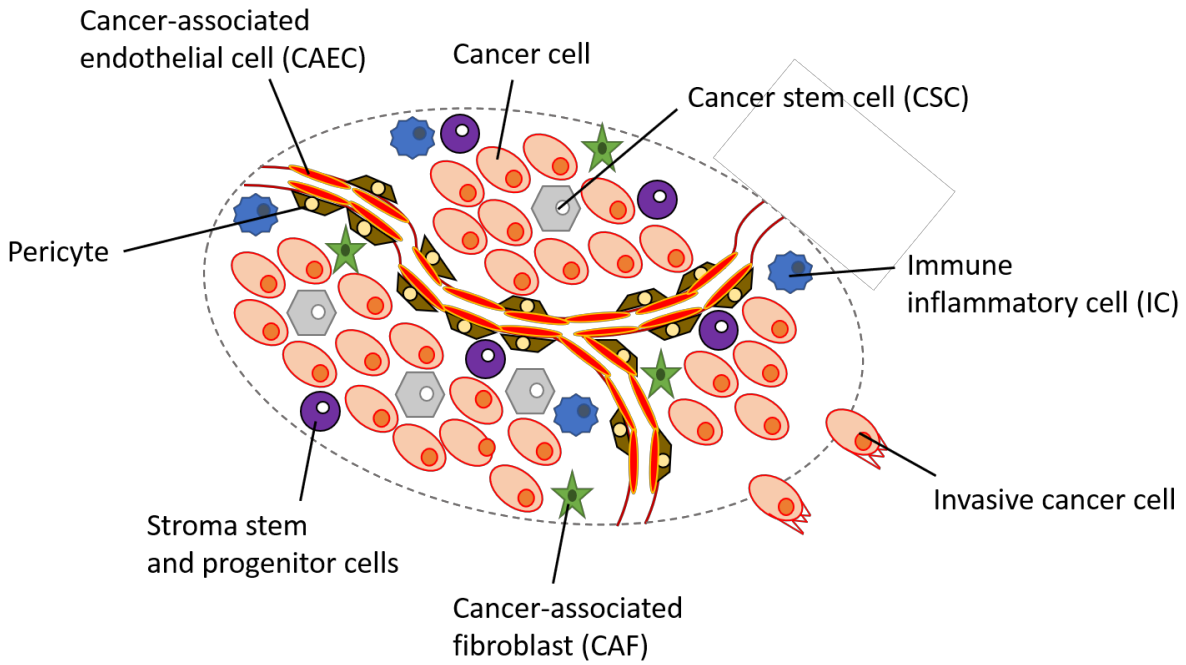

Figure 3. The primary tumor microenvironment. Tumor consists of not only homogenous cancer cells. Here a set of cell types presented, as the core of primary tumors, and known to contribute in the biology and regulatory signaling of most tumors. Figure reconstructed from [1].

Cancer cells are the foundation of the disease, initiate tumors and drive tumor progression forward. Initially, they form a homogeneous cell population, until later phases of tumor progression, when hyperproliferating cells create heterogenic clonal subpopulations.

CSCs are confirmed to be a common component of most tumors, however, earlier found to contribute only in hematopoietic malignancies [57], later were identified in breast carcinomas [58] as the cell type, that effectively seeds new metasasis. Moreover, cells with CSC properties are more resistant to numerous chemotherapeutic treatments [59-61]. CSC can be converted to stroma cells by the process of EMT (see below).

Fibroblast-like cancer cells, called *CAFs* are essential cell types of the supportive stroma. Animal studies highlights, that CAFs play important role in cancer cell proliferation, angiogenesis, invasion and metastases by promoting these mechanisms [62-65]. According to new findings in tumor metabolism, epithelial cancer cells can induce CAFs to secrete lactate and pyruvate (energy metabolites, resulting from Warburg-type aerobic glycolysis), that epithelial cells then utilize to facilitate tumor growth and angiogenesis. In this model, the epithelial cells instruct stroma cells to transform a wound-healing stroma, providing energy-rich microenvironment in a “host-parasite” way called “reverse Warburg effect” [66].

Distinctive gene expression profile of *CAECs,* and different cell-surface markers of normal cells compared to tumor endothelial cells confirm the conversion of normal endothelial

cells into CAECs [67-69]. CAECs ensure the development of tumor-associated angiogenesis and vascularization for the growing tumor tissue. Intratumoral vessels are often collapsed and nonfunctional, due to the high interstitial pressure, however, the functional vessels are located at the peripheries of tumors [1].

Pericytes are specialized mesenchymal cells, that cover the endothelial blood vessel from the outside, provide paracrine signals to the endothelial cells and synthesize the vascular basement membrane, thus support the tumor endothelium [63, 70].

Infiltrating cells of the immune system (ICs) are widely accepted to be the part of tumors. They can antagonize or promote tumor progression. In normal wound healing, immune cells transiently appear and disappear, versus their continuous presence in chronic diseases, among cancer [53]. ICs, including macrophages, neutrophils, B and T lymphocytes [52, 71, 72] release signaling molecules (tumor growth factor, angiogenic growth factor, chemokines and cytokines), that amplify inflammatory state, and may produce matrix-degrading enzymes, among matrix metalloproteinase-9 (MMP-9) and other matrix metalloproteinases (MMPs) [54, 73]. ICs are able to act as antitumor agents by inducing apoptosis (through producing reactive oxygen species), activating cytotoxic T cells, natural killer cells or B lymphocytes [74, 75]. Thus, ICs – neutrophils and lymphocytes - could help or deplete cell proliferation, tumor angiogenesis, invasion and metastatic behavior [54, 71-73, 76, 77].

ICs have been long known to recruit from the bone marrow, recent studies highlight that progenitors of CAFs, pericytes, and CAECs originating from the neighboring normal tissue, or via recruitment of bone marrow-derived stem or progenitor cells [78] (Table 1).

Table 1. Cell types in the tumor microenvironment. Table based on [1, 53, 57, 63, 78].

Cell type	Characteristic/function	Role in tumor progression	Self-renewal
Parenchyma			
Cancer cell	carrying oncogenic and tumor suppressor mutation	initiate cancer, proliferation	No
CSC	differentiate in well-characterized tumor cells	maintain propagation, form metastasis	Yes
Stroma (supportive cells)			
CAF	secrete growth factors, induce EMT, remodel ECM	growth, survival, migration	No
CAEC	signal-transduction, serve as channels for metastases	angiogenesis, vascularization, metastasis	No
Pericyte	synthesize basement membrane, provide paracrine signaling	support the tumor endothelium	No
IC	release signaling molecules, influence inflammatory state, induce apoptosis	proliferation, angiogenesis, invasion, metastasis (pro- or anti effect)	No

3.5. Epithelial to Mesenchymal Transition

In general, EMT is a cellular developmental process, that allows epithelial cells to turn into mesenchymal or mesenchymal-like cells, loose their apical-basal polarity, cell-cell contacts and gain invasive features [79]. EMT influences motility through mediating cell-cell adhesion-, and cell-ECM adhesion specific molecules, upon EMT the epithelial cytokeratin-based intermediate filament network is replaced with vimentin (VIM), actin stress fibers are formed and cells yield a more spindle-like shape [80, 81]. In EMT the expression of the mesenchymal CDH-2 increased, while an important epithelial marker (CDH-1) is down-regulated [82].

We distinguish between three types of EMT. Type I EMT is related to embryonic development, and it enables embryonic epithelial cells to become mesenchymal-like and travel to distant sites where new tissues and organs form. Type II EMT occurs in wound healing and fibrosis. During wound healing, changes upon EMT allow the injured edges to migrate to close the wound, and in this case, only cells of the leading edge seem to undergo EMT [79, 83].

Type III (oncogenic) EMT is not equivalent to developmental EMTs. Type III EMT is observed in carcinoma cells, is associated with tumor progression and metastasis, as it allows cancer cells to invade through the basement membrane and intravasate into the circulatory system [79, 83] (Figure 4).

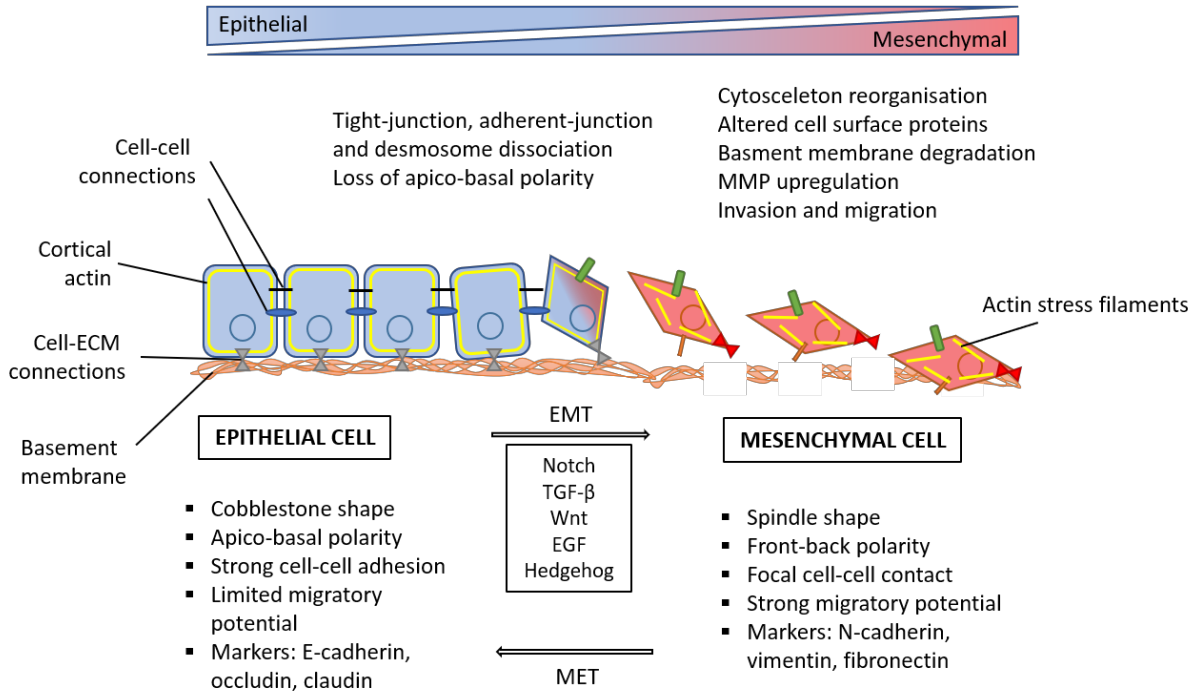

Figure 4. Oncogenic EMT of BC cells. During EMT, cells lose the connection between them and with the basement membrane, change their characteristic and start to migrate to other parts of the body. Meanwhile, cells reorganize the cytoskeleton, express different cell-surface proteins and well-characterized markers, becoming more mesenchymal-like cells. Once tumor cells went through EMT, they can undergo mesenchymal-to-epithelial transition (MET) that is the reverse process of EMT. Figure based on [79, 84].

The completeness of oncogenic EMT is often less, than that of type I EMT, depending on the cellular microenvironment, thus type III EMT can be regarded as a partial EMT process, in which, carcinoma cells gain mesenchymal features, but not fully lose epithelial characteristic. This intermediate phenotype represents a flexible state: the cells that already went through EMT, can undergo the reverse mechanism, called mesenchymal-epithelial transition (MET) during secondary tumor formation [85]. These new tumor colonies are histopathologically similar to those of carcinoma cells in the primary tumor that never underwent an EMT [84].

In summary, EMT can facilitate tumor progression through different ways: A) EMT can increase invasive and anti-apoptotic programs that drive cancer metastasis, B) EMT can generate structural end biochemical alterations of the tumor microenvironment, and C) EMT mediators can lead to the increment of CSC phenotype [38].

3.5.1. EMT and metastasis

Oncogenic EMT is observed in many BC models, and plays an important role in invasion and metastasis. Several EMT regulators are able to induce metastasis to distant

organs (mostly to the liver, brain, bones and lungs), and results poor disease outcomes. Distant metastases are generally characterized as having epithelial type morphology, and sometimes metastatic tumors have a greater degree of cellular differentiation as compared to the primary tumor [86], suggesting, that after EMT, the reverse mechanism (MET) occurred at some point. The existence of MET was further confirmed by the observation, that MET was highly dependent on signals from the host microenvironment [87, 88]. Moreover, Dykxhoorn and colleagues examined 4T1 cell series (isogenic mouse BC cell line series) with different metastatic potential [89, 90]. They found, that those 4T1 cell lines that were flexible - retained epithelial features (features of type III EMT), while also expressed mesenchymal characteristics - had high metastatic potential. The results highlight, that the cell line is capable to interchange between states if they receive the appropriate signal, thereby, can affect early or late stage metastasis.

3.5.2. EMT and breast cancer stem cells (BCSCs)

BCSCs play a major role in cancer growth and the formation of metastases, treatment resistance and disease recurrence. The proportion of BCSCs vary between cell models of BC. Usually, the proportion of BCSCs is small (e.g. 4T1 mouse BC), while certain cell lines contain high percentage up to 25% (e.g. SKBR-3 human BC) [91]. BCSCs show an invasive gene signature which correlates with enhanced metastasis and poor overall survival. A study highlights the metastatic potential of BCSCs [92]. In a murine model, metastases could re-create breast tumors when transplanted into immunosuppressed mice, and these metastases highly expressed BCSC markers.

There is no consensus on the existence, roles, functions and markers of BCSCs. BCSC are capable of self-renewal, and either divide symmetrically, producing further stem cells, or asymmetrically, to generate progenitor cells, that can differentiate into various cell types within the tumor. Classically, BCSCs are considered quiescent, with a slow capability to enter the cell cycle with increased resistance to apoptosis, thereby, BCSCs may hamper the effectiveness of surgery, radiotherapy or chemotherapy. Recent investigations suggest, that BCSCs can perform various biochemical changes in response to different microenvironmental conditions. In contrast to the Warburg paradigm of “aerobic glycolysis”, BCSCs are characterized by increased glycolytic flux, enhanced OXPHOS (oxidative phosphorylation), fatty acid oxidation and glutaminolysis [66]. Conflicting data suggest that BCSCs rely more on glycolysis than on mitochondrial oxidative metabolism, while others put forward, the dependence of BCSCs on OXPHOS and evidence a decrement in glycolysis. It stays probably closer to reality, that BCSCs have a plasticity in their metabolism: they can utilize glycolysis or OXPHOS as a

function of the microenvironment or the need of the cell. This plasticity confers them resistance to radiotherapy and chemotherapy [93]. From the perspective of cancer patients, inducing stem cells to enter the cell cycle and then target them with conventional anticancer therapies could be one possible solution for younger patients, or keep them in a dormant state would be more beneficial for elderly patients [94]. BCSCs are often identified by detection of the aldehyde dehydrogenase activity. Aldehyde dehydrogenase-1 (ALDH1), a detoxifying enzyme, is found in both normal mammary stem cells, and BCSCs. ALDH1 expression is recently associated with poor prognosis and decreased overall survival in human breast tumors [79, 95].

3.5.3. Molecular events of EMT in BC

Numerous mediators and molecular events are shown to drive EMT in BC. *DNA mutations*, *hypermethylation* or the *functional loss of* CDH1 is the most critical event connected to EMT. Transcriptional down-regulation of CDH1 seems to allow cancer cells abandon their original location and become more mobile, thereby, play a significant role in BC EMT, migration and invasion [96, 97]. Besides epigenetic and DNA mutations, *microRNAs* are a new class of EMT regulators, that inhibit gene expression at the post-transcriptional level, modifying EMT-inducing transcription factors. miRNA-335 is suggested to down-regulate metastatic genes in BC, based on recent studies [98, 99].

Numerous *transcription factors* have been found to drive EMT. Some of them exert their effects through the repression of CDH1: SNAI1, SNAI2, SNAI3, TWIST, FOXC1, FOXC2, ZEB1, ZEB2 and KLF8. These transcription factors play a crucial role in maintaining mesenchymal characteristics and in acquiring stem cell phenotype, as BCSCs display high expression of these factors [100]. Some of these transcription factors are able to induce EMT through *signaling mechanisms*, for example TGF-β, EGF, Wnt/ β-catenin, Notch and Hedgehog pathways [101]. SNAI1 can induce metastases by inducing immunosuppression, and SNAI and ZEB can induce EGFR/ErbB2 signaling, that also promote metastasis. Inhibition of these receptor pathways can reverse the aggressive BC phenotype into less aggressive cell form with epithelial-like features [102].

The *tumor microenvironment* can influence EMT as well, since MMPs can be up-regulated during the EMT process degrading the ECM and allowing cancer cells to migrate to different parts of the body [103]. At the metastatic site, in the absence of additional EMT modulators, the tumor cell could transform back to the original epithelial-like phenotype via the reverse process, called MET. The complex process of EMT suggests, that different molecules expound their effect together, strengthen or suppress the effect, to mediate EMT, rather, than master regulators acting on their own [101] (Table 2).

Table 2. EMT markers and regulators. The left column shows grouped markers and regulators, while the right column indicates whether they rather expressed in epithelial or mesenchymal cells, or promote epithelial or mesenchymal characteristics. Figure based on [97-101].

Marker	Epithelial or mesenchymal
CDH-1	Epithelial
CDH-2	Mesenchymal
VIM	
Fibronectin	
Krt 14	
MMPs	
Spp1	
Growth factor binding proteins	
MicroRNAs	**Epithelial or mesenchymal**
miRNA-335	Promote epithelial
Transcription factors	**Epithelial or mesenchymal**
SNAI1/2/3	Promote mesenchymal
TWIST	
FOXC1/2	
ZEB1/2	
KLF8	
Signaling/growth factor receptors	**Epithelial or mesenchymal**
TGF-β	Promote mesenchymal
EGF/EGFR	
Notch	
Wnt/ β-catenin	
Hedgehog	
ER	

3.6. The human microbiome

The term microbiome and metagenome are often used as synonyms, but express two different meanings, whereas, microbiome indicates the entirety of microbes, the metagenome refers to the totality of genomes of the microbiota, and is often used to describe the unit of microbial properties encoded by the microbiota [104]. The term „human microbiota" is applied to the sum of microbes that live in numerous habitats of our body (gut, skin, vagina, mouth, nose, conjunctiva, among others). The microbiota of each organ is different and characteristic, it has important and functionally relevant individual variability between individuals and is a potential determinant of disease (such as cancer) [105].

3.6.1. The human gut microbiota

A large number of diverse microbial species (~10^{14} bacteria) colonize the human gastrointestinal (GI) tract. Their collective bacterial metagenome harbors 150-fold more genes than the human genome [105]. A complete study identified 9.9 million microbial genes across the fecal microbiome [106]. The human gut microbiome serves a good model for investigating host-microbiome-diseases interactions. Main phyla of the GI tract are *Firmicutes, Bacteroides,*

Actinobacteria, Proteobacteria, Fusobacteria, Verrucomicrobia, Tenericutes and Lentisphaerae (Table 3). Main genera are *Bacteroides, Clostridium, Faecalibacterium, Eubacterium, Ruminococcus, Peptococcus, Peptostreptococcus, Lactobacillus, Streptococcus, Streptomyces* and *Bifidobacterium* [107].

Table 3. The connection between gut microbiota, BC, cadaverine and lithocholic acid (LCA) production. The first column shows the main bacterial phyla in the GI tract, red color shows known altered phyla in BC (changes occur between stage I/II and stage III), cadaverine producing phyla marked with green, while blue phyla sign LCA producing bacteria. Figure based on [105, 108, 109].

GI tract main bacterium phyla	Alterations in BC (between stages)	Cadaverine producing bacterium phyla	LCA producing bacterium phyla
Firmicutes	***Firmicutes***	***Firmicutes***	***Firmicutes***
Bacteroides	***Bacteroides***	***Bacteroides***	***Bacteroides***
Actinobacteria		***Actinobacteria***	
Proteobacteria		***Proteobacteria***	***Proteobacteria***
Fusobacteria		***Fusobacteria***	
Verrucomicrobia			
Tenericutes			
Lentisphaerae			

The human gut microbiota is helpful in digestion, metabolism, and plays important role in human health. It plays a critical role in maturation, immune response, provide protection against pathogen overgrowth, helps to maintain intestinal barrier function, influence host-cell proliferation and vascularization, regulate intestinal endocrine functions, neurologic signaling, bone density, provide a source of energy biogenesis, biosynthesize vitamins, neurotransmitters, metabolize bile salts, react or modify drugs and eliminate exogenous toxins [2].

Several internal and external factors influence the gut microbiota, including age, diet, host genetic features, maternal colonization, hygiene, xenobiotic and antibiotic exposure, stress or travelling. The gut microbiota dysbiosis – imbalances in the function and composition of the intestinal microbes – can promote numerous diseases ranging from localized GI disorders to metabolic, cardiovascular, neurologic, respiratory, hepatic disorders and cancer [2] (Figure 5). Moreover, studies show, that discrete presence of some bacterial species or changes in the abundance of certain microorganisms can exert pathogenic effects that facilitate disease development [110, 111].

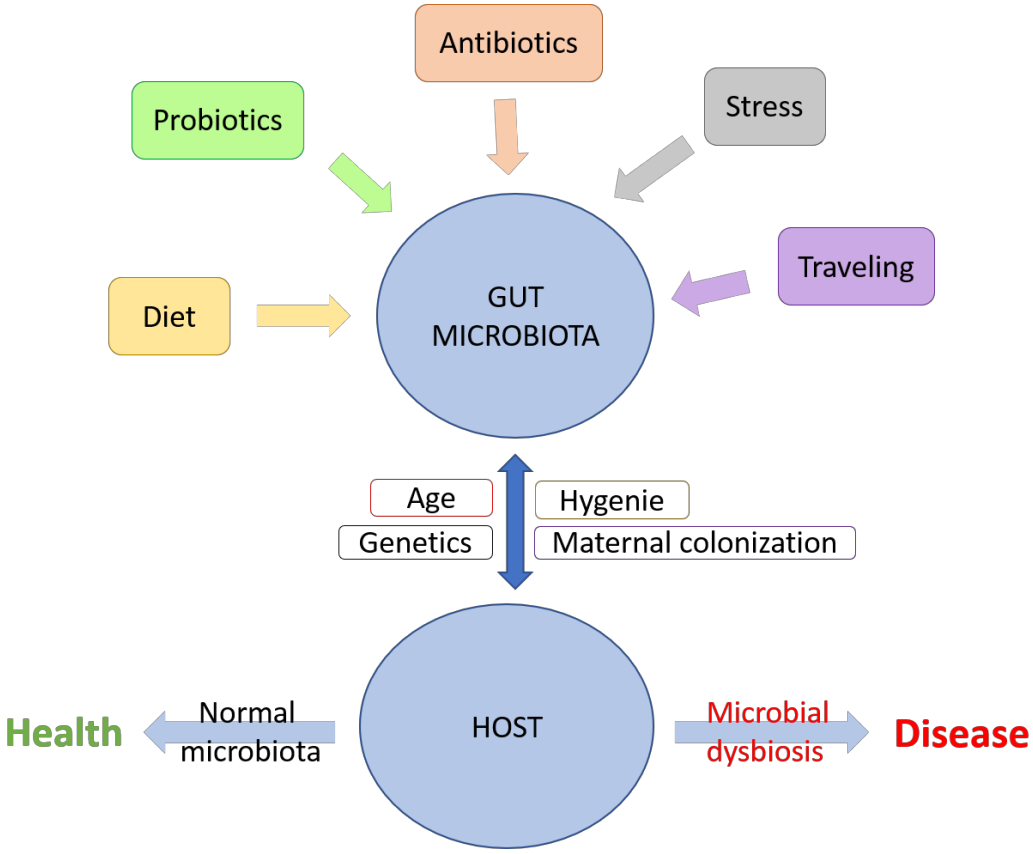

Figure 5. Host-microbiome-disease connection. Several external and internal signals can affect to the microbiome. Through the composition and bacterial metabolism, the microbiota influences the host, contributing health or disease development, while the host affect back to the microbiome through hygiene and other internal signals. Figure based on [2].

Some metabolites have been identified as the microbes' own product, other metabolites are created by modification of certain products of the host, while further metabolites produced both by the host itself and by the microbiome as well in parallel.

3.6.2. Connection between gut microbiome and BC

Bacterial communities within the host are suggested to be an additional environmental factor related to BC [37]. Microbial metabolites generated in the GI tract can reach distant parts of the body through the bloodstream, and exert their effect in organs other than the GI tract.

The link between BC and GI microbiome dysbiosis has been investigated in case-control studies, however, the studies targeting this relationship are quite limited so far. Some papers confirm that in BC, beside of the weakness of immune system, a huge decrement occurs in the metabolic ability of the microbiome [112]. A case-control study comparing the fecal microbiota between control and BC patients shows significantly altered microbiome

composition and less diverse gut bacteria among BC patients. They found increased abundance of *Clostridiacea, Faecalibacterium* and *Ruminococcaceae* and decreased *Dorea* and *Lachnospiraceae* taxa [11]. Furthermore, reduced microbiota diversity characterize obese patients, which is a well-known risk of BC [113].

Changes in the composition of the microbiota exist not only between control and BC patients, but between certain BC stages as well [114]. For example, patients with grade III cancer have elevated absolute numbers of *Blautia spp*. compared with grade I patients. Another study shows that in clinical stage groups II/III, patients were significantly higher number of *Bacteroidetes, Clostridium leptum cluster and Blautia spp* [112] (Table 3).

3.7. Polyamines and the role of cadaverine

Polyamines are organic compounds, polycations, containing more than two amino groups. Low molecular weight linear polyamines are present in all living organism, the most common representatives are spermine, spermidine, putrescine and cadaverine. Between species, polyamine concentration and composition differ, for example, cadaverine is well-characterized in plants and bacteria, while show low abundance in most other species, in contrast with spermine, spermidine or putrescine [115-117].

Intracellular polyamine levels are strictly regulated through biosynthesis, transport and catabolism. They are mainly synthetized from the amino acids methionine, ornithine, arginine and lysine by decarboxylase enzymes. A less common biogenic amine, cadaverine, is formed through the direct decarboxylation of L-lysine catalyzed by lysine decarboxylase (LDC). Main cadaverine producing bacteria are *Escherichia coli (E. coli), Raoultella ornithinolytica, Enterobacteriaceae bacteria, Edwardsiella tarda, Hafnia alvei, Aeromonas veronii, Clostridium perfringens, Staphylococcus* and *Streptomyces species [108].* They belong to the *Firmicutes, Bacteroides, Actinobacteria, Proteobacteria* and *Fusobacteria* phyla (Table 3). The reference serum concentration of cadaverine is 0.1 - 0.8 μM as measured in healthy volunteers [118, 119]. Cadaverine plays significant role in cell survival at acidic pH [120], cell signaling, stress response and is also related to animal growth and development [121], cell proliferation and tumorigenesis [122, 123]. Moreover, cadaverine is an essential component of the cell wall, and plays an important role in the structural linkage between the outer membrane and peptidoglycan in bacteria [124] (Figure 6).

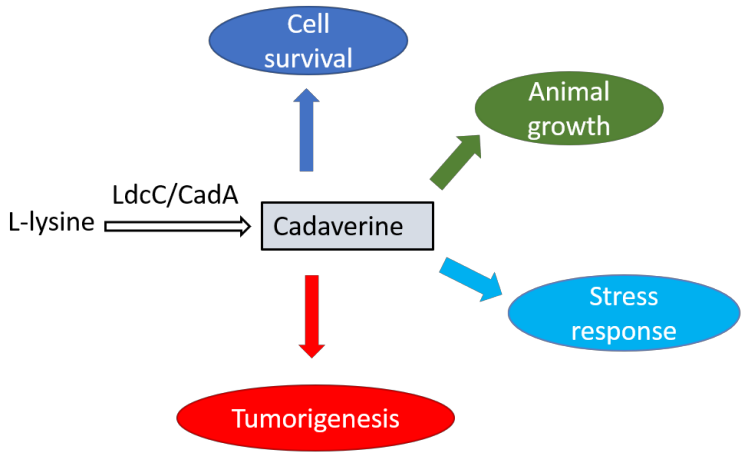

Figure 6. The roles of cadaverine in the cell. Cadaverine plays significant role in cell growth and development, cell survival in acidic pH, stress response and in tumorigenesis. Figure based on [120, 123, 124].

LDC is widely distributed among prokaryotes and eukaryotes. In *E. coli* two types of LDC were discovered: the constitutive LdcC and the acid inducible CadA. They show high sequence conservation with 69% identity, however, their optimal pH, stability and decarboxylation activity differ [125, 126]. The optimal concentration of cadaverine is maintained in *E. coli* by *the* cadaverine regulatory system that has two main components: the cadBA operon – that codes for lysine decarboxylase (CadA) and lysine/cadaverine antiporter (CadB) – and the regulatory inner membrane protein (CadC), which is responsible for pH sensing [127, 128] (Figure 7).

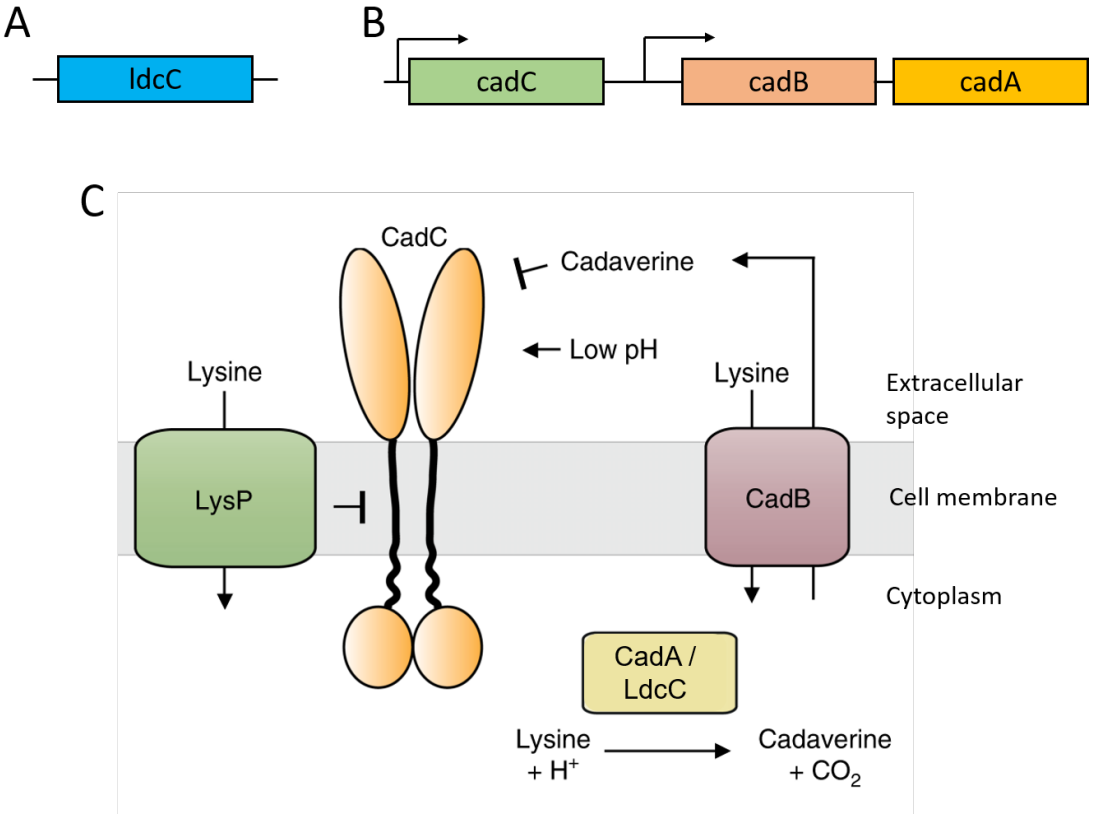

Figure 7. E. Coli cadaverine regulatory system. (A) Constitutive ldcC operon. (B) Acid inducible cadBA operon. (C) In a lysine-rich environment, CadC activates expression of the cadBA operon. CadA and LdcC convert lysine to cadaverine. The antiporter CadB transports lysine into the cells and exports cadaverine. External cadaverine has a feedback inhibitory effect on CadC activity, while low pH increases its activity. ldcC: LdcC coding region, LdcC: constitutive lysine decarboxylase, cadA: CadA coding region, CadA: acid-inducible lysine decarboxylase, cadB: CadB coding region, CadB: lysine/cadaverine antiporter, cadC: CadC coding region, CadC: regulatory protein, cadBA transcription activator, LysP: lysine-specific transporter and negative regulator of cadBA. (modified figure from [128]).

Recent studies have discovered trace amine-associated receptors (TAARs) as recognition receptors of biogenic amines. First, TAAR13c was identified to specifically recognize cadaverine in zebrafish [129]. All TAARs except TAAR1 function as olfactory receptors in rodents, primates and fish, and they share a strong evolutionary relationship with biogenic amine G-protein coupled receptors (GPCRs). These receptors are characterized by highly conserved domains: a 7-transmebrane domain, connected with 3 extracellular and 3 intracellular loops [130]. In mammals, TAAR13c is absent and other TAARs take over its role. In these cases, other TAARs were sequentially identified which detect the carrion odor cadaverine. TAAR13c has two main characteristics that allow cadaverine binding: a negatively charged $Asp_{3.32}$ – that supports amine recognition – and a second aspartate at position 5.42 or 5.43. Based on these molecular features, structural studies found similar TAARs in humans (TAAR6 and TAAR8), mice (TAAR6 and TAAR8b) and rats (TAAR6 and TAAR8a), that could be responsible for responding to cadaverine [131]. In humans TAAR1 is mostly expressed in

the brain, and - together with TAAR2 - is important in mediating amine-induced leukocyte functions [132]. TAAR3 and TAAR4 are encoded by pseudogenes, TAAR5 is a highly sensitive olfactory receptor, TAAR6 is associated with schizophrenia and bipolar disorders [133]. TAAR7 is not expressed in humans, while TAAR8 often uses TAAR1 agonists and downstream signaling pathway [134]. TAAR9 is a functional receptor in most of the human population, although, current understanding of TAAR-mediated functions and signaling is ill-characterized (Figure 8).

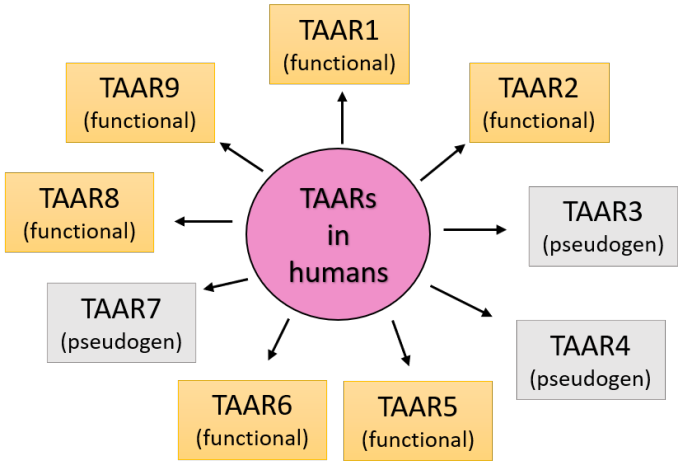

Figure 8. The family of TAARs in humans. Functional TAARs recognize ligands, and collect chemical signals from the environment. Most TAARs retain amine recognition motifs conserved in biogenic amine receptors. TAARs, existing as pseudogenes, have sequences similar to normal genes but due to gene mutation this pseudogene is not functional, and usually not transcribed. Figure reproduced from [135].

However, TAAR family remains largely understudied as compared to other GPCRs, a recent study highlights the association between TAAR1 overexpression and positive survival rate among BC patient [136]. These results suggest, that the family of TAARs may have important role in BC pathology.

3.8. Bile salt biotransformation and LCA

BAs are synthesized from cholesterol in hepatocytes. Two main primary BAs – cholic acid (CA) and chenodeoxycholic acid (CDCA) – are produced in the human liver. Primary BAs are subsequently conjugated to glycine or taurine. These fully ionized BA salts are carried to the gallbladder to concentrate. Bile salts are highly effective detergents, after a meal they get secreted to the intestine [137], where BAs promote the emulsification, absorption and digestion of lipids and lipid-soluble nutrients. More than 95% of the BAs are reabsorbed in the distal ileum and return to the liver for reuse. This process is called “enterohepatic circulation” and

occur four to twelve cycles a day. While bile salt absorption is highly effective (~95%), still 200-600 mg of bile salts leave the enterohepatic circulation daily, and become substrates for bacterial transformation in the colon [138] (Figure 9). The transformation of bile salts occurs with the contribution of bile salt hydrolase (BSH) and hydroxysteroid dehydrogenase (HSDH) enzymes, expressed by intestinal bacteria.

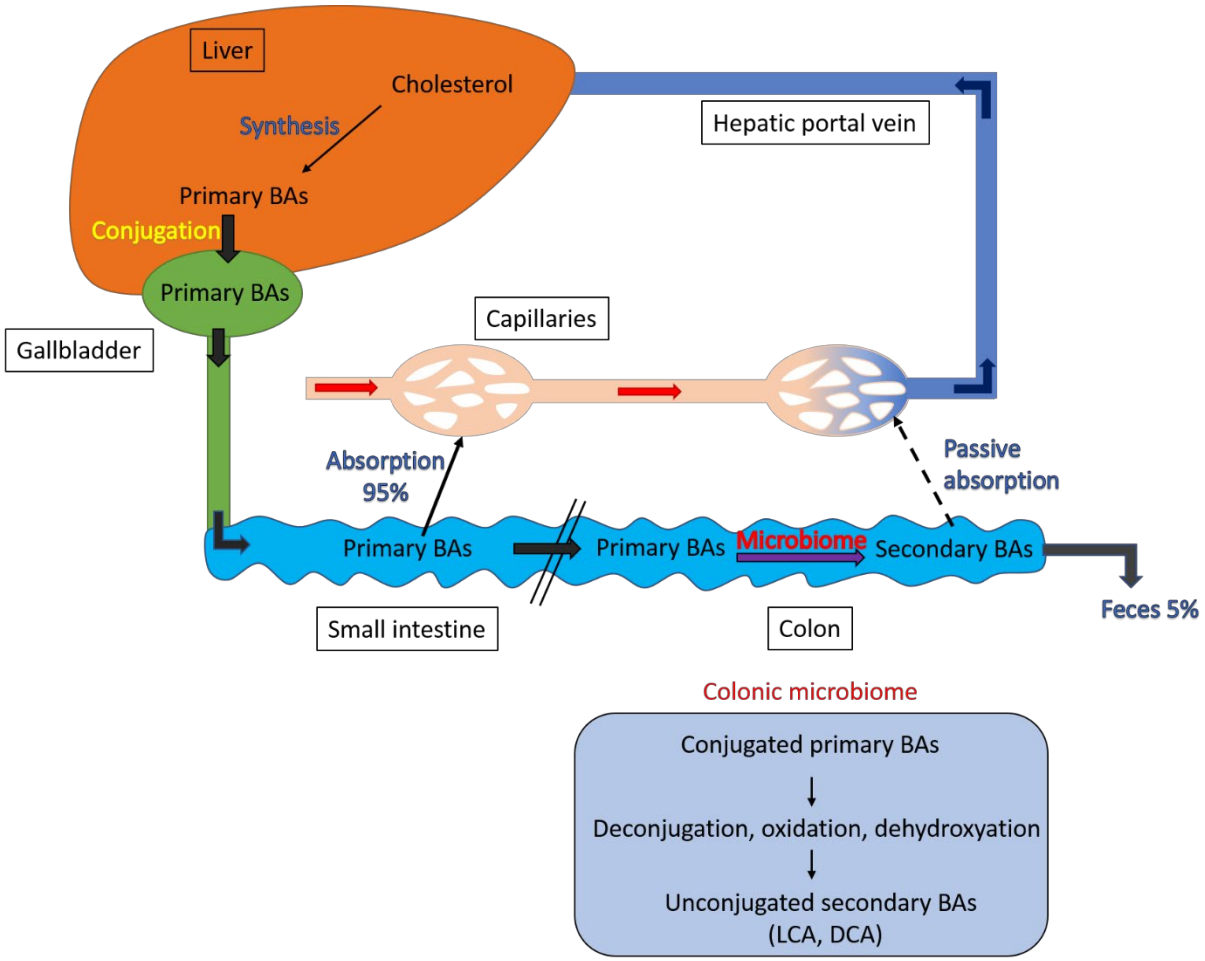

Figure 9. The enterohepatic circulation of BAs. Primary BAs synthesized in the liver, and concentrated in the gallbladder. Once they released, they go to the intestines where transformed to secondary BAs by microbes (mainly in the large intestine). 95% of BAs are actively reabsorbed from the small intestine to the portal vein, while approximately 5% lives the body with the feces daily. Figure based on [109, 138].

Taurine and glycine deconjugation, oxidation and epimerization have several benefits to the microbiome. It has been highlighted that BSH activity can be a way for bacterial species to detoxify BAs, while deconjugation was found to improve the bacterial colonization of GI tract, moreover, BA conjugates serve as substrates for microbial metabolism and provide energy [138, 139]. After conjugated BAs are deconjugated, bacterial 7α/β-dehydroxylation (7α/β-HSDH) of CA and CDCA occurs, causing formation of the secondary BAs deoxycholic acid (DCA) or LCA.

The most important bacterial bile salt biotransformation is 7α-dehydroxylation in the human GI tract, although some intestinal anaerobic bacteria are capable of both 7α- and β-dehydroxylating activities [140]. LCA is a hydrophobic secondary BA that is primarily formed by the intestinal bacteria through 7α-dehydroxylation of CDCA or 7β-dehydroxylation of ursodeoxycholic acid (UDCA). Main LCA producing bacteria are *Bacteroides fragilis, Bacteroides intestinalis, Clostridium scindens, Clostridium sordelli, Clostridium hylemonae and E. coli* [109]. These bacteria belong to the phyla *Firmicutes, Bacteroides and Proteobacteria* (Table 3). Most of deconjugated LCA is lost in feces, therefore, it dominates in human fecal samples.

The BA-inducible (bai) operon is a highly conserved and complex gene organization system, in which baiH codes the enzyme 3-dehydro-4-7β-oxidoreductase, that is responsible for LCA production [109, 141] (Figure 10).

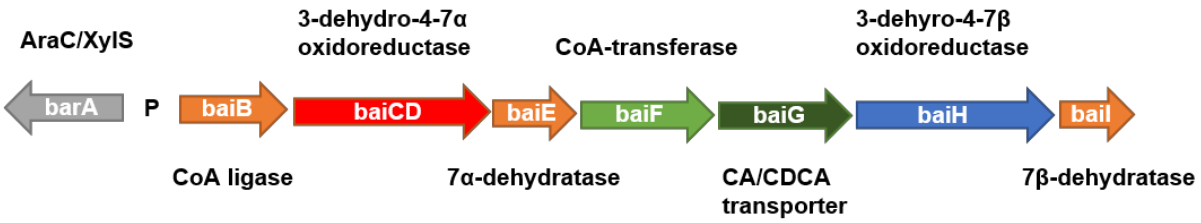

Figure 10. The complex gene organization system of Clostridium hylemonae bai operon. Figure reproduced from [141].

LCA is recognized to exert its effect through farnesoid X receptor (FXR), liver X receptor (LXR), pregnane X receptor (PXR), constitutive androstane receptor (CAR), vitamin D receptor (VDR) or G protein-coupled BA receptor (TGR5) signaling [142-144]. Through these receptors, LCA affects a wider range of biological activities than initially highlighted. They can activate different signaling pathways (cell death or survival), they are involved in energy metabolism, inflammatory response and can protect the intestinal mucosa from bacterial invasion (antimicrobial property) [145].

Secondary BAs, produced by the intestinal flora, appear in peripheral tissues, like liver, kidney, heart, where they exert hormone-like effects. It seems like they are in connection with various kinds of carcinomas, gallstones and chronic inflammatory diseases, based on recent studies [28, 146, 147]. The reference serum concentration of LCA is 30-50 nM, however, in the breast tissue higher LCA concentrations (up to 1 μM) were reported [148].

4. OBJECTIVES

The bacterial metabolites produced by the gut microbiota (among LCA and cadaverine) play significant role in regulating the metabolism and energy homeostasis of the host, while, through numerous internal and external factors (diet, hygiene, immune system etc.) the host can modulate the microbiome. These metabolites – through the circulatory system – can reach and affect tumor cells in distant locations in the human body (Figure 11). In this study we wanted to highlight the strong connection between microbiome, host and BC.

We planned to:

- Characterize the effect of LCA and cadaverine on different type of BC cell lines.
- Identify the molecular mechanisms through which these bacterial metabolites exert cytostatic activity.
- Investigate the changes of tumor hallmarks and the biological effects of metabolites in mouse model. Examine the level of LCA in BC.
- Measure the amount of bacteria/enzymes producing these metabolites in BC patients.

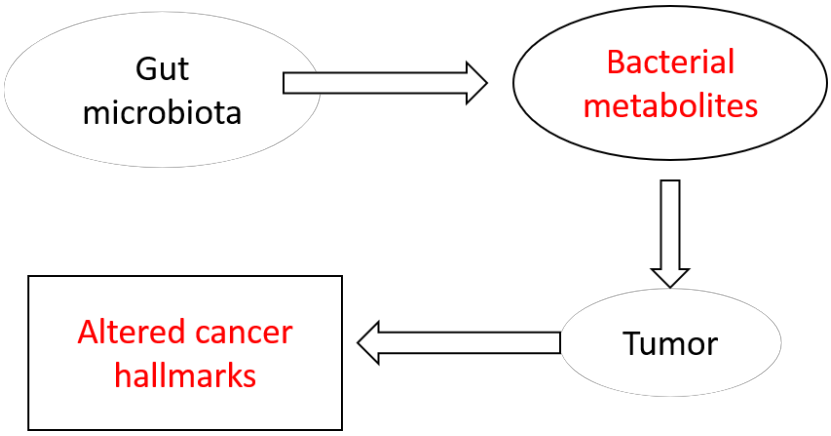

Figure 11. Schematic figure of the hypothesis. The intestinal flora produces bacterial metabolites that can reach tumor cells through the circulatory system, and thus alter different hallmarks of cancer cells.

5. MATHERIALS AND METHODS

Chapter based on [149] and [150].

5.1. Chemicals

Chemicals, among them, cadaverine and LCA were from Sigma-Aldrich (St. Louis, MI, USA) unless otherwise stated.

5.2. Cell culture

4T1 murine BC cells, ZR-75-1 human BC cells were maintained in RPMI-1640 (Sigma-Aldrich, R5886) medium containing 10 % FBS, 1 % penicillin/streptomycin, 2 mM L-glutamine and 1 % pyruvate at 37 °C with 5 % CO_2.

MDA-MB-231 and SK-BR-3 human BC cells were maintained in DMEM (Sigma-Aldrich, 1000 mg/l glucose, D5546) containing 10 % FBS, 1 % penicillin/streptomycin, 2 mM L-glutamine and 10 mM HEPES at 37 °C with 5 % CO_2.

MCF7 human BC cells were maintained in MEM (Sigma-Aldrich, M8042) medium containing 10 % FBS, 1 % penicillin/streptomycin, 2 mM L-glutamine and 10 mM HEPES at 37 °C with 5 % CO_2.

Human primary fibroblast cells were maintained in DMEM (Sigma-Aldrich, 1000 mg/l glucose, D5546) containing 20 % FBS, 1 % penicillin/streptomycin, 2 mM L-glutamine and 10 mM HEPES at 37 °C with 5 % CO_2.

First we have chosen 4T1 (TNBC) cells for our experiments because this cell line is suitable for mouse experiments. MCF-7 and ZR-75-1 cell lines are ER^+PR^+ cell lines, while MDA-MB-231 and SKBR-3 cells are ER^-PR^-. Primary human fibroblasts were used as a reference cell line.

5.3. Sulphorhodamine B assay

Cells were seeded in 96-well plates (4T1- 1500 cells/well; MDA-MB-231 and ZR-75-1- 3000 cells/well; SK-BR-3; MCF7; human fibroblast- 5000 cells/well) and were let to attach overnight. Cells were treated with different concentrations (0.1 μM, 0.3 μM, 0.8 μM) of cadaverine (Sigma Aldrich, C8561) for 48 hours. After 2 days cells were fixed by the addition of 50 % trichloroacetic acid (TCA, final concentration: 10 %) and the plate was incubated for 1 hour at 4 °C. The plate was then washed 5 times with water and was stained with 0.4 % (w/v) Sulphorhodamine B solution in 1 % acetic acid. Unbound dye was removed by washing 5 times

with 1 % acetic acid. Bound stain was solubilized with 10 mM Tris base and the absorbance was measured at 540 nm.

5.4. Colony formation assay

Cells were seeded in 6-well plates (4T1- 750 cells/well; MDA-MB-231, SKBR-3, ZR-75-1; MCF-7- 1000 cells/well) in complete medium and were treated with cadaverine for 4 days. At the end of the treatment plates were washed in PBS twice. Colonies were fixed in 4 % PFA for 30 minutes, dried on air and stained with the solution of May-Grünwald-Giemsa for 30 minutes. Plates were then washed with water and the colonies, containing at least 50 cells, were counted using Image J software.

5.5. Detection of cell death

5.5.1. Propidium iodide (PI) uptake

Cells were seeded in 6-well plate (MDA-MB-231, ZR-75-1 and MCF-7- 100000 cells/well; SKBR-3; human fibroblast- 200000 cells/well). After 2 days of cadaverine treatment cells were stained with 100 µg/ml PI for 30 min at 37 °C. Supernatant was collected in FACS tubes, cells were washed with PBS and collected in the same FACS tubes (trypsin: PBS 1:1) then samples were analyzed by flow cytometry (FACSCalibur, BD Biosciences).

5.5.2. Apoptosis detection using Annexin-V-FITC staining

4T1 cells were seeded in 6-well plates (50000 cells/well) and treated with the indicated cadaverine concentrations for 2 days. Cells were harvested in FACS tubes, washed once with cold PBS and stained with 100 µg/ml PI solution and 5 µl FITC Annexin V (Component A) according to the instructions of the apoptosis kit. The number of apoptotic cells was measured with flow cytometry, and analyzed using Flowing Software 2.5.1.

5.6. Electric cell-substrate impedance sensing (ECIS)

4T1 cells were seeded on type 8W10E arrays (20000 cells/well) and were let to attach overnight. Next day cells were treated with 0.1 µM cadaverine. ECIS (Electric cell-substrate impedance sensing) model Zθ, Applied BioPhysics Inc. (Troy, NY, USA) was used to monitor transcellular electric resistance of control and cadaverine treated cells for 20 hours before the treatment, and total impedance values were measured for additional 48 hours upon cadaverine treatment. Multifrequency measurements were taken at 62.5, 125, 250, 500, 1000, 2000, 4000, 8000, 16000, 32000, 64000 Hz. The reference well was set to a no-cell control with complete medium. ECIS measurements are used to assess cell-to-cell and cell-to-surface connections.

5.7. Scratch assay

4T1 cells were seeded in 6-well plates (150000 cells/well) and were grown overnight. The plates were manually scratched with sterile 200 µl pipette tip, followed by washing the cells with complete growth medium. Then cells were treated with 0.1 µM cadaverine in a 37°C thermostat and were monitored every hour for 36 hours using JuLi Br Live cell movie analyzer (NanoEnTek Inc., Seoul, Korea). Scratch assays were employed to assess cell movement.

5.8. Invasion assay

Matrigel invasion assay was carried out on 4T1 cells using Corning BioCoat Matrigel Invasion Chamber (354480). 4T1 cells were seeded in the chambers (50000 cells/well) in serum free medium, and were grown overnight. Cells were then treated with the indicated concentrations of cadaverine. The lower chamber contained full 4T1 medium with 100 ng/ml SDF1-alpha (Sigma, SRP4388) as chemoattractant. After 48 hours of cadaverine treatment cells were prepared according to the manufacturer's instructions (Figure 12) and stained with Hematoxylin-Eosin (VWR, 340374T and 341972Q) dye. Cells were then pictured with Opera Phenix High Content Screening System and pictures were analyzed using Harmony 4.6 Software. Invasion index was calculated from the percentage of invading cells through matrigel membrane and control membrane, as follows:

$$\%\ Invasion = \frac{Mean\ of\ cells\ invading\ through\ Matrigel\ insert\ membrane}{Mean\ of\ cells\ invading\ through\ Control\ insert\ membrane} * 100$$

$$Invasion\ index = \frac{\%\ Invasion\ Test\ Cell}{\%\ Invasion\ Control\ Cell}$$

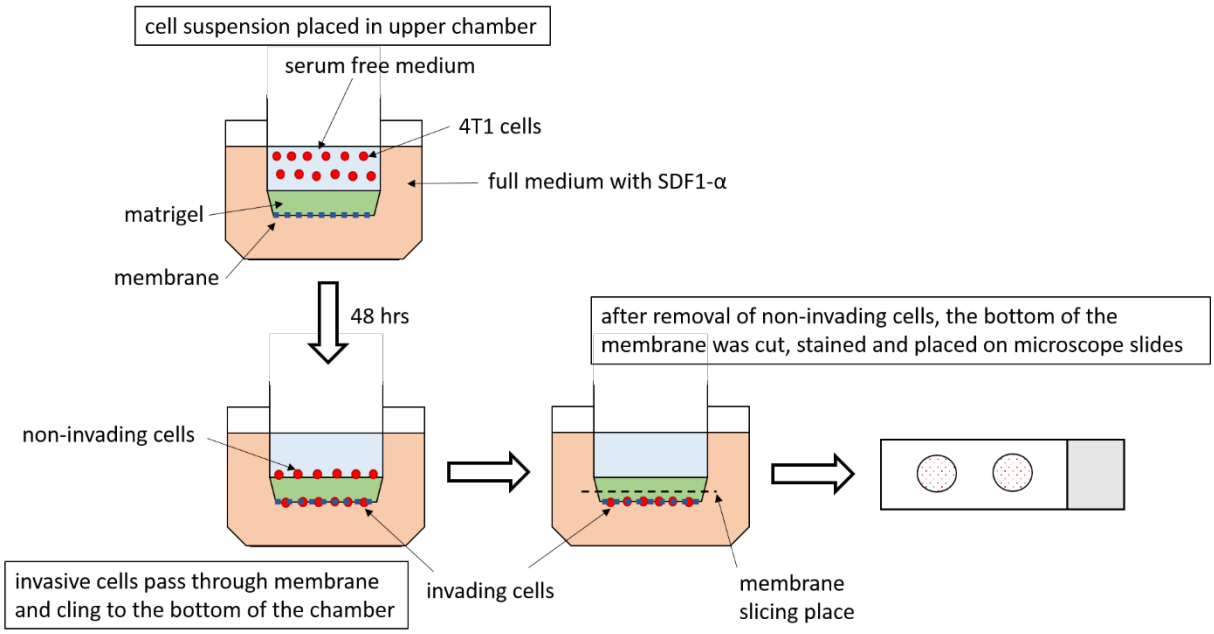

Figure 12. Schematic figure of invasion assay. Cells were seeded in the upper chamber, and treated with cadaverine. After 48 hours, non-invading cells were removed and the membrane was cut off with the invaded cells on the bottom. Cells were then fixed, stained and placed on microscope slides for imaging.

5.9. Immuncytochemistry

4T1 cells were grown on coverslips, and treated with the indicated concentration of cadaverine for 48 hours. Cells were washed with PBS, fixed with 4 % PFA for 15 minutes and permeabilized using 1 % Triton X-100 for 5 minutes. After washing twice with PBS, cells were blocked with 1 % BSA for one hour at room temperature.

5.9.1. Assessment of changes in actin morphology

To investigate the effect of TAARs, 5 μM NF449 (Bio-Techne R&D Systems Kft, 627034-85-9) G-protein inhibitor [151] was also added to cadaverine-treated cells. For direct labelling of the actin cytoskeleton, fixed and blocked cells were incubated with Texas Red-X Phalloidin (1:150; Thermo Fisher Scientific) for an hour, followed by several washing steps with PBS.

5.9.2. Assessment of MMP9 expression levels

For visualizing MMP9 protein in 4T1, MDA-MB-231 and SKBR3 cells, mMMP9 primary antibody (1:1000, Abcam) was applied overnight on cells in a humid chamber at 4 °C. Subsequently, primary antibody was visualized by a goat anti-rabbit secondary antibody (1:500, Thermo Fisher Scientific).

Cell nuclei were visualized with TO-PRO-3 iodide (1:1000, Thermo Fisher Scientific), or DAPI (1:10, Thermo Fisher Scientific) in both experiments. Coverslips were rinsed and mounted in Mowiol/Dabco solution. Confocal images were acquired with Leica SP8 confocal microscope and LAS AF v3.1.3 software. Intensity was calculated using Image J software. Materials used in immunocytochemistry assays are summarized in Table 4.

Table 4. List of antibodies used for Immuncytochemistry

Antibody	Concentration	Vendor
anti MMP9 antibody	1:1000	Abcam (ab38898)
Goat anti-Rabbit IgG (H+L) Cross-Adsorbed Secondary Antibody (Alexa Fluor 488)	1:500	Thermo Fisher Scientific (A11008)
Texas Red™-X Phalloidin	1:250	Thermo Fisher Scientific (T7471)
TO-PRO®-3	1:1000	Thermo Fisher Scientific (T3605)
DAPI	1:10	Thermo Fisher Scientific (R37606)

5.10. Measuring “stem cell-ness”

5.10.1. Seahorse metabolic flux analysis

4T1 cells were seeded in 96-well Seahorse assay plate (1500 cells/well) and treated with vehicle and cadaverine for 48 hours. XF96 oximeter (Seahorse Biosciences, North Billerica, MA, USA) was used to monitor the changes in oxygen consumption rate (OCR) and in extracellular acidification rate (ECAR) after cadaverine treatment. Changes were measured in every 30 minutes to monitor the effect of cadaverine. Data were normalized to protein content.

5.10.2. Aldefluor assay

Aldehyde dehydrogenase (ALDH) activity was determined on cadaverine treated 4T1 and MDA-MB-231 cells using Aldefluor Stem Cell kit (StemCell Technologies, Vancouver, Canada, #01700) [95]. Cells were seeded on 6 well plates (4T1- 50000 cells/well) or on 24 well plates (MDA-MB-231- 50000 cells/well) and treated with different concentration of cadaverine for 2 days. Cells were then collected and prepared according to the manufacturer’s instructions. We used SKBR-3 cell line for positive control based on the manufacturers’ instructions. Changes in the level of ALDH was measured using flow cytometry and the results were analyzed with Flowing Software 2.5.1.

5.11. Determination of lipid peroxidation

Lipid peroxidation was measured by determining the production rate of thiobarbituric acid reactive substrate (TBARS). 4T1 cells were seeded in T75 flasks and allowed to adhere overnight. Cells were exposed to cadaverine for 48 hours, then collected by centrifugation. 8.1 % SDS, 20 % acetic acid, 0.8 % thiobarbituric acid (TBA) and distilled water was added to the pellet and was heated at 96°C for 1 hour in thermoblock. Samples were cooled on ice and centrifuged, the absorbance of the supernatant was measured at 540 nm [152].

5.12. Transfections

MDA-MB-231 cells were seeded on 24-well plate with or without coverslip, in 50000 cells/well density. Next day, cells were treated with vehicle or 0.3 μM cadaverine and were transfected with human TAAR1 siRNA (Thermo Fisher Scientific, s223306) in 10 nM final concentration, human TAAR8 siRNA (Thermo Fisher Scientific, s223302) or human TAAR9 siRNA (Thermo Fisher Scientific, s38008) in 30 nM final concentration, or with control siRNA (Thermo Fisher Scientific, 4390843) in 30 nM final concentration. siRNAs were diluted in OptiMEM (Thermo Fisher Scientific, 31985062). 3 μl RNAiMAX transfection reagent (Thermo Fisher Scientific,13778) was used in each well according to the manufacturer's instructions. Cells were incubated in 37°C with 5% CO_2 for 48 hours. Then MMP9 and TexasRed-X Phalloidin immunocytochemistry were carried out on cells on coverslip, and Western blot analysis was carried out on cells grown in plates without coverslip.

5.13. mRNA isolation and RT-qPCR

Total RNA from cells were prepared using TRIzol reagent (Invitrogen, TR118). 2 μg RNA was reverse transcribed using High Capacity cDNA Reverse Transcription Kit (Applied Biosystems, Foster City, CA, USA, 4368813) according to the manufacturer's instructions. qPCRBIO SyGreen Lo-ROX Supermix (PCR Biosystems Ltd, London, UK, PB20.11-05) was used for the qPCR reactions, the expression level of the genes was detected with Light-Cycler 480 Detection System (Roche Applied Science). Geometric mean of 36B4 and cyclophilin or GAPDH was used for normalization. Primers are listed in Table 5.

Table 5. Primers used in the RT-qPCR reactions

Gene Symbol	Murine forward primer (5'-3')	Murine reverse primer (5'-3')
MMP2	TGGGGGAGATTCTCACTTTG	CATCACTGGGACCAGTGTCT
MMP3	TGGGACTCTACCACTCAGCCAAG	TGCACATTGGTGATGTCTCAGGT
MMP9	CATTCGCGTGGATAAGGAGT	ACCTGGTTCACCTCATGGTC
Krt14	GAAGAGGCCAACACTGAACTGGA	AGGCTCTGCTCCGTCTCAAACTT
Spp1	GATTGGCAGTGATTTGCTTTTGC	TTCTGCTTCTGAGATGGGTCAGG
FgfBp1	CAAGGTCCAAGAAGCTGTCTCCA	AGCTCCAAGATTCCCCACAGAAC
Notch1	CCTTCACCTGTCTGTGTCCACCT	TCACAGTGGTACTGCGTGTTGGT
Tgfb3	GGCGTCTCAAGAAGCAAAAGGAT	CCTTAGGTTCGTGGACCCATTTC
Erbb3	TACTTGCCTCTGGGCTCTCTCCT	CACCTGGACTTGACTCGGTGACT
Er1	GACCATGACCCTTCACACCAAAG	CTCGGGGTAGTTGAACACAGTGG
IgfBp4	CAAGATGAAGATCGTGGGGACAC	CAGTTTGGAATGGGGATGATGAA
36B4	AGATTCGGGATATGCTGTTGG	AAAGCCTGGAAGAAGGAGGTC
Cyclophilin A	TGGAGAGCACCAAGACAGACA	TGCCGGAGTCGACAATGAT
GAPDH	CAAGGTCATCCATGACAACTTTG	GGCCATCCACAGTCTTCTGG

5.14. Fecal protein sample preparation

RIPA buffer (50 mM Tris, 150 mM NaCl, 0.1 % SDS, 1 % Triton X-100, 0.5 % sodium deoxycholate, 1 mM EDTA, 1 mM Na_3VO_4, 1 mM NaF, 1 mM PMSF, protease inhibitor cocktail) was used to lyse cells of fecal samples of *cohort 2*. Samples were sonicated (Qsonica Q125 Sonicator, Newtown, Connecticut) 3 times for 30 seconds with 50% amplitude. After centrifugation, 25 µl 5 X SDS sample buffer (50 % glycerol, 10 % SDS, 310 mM Tris HCl, pH 6.8, 100 mM DTT, 0.01 % bromophenol blue) and 8 µl β-mercaptoethanol were added to every 100 µl supernatant. Samples were heated 10 minutes at 96 °C and kept on ice until loading.

5.15. SDS-PAGE and Western blotting

Protein extracts were separated on 8% SDS polyacrylamide gels and transferred onto nitrocellulose membranes by electroblotting. Then membranes were blocked with 5 % BSA, and incubated with anti-LDC primary antibody (1:100, Abcam), anti-TAAR1 polyclonal antibody (1:1000, Thermo Fisher Scientific), anti-TAAR8 polyclonal antibody (1:1000, Thermo Fisher Scientific) or anti-TAAR9 polyclonal antibody (1:1000, Biorbyt) for overnight at 4 °C. The membranes were washed with 1X TBS-TWEEN and incubated with IgG HRP conjugated secondary antibody (1:2000, Cell Signaling Technology). Bands were visualized by enhanced chemiluminescence reaction (SuperSignal West Pico Solutions, Thermo Fisher Scientific, 34578) using Chemidock Touch system. Densitometry was performed using the Image J software. Primary and secondary antibodies, used in this study, are listed in Table 6.

Table 6. List of antibodies used for Western blot

Antibody	Concentration	Vendor
Anti-LDC, constitutive antibody	1:100	Abcam (ab193351)
anti-rabbit IgG, HRP-linked antibody	1:2000	Cell Signaling Technology (#7074)
TAAR1 polyclonal antibody	1:1000	Thermo Fisher Scientific (PA5-23141)
TAAR8 polyclonal antibody	1:1000	Thermo Fisher Scientific (OSR00118W)
TAAR9 polyclonal antibody	1:1000	Biorbyt LLC (orb165536)

5.15.1. Validating of E. coli LdcC antibody

DH5α *E. coli were* seeded in liquid LB medium. Cells were incubated at 37°C overnight with gentle shaking. *E. coli* cells were then collected with centrifugation and proteins were isolated using RIPA buffer (50 mM Tris, 150 mM NaCl, 0.1 % SDS, 1 % TritonX 100, 0.5 % sodium deoxycholate, 1 mM EDTA, 1 mM Na_3VO_4, 1 mM NaF, 1 mM PMSF, protease inhibitor cocktail). Cell wall and membrane were disrupted using ultrasound sonicator (Branson Ultrasonic Sonifier S-250A, Thermo Fisher Scientific) 3 times for 30 seconds at 50 % amplitude. Samples were analyzed by SDS-PAGE followed by Western blotting (Figure 26A).

5.16. Animal studies

Animal experiments were approved by the Institutional Animal Care and Use Committee at the University of Debrecen and the National Board for Animal Experimentation (1/2015/DEMÁB) and were carried out according to the NIH guidelines (Guide for the care and use of laboratory animals) and applicable national laws. Animal studies are reported in compliance with the ARRIVE guidelines [153, 154].

We used BALB/c female mice (4 months of age, 20-25g). Animals were bred in the “specific pathogen free” zone of the Animal Facility at the University of Debrecen, and kept in the “minimal disease” zone during the experiments. 4 mice were housed in one cage (standard block shape 365 × 207 × 140 mm, surface 530 cm^2; 1284 L Eurostandard Type II. L from Techniplast). Dark/light cycle was 12 h, and temperature was 22 ± 1°C. Mice had ad libitum access to food and water (sterilized tap water). Researchers administering LCA, cadaverine and vehicle solutions were blinded. Treatment was administered every day at the same time. Schematic picture of animal studies shown on Figure 13.

5.16.1. Tumor injection

Tumor was formed in mice by the grafting of 4T1 cells. Cells were suspended ($2x10^6$/mL) in ice cold PBS-matrigel (1:1, Sigma-Aldrich) at 1:1 ratio. Female BALB/c mice

received 50 µL injections to the inguinal fat pads below the lower abdominal nipples on both sides (10^5 cells/injection site) (Figure 13).

5.16.2. LCA treatment

A total of 28 mice was used in this study. Animals received daily oral LCA treatments. LCA stock was prepared in 96% ethanol at 100x concentration (7.5 mM) and stored at -20°C. LCA stock was diluted each day to a working concentration of 75 µM in sterile PBS immediately before the treatment. Ethanol vehicle (1% in PBS) was prepared and diluted similarly. Animals received a daily oral dose of 200 µL/30 g bodyweight from the LCA solution or the vehicle. Treatment was administered every day during the morning hours between 8 am and 10 am. Mice were sacrificed on day 18 post grafting (Figure 13).

5.16.3. Cadaverine treatment

32 female mice were used in the cadaverine study, 16 randomly selected control and 16 cadaverine fed mice. The study was performed in two runs at two different occasions. Data from the runs were pooled. Animals received daily oral cadaverine treatment. Cadaverine stock was prepared in sterilized tap water at 100x concentration (15 mM) and the stock was stored at -20°C. Cadaverine stock was diluted each day to a working concentration of 150 µM in sterile tap water before the treatment. Animals received a daily oral dose of 100 µl/30 g bodyweight from cadaverine solution or vehicle (sterilized tap water). Treatment was carried out between 9 am and 11 am. Mice were sacrificed on day 16 post grafting (Figure 13).

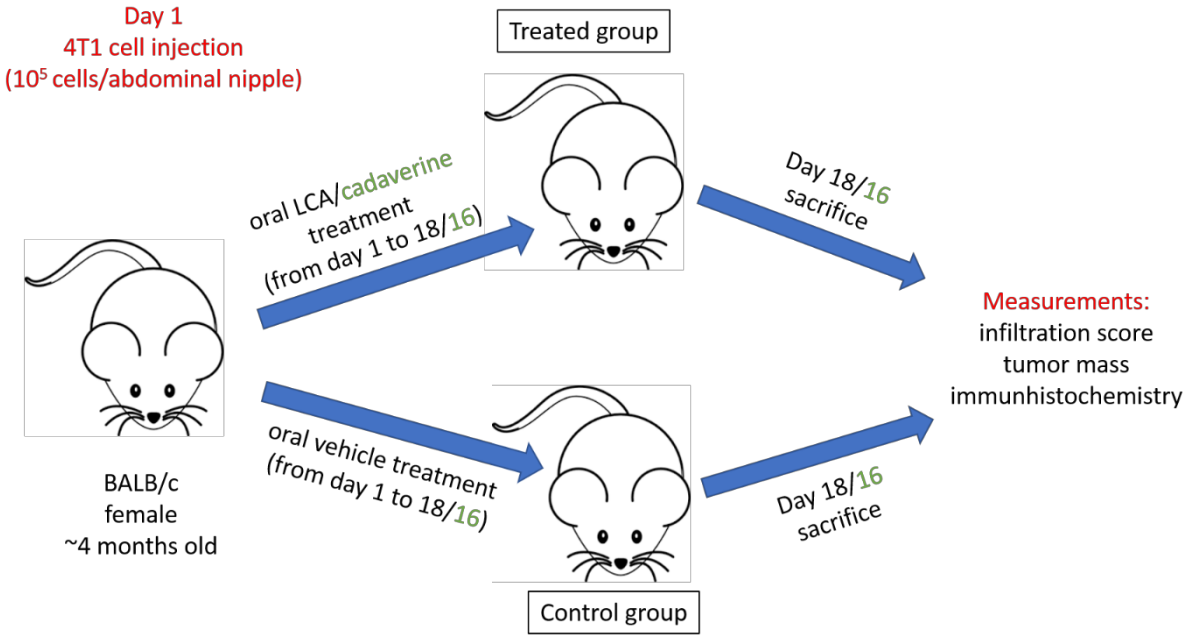

Figure 13. Main steps of animal studies. On first day cells were injected into the inguinal fat pads below the lower abdominal nipples, and mice got their first oral LCA (LCA study) or cadaverine (cadaverine study), and vehicle treatment. From day 2 to 18/16 mice in treated group got LCA or cadaverine daily, while in control group mice got sterilized tap water p.o. q.d. Then mice were sacrificed and measurements and calculations were carried out on samples (black number 18 indicate the endpoint of LCA while green number 16 indicate the end point of cadaverine treatment).

5.16.4. Infiltration score, tumor mass and TIL calculation

During autopsy primary tumors were scored based on their infiltration rate into surrounding tissues based on macroscopic appearance of the tumor as follows:

- "*Low infiltration*" class means that primer tumor remained in the mammary fat pads without any attachment to muscle tissues.
- In case the tumor mass attached to the muscle tissue but did not penetrate to the abdominal wall, it classified as a "*medium infiltration*" tumor.
- If the tumor grew into the muscle tissue and totally penetrated the abdominal wall, it was scored as a "*high infiltration*" tumor.

Both *primary and metastatic tumor masses* were removed from mice and were measured. (Figure 13).

Tumor infiltrating lymphocyte (TIL) content was counted in sections of HE-stained, formalin-fixed, paraffin embedded tumor tissues as the number of TILs per 100 tumor cells.

Nuclear pleomorphism was scored according to the following instructions:

- 1 point: small nucleus, uniform shape, normal chromatin
- 2 points: medium sized nucleus with different shape and size, visible nucleolus
- 3 points: big, pleiomorf and vesicular nucelus, more visible nucleolus

Mitosis was calculated based on the following scores:

- 1 point: less than 6 mitotic cells
- 2 points: 7-13 mitotic cells
- 3 points: more than 14 mitotic cells

5.17. Human studies

5.17.1. Fecal DNA samples from NCI (Cohort 1.)

Human fecal samples were collected from healthy women and BC patients between age 50-74 by collaborators at the National Cancer Institute (NCI), Kaiser Permanente Colorado (KPCO), the Institute for Genome Sciences at the University of Maryland School of Medicine, and RTI International (see details in Table 7, *Cohort 1*).

Table 7. Patient cohorts

Cohort 1.	healthy	patient	of which			
			stage 0	stage 1	stage 2	stage 3
number	48	46	11	23	10	2
age (years)	50 - 74					

This cohort was published in **[11]**. Staging of the patients was performed according to **[155]**.

Cohort 3.	healthy	patient	of which				
			stage 0	stage 1	stage 2	stage 3	stage 4
number	56	56	-	16	25	10	5
age (years)	59.1±7.3	60.7±8	-	61.8±5.5	61.5±8.6	60.6±8.2	53.8±10

Patients were recruited at the Medical Center of the University of Debrecen. Patients with other cancers, inflammatory diseases, diseases affecting the GI tract and the liver or receiving antibiotics were excluded from the study.

The study protocol and all study materials were approved by the Institutional Review Boards at KPCO, NCI, and RTI International (IRB number 11CN235). All methods were performed in accordance with the relevant guidelines and regulations. 10 ng of DNA was used for qPCR reactions.

The abundance of the bacterial DNA coding LDC was determined in these fecal NCI samples. Primers are listed in Table 8. The amplicons were subsequently sequenced using the same primers.

Table 8. Primers for the determination of the abundance of CadA and LdcC using qPCR

Organism and gene name	Forward primer (5'-3')	Reverse primer (5'-3')
E. coli LdcC	CGGCCCTTATAACCTGCTGTTTC	CCTTGTGCCAGATCCTGAATACG
E. coli CadA	GTCTGTGCGGCGTTATTTTTGAC	CACCCAGCGCATATTCAAAGAAG
Enterobacter cloacae LdcC	ATATGATCTGAACCTGCGGGTGA	AGGTTCTCCAGCTCAACGGTTTC
Hafnia alvei LdcC	GGTGAACTGGGTTCTCTGCTTGA	AGCGGGTGCTGAGTACATACCAA

baiH abundance was assessed by amplifying baiH ORF from NCI fecal DNA samples. Primers are listed in Table 9. The amplicons were subsequently sequenced using the same primers as listed in Table 9.

Table 9. Primers used for the determination of baiH abundance using qPCR

Organism	Forward primer (5'-3')	Reverse primer (5'-3')
Bacteroides fragilis	CGGGCAGATCGATGTACTGGT	AGTACCATTCGAATCGGCCGT
Bacteroides thetaiotaomicron	CCCATCATGACCACTCACGGA	AAGAACCAGTCCCGGTGCTAC
Escherichia coli	TATGGCGTTTGACCTGGGTGA	CAAAGGAACAGCGCTGCGTTA
Clostridium scindens	GATGAGCTGGAGACCACCCTG	GTAGCCGTAGTCTCGCTGTCA
Clostridium sordelli	TGCCATACTCCTGAAATCGAGT	TCCCATCTTTCTTCAAATGTACGCT
Staphylococcus haemolyticus	CGTTTCTGTCGTGATAATGCCCT	GGCGTGTTTGAATGGTCGCTT
Pseudomonas putida	GGGCGATGCACTGGACTTCTA	ATGTGGGTGTTGTCCTCGAGG

5.17.2. Fecal samples from BC patients (Cohort 2.)

On the course of the study, we began to build up a fecal biobank. The collection and biobanking of feces were authorized by the Hungarian National Authority (ETT). Patients and healthy volunteers meeting the following criteria were excluded from the study according to the corresponding national guideline for fecal transplantation [156]: 1) who have previous history of BC or had been operated due to neoplasia, 2) who have a disease of unknown origin, 3) who have chronic contagious disease, 4) who had contagious diarrhea 6 months prior to enrollment, 5) who had been taken antibiotics in the 6 months prior to enrollment, 6) who had chemotherapy, biological therapy or immunosuppressive therapy 6 months prior to enrollment, 7) who used intravenous drugs 12 months prior to enrollment, 8) who had piercing, tattooing, acupuncture or other endangering behavior or action 12 months prior to enrollment, 9) who had exposition to an allergen to which the enrolled individual had been sensitized to, 10) who underwent colonoscopy 12 months prior to enrollment. First morning feces were sampled; samples were frozen and deposited in the biobank two hours after defecation. Samples were stored at -70 ^{o}C until subsequent use.

5.17.3. Human serum samples (Cohort 3.)

The study in which human female serum samples were collected from healthy subjects and BC patients (see details in Table 7, *Cohort 3*) was developed by collaborators at the University of Debrecen, Department of Laboratory Medicine (Hungary). The study protocol and all study materials were approved by the Institutional and Hungarian Review Boards (3140-2010). For the determination of serum BA profile, first a reversed-phase high-performance liquid chromatography was carried out on samples. Bile acids, separated on the column, were mixed with NAD-containing mixture and migrated through a 3α-hydroxysteroid dehydrogenase (3α-HSD) immobilized enzymic column. 3α-HSD column generates NADH (and 3-keto bile acids) consuming NAD. Finally, NADH (generated by the ensymic reaction) was measured using fluorescent detection at 460 nm as described in [157, 158].

5.18. Database screening

The kmplot.com database was used to study the connection between gene expression levels and BC survival. The association of known mutations with BC was retrieved from www.intogen.org/. Gene expression profiles were retrieved from the Gene expression omnibus (www.ncbi.nlm.nih.gov/geoprofiles/). The sequence of the CadA, LdcC and baiH ORF or the bai operon were retrieved from the KEGG (www.genome.jp/kegg/) and the PATRIC (www.patricbrc.org/) databases. We assessed the NCBI GEO Profiles with the term “LDC and breast cancer” and the GENT database with the keywords ”TAAR1”, ”TAAR8” and ”TAAR9”.

5.19. Statistical analysis

We used two tailed Student’s *t*-test for the comparison of two groups unless stated otherwise. Fold data for human sample analysis were $\log_2$ transformed to achieve normal distribution. For multiple comparisons one-way analysis of variance test (ANOVA) was used followed by Tukey’s honestly significance (HSD) post-hoc test. Data is presented as average ± SEM unless stated otherwise. Texas Red-X Phalloidin-labelled fluorescent pictures were analyzed using Cell Profiler 2.0 followed by Advanced Cell Classifier 3.0. FACS results were analyzed using Flowing Software 2.0. Statistical analysis was done using Origin 8.6 or GraphPad Prism 6 software, unless stated otherwise (Table 14).
On the figures *, ** and *** indicate statistically significant difference between control and treated groups at $p<0.05$, $p<0.01$ or $p<0.001$, respectively.

6. RESULTS

Chapter based on [149] and [150].

6.1. Cadaverine reduces BC aggressiveness

6.1.1. Cadaverine treatment reduces metastasis formation in 4T1-grafted mice

As first step, we investigated the effects of cadaverine supplementation to mice homotopically grafted with 4T1 BC cells (200000 cells/mouse). Cadaverine supplementation (500 nmol/ kg p.o. q.d.) did not alter the number of primary tumors that grew in the grafted mice (Figure 14A), but there was a trend towards tumor with lower mass (Figure 14B). In line with that, the number of metastases decreased (Figure 14C) and, as with the primary tumors, there was a trend for smaller tumors in the cadaverine-treated mice (Figure 14D).

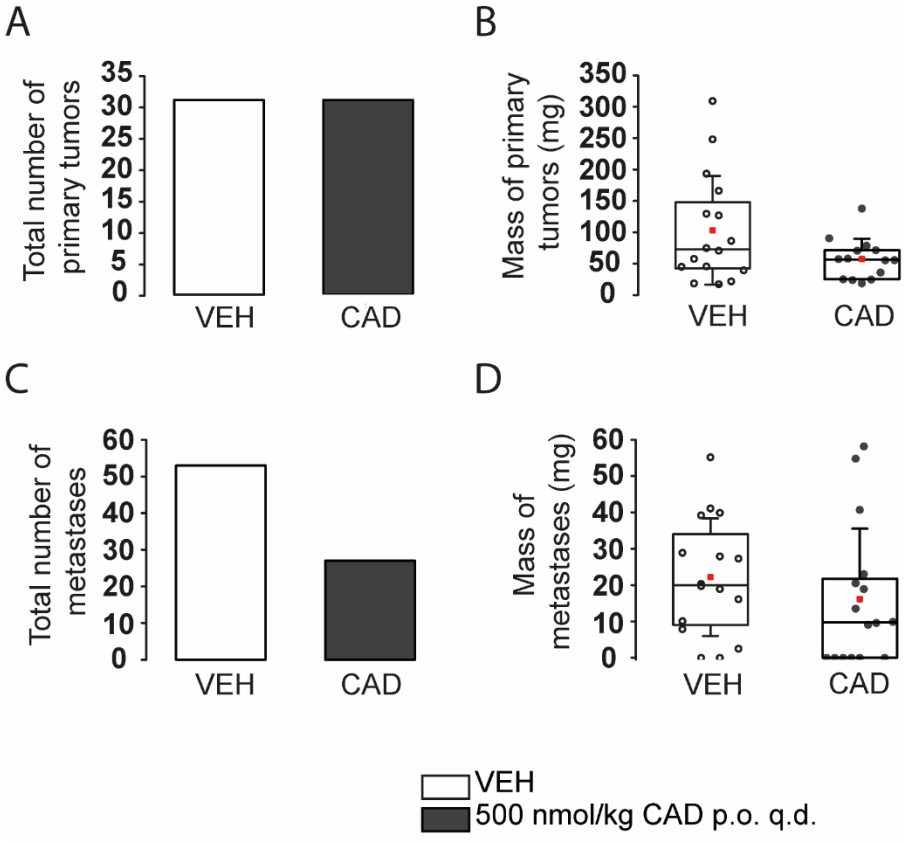

Figure 14. Cadaverine treatment decreases tumor mass in BALB/c mice. Female BALB/c mice were grafted with 4T1 cells as described, and were treated with cadaverine (CAD group) or vehicle (VEH group) (n=16/16) for 16 days before sacrifice. In VEH and CAD group **(A)** the number and **(B)** mass of primary tumors were counted, and the **(C)** number and **(D)** mass of metastases were measured upon autopsy.

Importantly, cadaverine treatment decreased the invasivity of the primary tumors (Figure 15A). Histological examination of the primary tumors revealed that cadaverine treatment

decreased the rate of mitosis (Figure 15C-D), and the heterogeneity of nuclear morphology (Figure 15B).

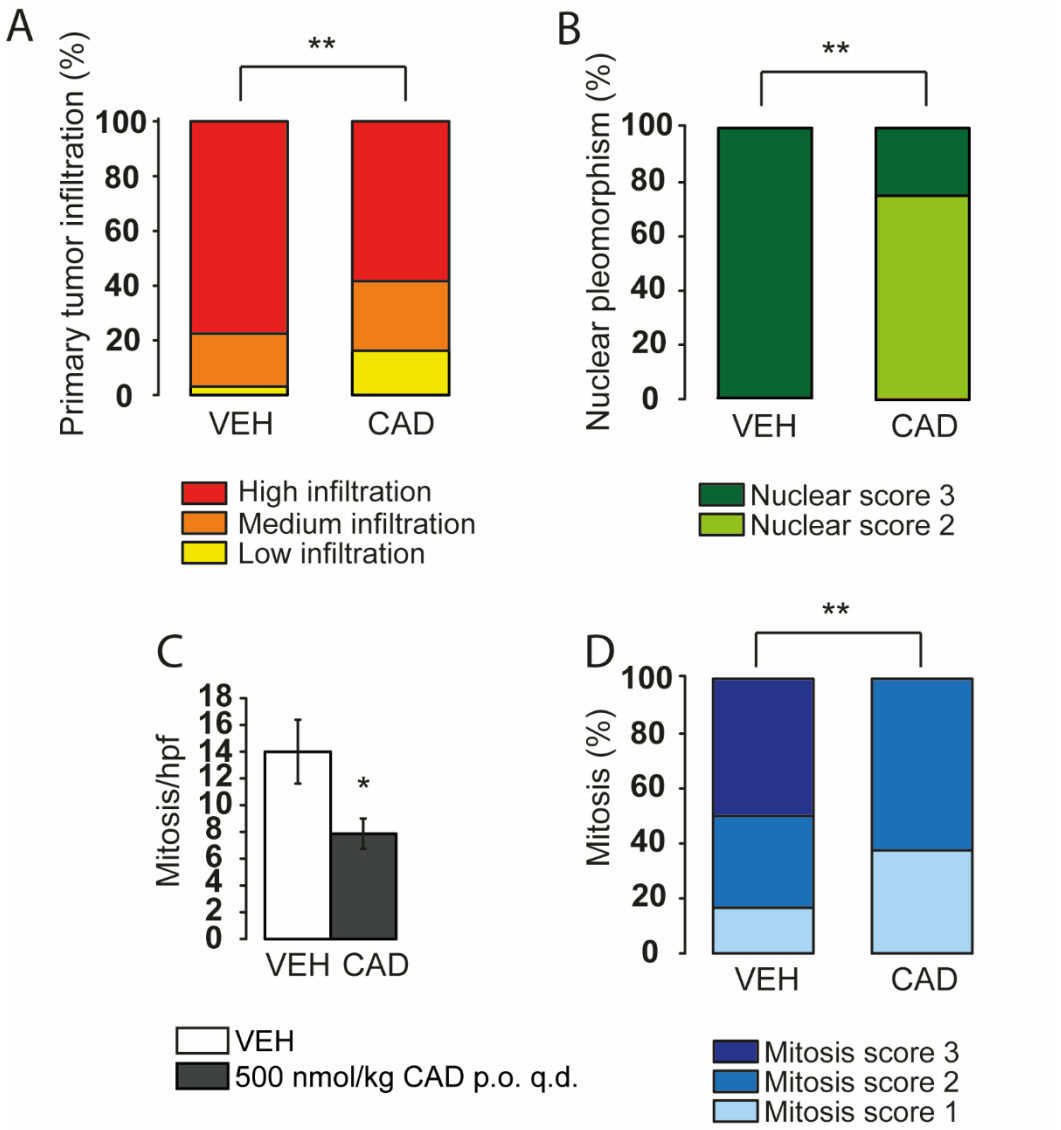

Figure 15. Cadaverine treatment reduces breast cancer aggressiveness in vivo. Female BALB/c mice were grafted with 4T1 cells as described and were treated with (CAD group) or vehicle (VEH group) (n=16/16) for 16 days before sacrifice. 6 samples from CTL group and 8 samples from cadaverine group underwent histological analysis. **(A)** Upon autopsy, the infiltration rate of the primary tumor was scored. **(B-D)** Primary tumors were formalin-fixed and were embedded into paraffin, then sections were hematoxylin-eosin stained and were scored for **(B)** nuclear pleomorphism, **(C)** mitosis/high-power field and **(D)** mitosis.

6.1.2. Cadaverine administration does not impair BC proliferation

We investigated whether cadaverine administration could influence the proliferation of cultured BC cell lines. We used five different established BC cell lines of which four were of human (MD-MBA-231, SKBR3, ZR-75-1 and MCF7), while one was of murine origin (4T1). The cadaverine concentration that we used corresponded to the reference concentration of

cadaverine in human serum (0.1-0.8 μM)[118, 119]. Cadaverine slowed the proliferation of 4T1, MDA-MB-231 and SKBR-3 cells as measured in SRB assay (Figure 16A) or in colony forming assays (Figure 16B), although the changes were not statistically significant. Importantly, the same concentrations of cadaverine did not hinder the proliferation of non-transformed primary human skin fibroblasts (Figure 16A). We assessed whether slower proliferation could be due to the toxicity of cadaverine to cells. The proportion of the PI positive cells did not increase upon cadaverine treatment (Figure 16D), nor did the apoptotic fraction in 4T1 cells (Figure 16C).

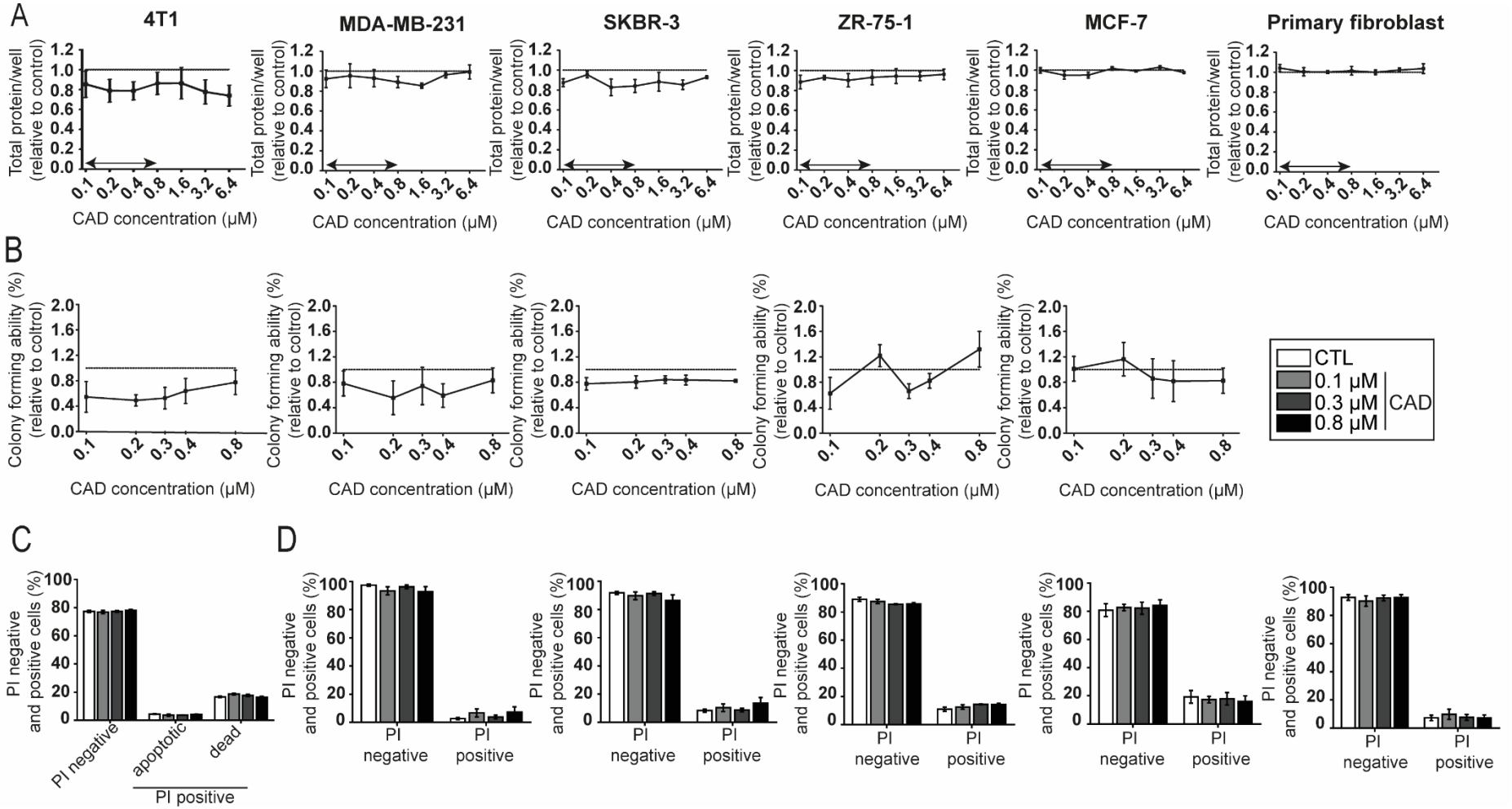

Figure 16. Cadaverine administration slightly impair BC proliferation. **(A)** 4T1 (n=6 in octuplicates), MDA-MB-231 (n=3 in octuplicates), SKBR-3 (n=3 in octuplicates), ZR-75-1 (n=3 in octuplicates) and MCF-7 (n=3 in octuplicates) BC cells and primary fibroblasts cells were treated with cadaverine in the concentrations indicated for 48 hours then total protein concentrations were determined in SRB assay. Values are expressed as fold change, where 1 means protein content in the control cells (indicated by a dotted line). **(B)** 4T1, MDA-MB-231, SKBR-3, ZR-75-1 and MCF-7 (n=3 for each in one replicate) cells were treated with cadaverine in the concentrations indicated for 4 days. Colonies were then stained according to May-Grünwald-Giemsa

and counted using Image J software (n=3). **(C)** 4T1 cells (n=3 in triplicates) were treated with cadaverine in the concentrations indicated for 48 hours. Cells were stained with Annexin-FITC-PI Apoptosis Kit and analyzed by flow cytometry (n=4). **(D)** 4T1 (n=3 in triplicates), MDA-MB-231 (n=4 in triplicates), SKBR-3 (n=4 in triplicates), ZR-75-1 (n=3 in triplicates), MCF-7 (n=3 in triplicates) and primary fibroblasts cells were treated with cadaverine in the concentrations indicated for 48 hours. Dead cells were stained with PI and analyzed by flow cytometry.

6.2. Cadaverine revert EMT and suppress invasion ability

We assessed whether cadaverine treatment can revert mesenchymal-like cancer cells to epithelial-like cells. First, we performed a measurement in the ECIS system in which 0.1 μM cadaverine increased resistance, suggesting better adherence of cells (Figure 17).

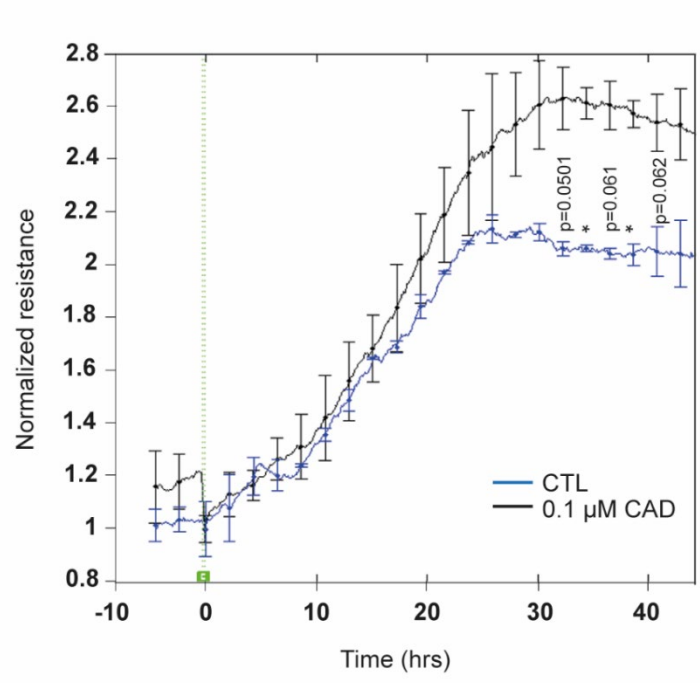

Figure 17. ECIS measurement of the changes in total cell impedance. In control and cadaverine-treated 4T1 cells total cellular impedance was measured by ECIS (n=2 in duplicate). Increased impedance suggests stronger cell-cell and cell-surface connections.

To verify these findings, we stained cells with Phalloidin-Texas Red to visualize the arrangement of the actin cytoskeleton. Cadaverine treatment changed the fibroblast-like morphology of the 4T1 cells to a rather cobblestone-like morphology (Figure 18A) that is characteristic for epithelial cells. Treatment of MDA-MB-231 cell line with cadaverine led to similar morphological changes (Figure 18B).

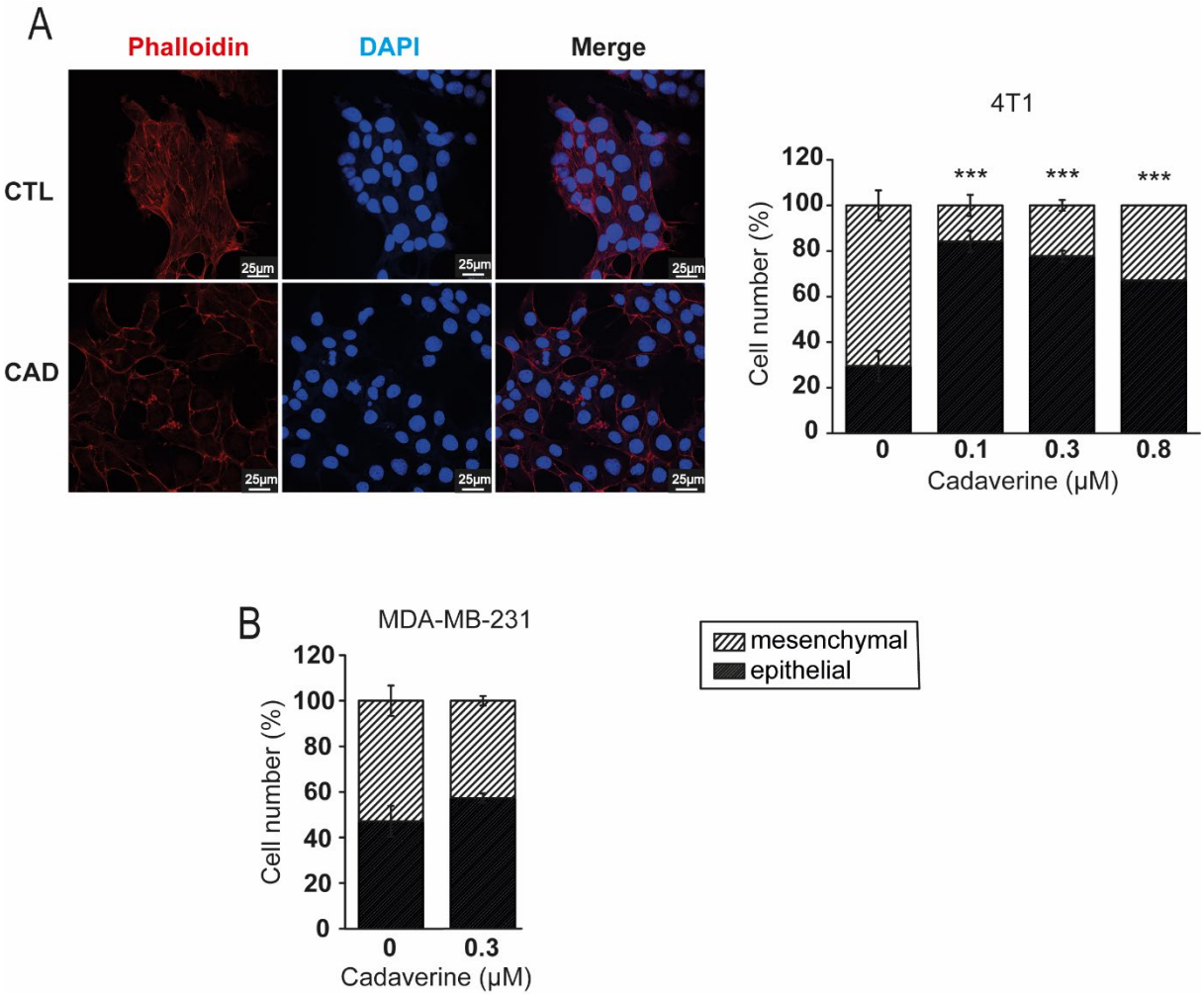

Figure 18. Changes in actin morphology. Morphology of the actin cytoskeleton was assessed after Texas Red-X Phalloidin+To-Pro-3 staining of **(A)** 4T1 cells (n=2 in triplicates) (representative picture of 4T1 control and 0.1 µM cadaverine-treated cells). Ratio (%) of epithelial and mesenchymal cells was shown on bar charts, and **(B)** MDA-MB-231 (n=1 in triplicates).

To gain insight into the molecular mechanism through which MET takes place we performed an RT-qPCR screen on EMT genes. The assay revealed differential expression of 11 genes of which most were suppressed after cadaverine treatment. MMP2, MMP3 and MMP9 support movement; Tgfb3, FgFbp1, Erbb3 and Er1 support proliferation; while Krt14, Notch1, CDH1, IgFbp4 and Spp1 support cell adhesion (Table 10) (Figure 19A-C).

Table 10. List of EMT genes differentially regulated upon cadaverine treatment.

Abbreviation	Gene name	Category
MMP2	Matrix Metalloproteinase 2	ECM and cell adhesion
MMP3	Matrix Metalloproteinase 3	
MMP9	Matrix Metalloproteinase 9	
Krt14	Keratin 14	
CDH1	E-cadherin	
Spp1	Secreted Phosphoprotein 1	
FgfBp1	Fibroblast Growth Factor Binding Protein 1	Cell growth and proliferation
Notch1	Notch 1	
Tgfb3	Transforming Growth Factor Beta 3	
Erbb3	Human Epidermal Growth Factor Receptor 3	
Esr1	Estrogen Receptor 1	
IgfBp4	Insulin Like Growth Factor Binding Protein 4	

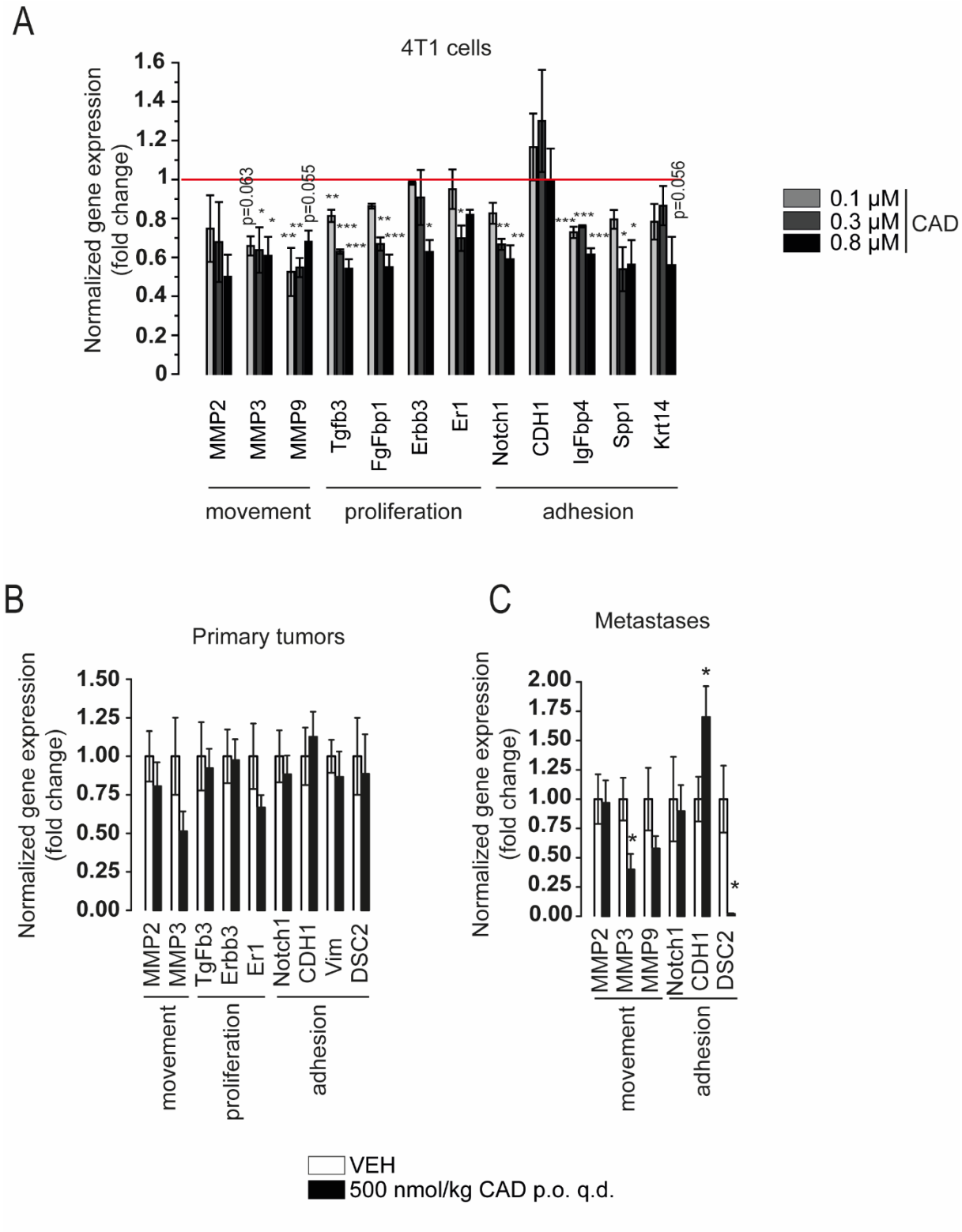

Figure 19. Cadaverine treatment reverses EMT of BC cells. **(A-C)** Expression of a set of genes involved in EMT were assessed by RT-qPCR in **(A)** 4T1 cells (n=3), **(B)** primary tumors (n=16/16) and in **(C)** metastases (n=16/16). All data is expressed as fold change. The red line that equals to 1 (no change) indicate the average of the control samples.

In line with these observations, cadaverine-treated cells were slower in migrating to open areas in scratch assays (Figure 20A) and also performed worse in Boyden-chamber transmigration tests (Figure 20B).

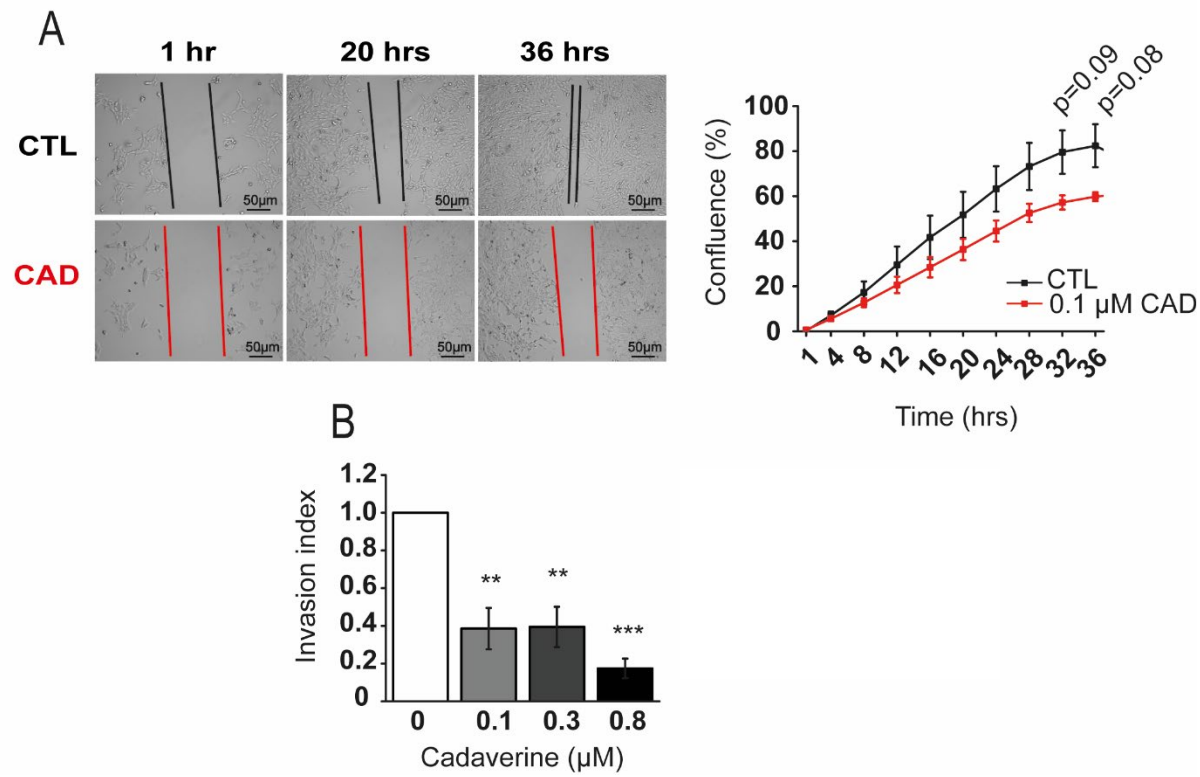

Figure 20. Cadaverine treatment reduce movement and invasion ability of 4T1 cells. **(A)** After scratching a 4T1 cell layer, cells were treated with 0.1 µM cadaverine for 36 hours. Subsequent closure of the wound was assessed by the JULI-Br live cell analyzer system (n=2). **(B)** 4T1 cells were treated with the indicated concentrations of cadaverine for 48 hours and subsequently invasion capacity of the cells was measured using the Corning Matrigel invasion chamber. Cells were counted using the Opera HCS system and invasion index was calculated.

These data were further supported by the observation that MMP9 expression was suppressed by cadaverine treatment in 4T1 cells (Figure 21A), as well as in MDA-MB-231 (Figure 21B) and SKBR-3 BC cell lines (Figure 21C).

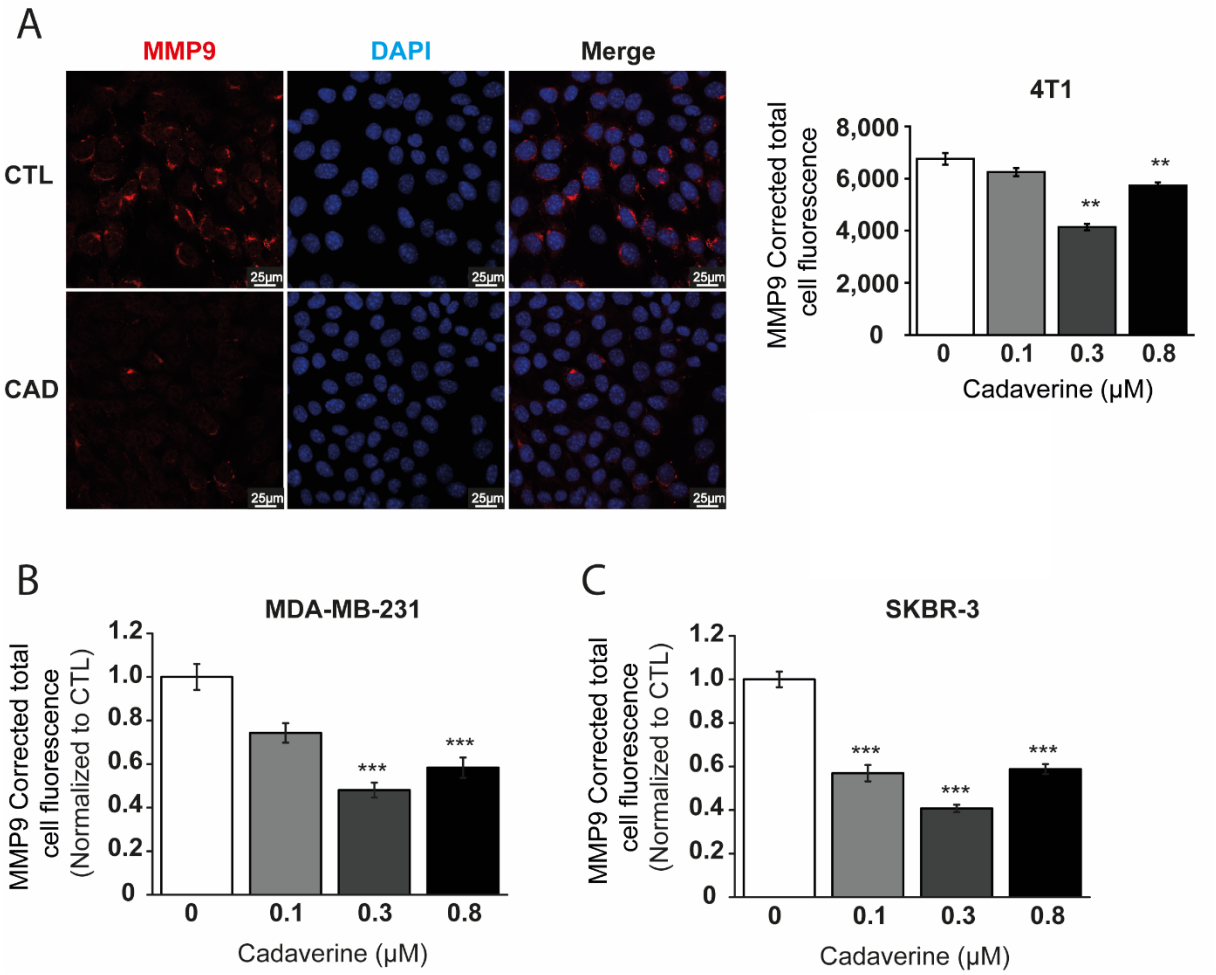

Figure 21. Cadaverine treatment attenuate movement of cells. **(A-C)** Cells were treated with vehicle and cadaverine for 48 hours, then cells were stained for MMP9 and nucleus (DAPI) and sections were analyzed by confocal microscopy using a Leica SP8 confocal system. MMP9 content was calculated from the total cellular fluorescence of **(A)** 4T1 cells measured by the Image J software, **(B)** of MDA-MB-231 cells (n=2, triplicates) measured by Cell Profiler 2.0 software, and **(E)** of SKBR-3 cells (n=2, triplicates) measured by Cell Profiler 2.0 software.

We assessed metabolic changes evoked by cadaverine administration using the Seahorse metabolic flux analyzer. Cadaverine treatment reduced glycolytic flux (Figure 22A) that is a characteristic of BC stromal cells [66]. Therefore, we assessed the “stem-ness” of 4T1 cells using the aldefluor assay and found a mild reduction in cancer cell “stem-ness” (Figure 22B). We found similar reductions in cancer cell “stem-ness” in MDA-MB-231 cells upon cadaverine treatment (Figure 22C). We did not detect changes in lipid oxidation (Figure 22D).

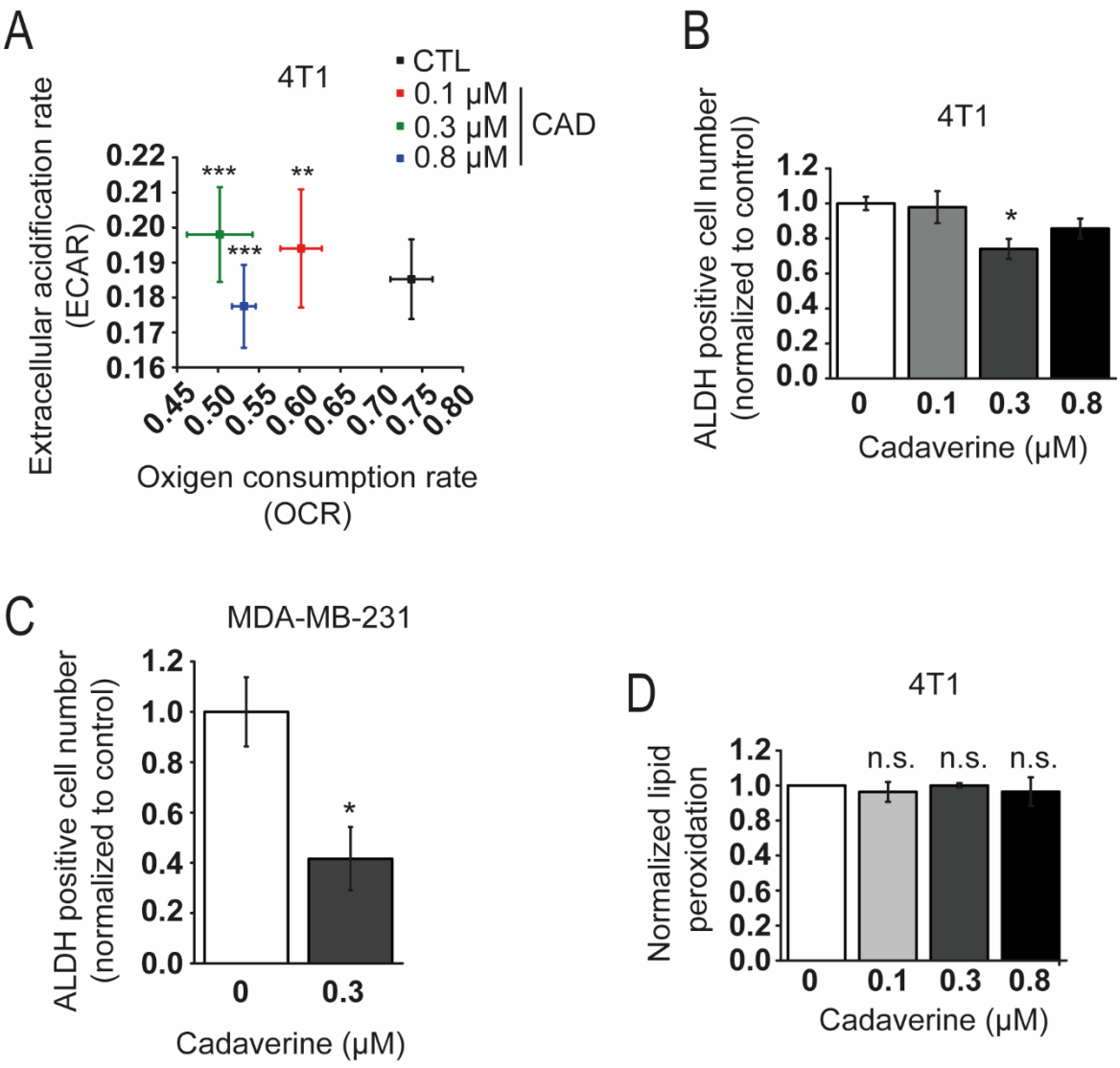

Figure 22. Cadaverine treatment alter mitochondrial oxidation, "stem-ness" but does not influence lipid peroxidation. **(A)** 4T1 cells were treated with vehicle or cadaverine for 48 hours (n=3 in 24 replicates), then cells were subjected to a Seahorse XF96 analysis. OCR and ECAR were measured and plotted. **(B)** 4T1 cells and **(C)** MDA-MB-231 cells (n=2, duplicates) were treated with vehicle and cadaverine for 48 hours (n=3 in triplicates), then cells were subjected to an Aldefluor assay. **(D)** Lipid peroxidation was measured by determining the production rate of thiobarbituric acid reactive substrate (TBARS). n.s. – not significant

6.2.1. Cadaverine exert its beneficial effects through TAARs

The trace amino acid receptor family serve as receptors for cadaverine [159]. Although, most studies on TAAR focused on olfaction [159], a study linked TAAR1 to BC [136]. Indeed, higher expression of TAAR1, TAAR2, TAAR5, TAAR8 (in ER- cases) and TAAR9 provided better survival in BC (Figure 23; Table 11).

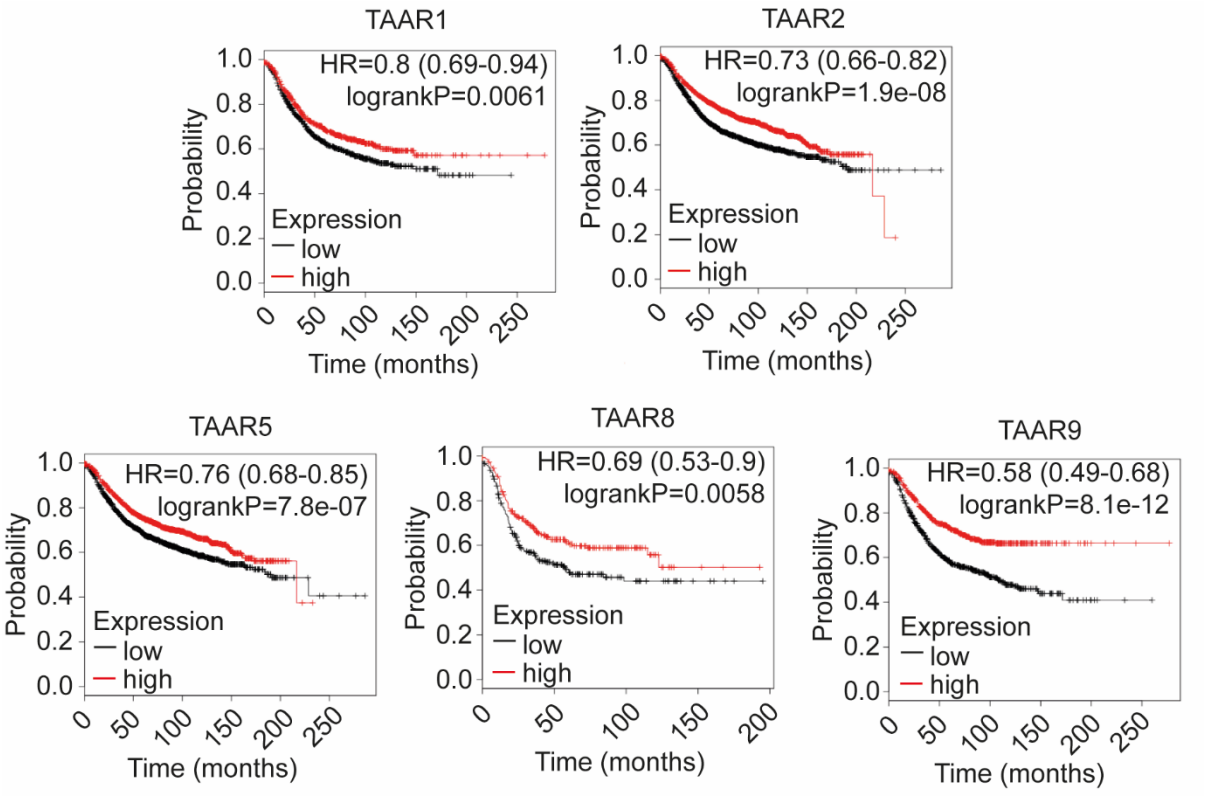

Figure 23. Kaplan-Meier plots show the connection between TAARs and BC survival. High expression of these receptors correlates with better BC survival. Significance data refers to all BC cases, except on TAAR8 plot, where ER$^-$ results are pictured. Kaplan-Meier plots, HR (with 95% confidency intervalls) and P values were exported directly from www.kmplot.com databese.

Table 11. Connection between TAARs and BC Patient survival. First column shows different breast cancer groups. Values were exported from www.kmplot.com database. Hazard Ratio (HR) indicates the probability of death in high TAAR expression group, while P-values sign the difference between high and low expression groups.

TAAR1 (1553930_at)	**HR (Hazard Ratio)**	**P-value (Log Rank Test)**
All BCs, N=1764	0.8	**6.1×10^{-3}**
ER(-), N=516	0.77	0.054
ER(+), N=1248	0.83	0.052
Basal subtype, N=360	0.66	**0.011**
Luminal B, N=407	0.67	**0.01**
TAAR2 (221394_at)	**HR (Hazard Ratio)**	**P-value (Log Rank Test)**
All BCs, N=3951	0.73	**1.90×10^{-8}**
ER(-), N=869	0.65	**6.20×10^{-5}**
ER(+), N=2061	1.07	0.4
Basal subtype, N=618	0.66	**1×10^{-3}**
Luminal B, N=1149	0.66	**3.10×10^{-5}**
TAAR5 (221459_at)	**HR (Hazard Ratio)**	**P-value (Log Rank Test)**
All BCs, N=3951	0.76	**7.80×10^{-7}**
ER(-), N=869	0.75	**8.3×10^{-3}**
ER(+), N=3082	0.8	**6.00×10^{-4}**
Basal subtype, N=618	0.73	**0.016**
Luminal B, N=1149	0.62	**1.00×10^{-6}**
TAAR8 (1553552_at)	**HR (Hazard Ratio)**	**P-value (Log Rank Test)**
All BCs, N=1764	0.94	0.42
ER(-), N=516	0.69	**5.8×10^{-3}**
ER(+), N=1248	1.1	0.31
Basal subtype, N=360	0.64	**7.8×10^{-3}**
Luminal B, N=407	0.97	0.85
TAAR9 (1553066_at)	**HR (Hazard Ratio)**	**P-value (Log Rank Test)**
All BCs, N=1764	0.58	**8.10×10^{-12}**
ER(-), N=516	0.55	**1.40×10^{-5}**
ER(+), N=1248	0.6	**2.30×10^{-7}**
Basal subtype, N=360	0.5	**4.80×10^{-5}**
Luminal B, N=407	0.69	**0.017**

First, as TAAR receptors are G protein-dependent receptors [159], we assessed their involvement by treating 4T1 cells with NF449, a Gsα-subunit-selective G-protein antagonist, a treatment that abolished the anti-EMT effect of cadaverine (Figure 24A). Next, we silenced TAAR1, TAAR8 and TAAR9 in MDA-MB-231 cells (Figure 24B). The silencing of TAAR1, TAAR8 and TAAR9 prevented the cadaverine-elicited mesenchymal-to-epithelial transition

and the silencing of TAAR8 and TAAR9 prevented the cadaverine-induced decrease in MMP9 expression (Figure 24C-D).

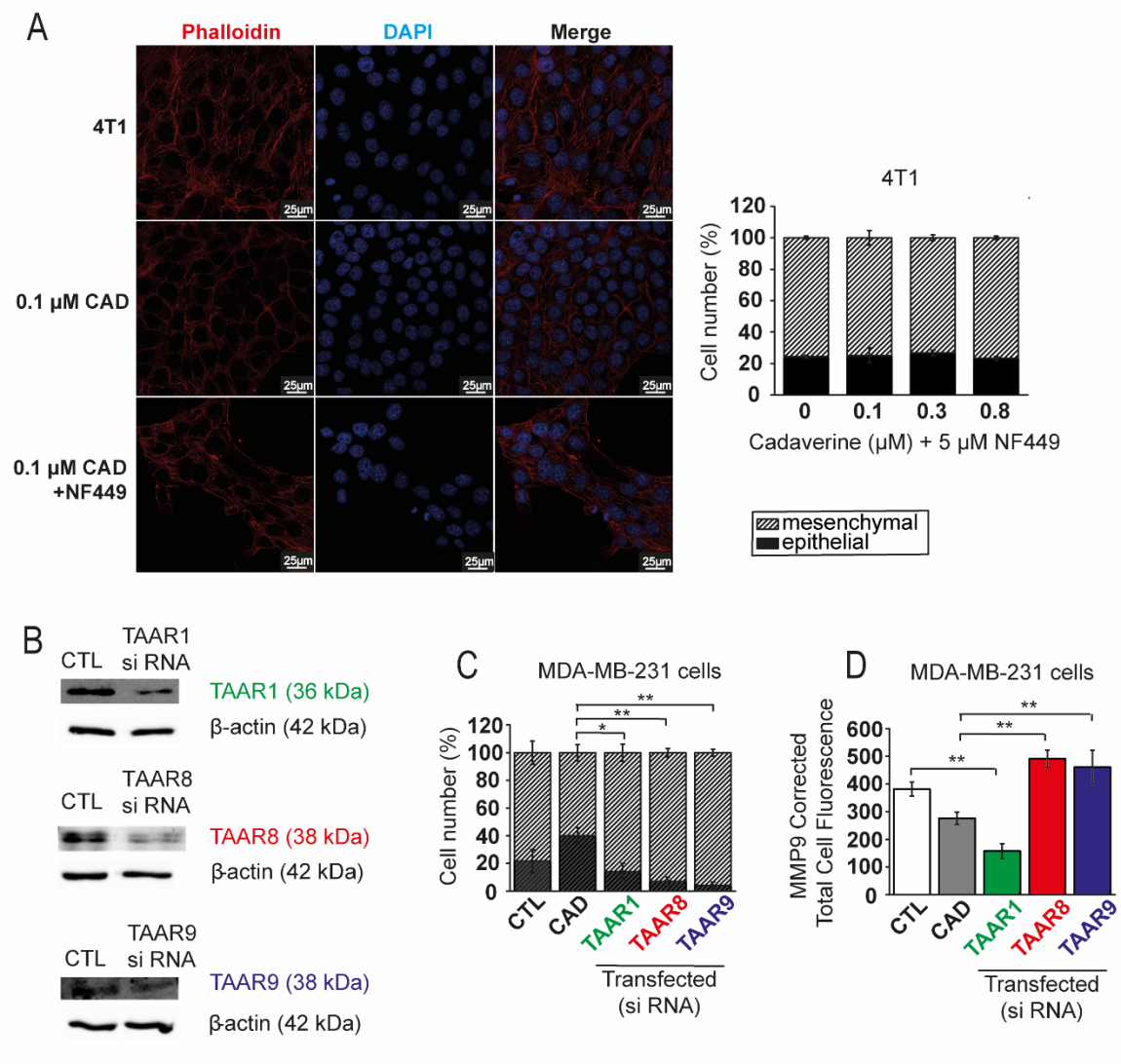

Figure 24. TAARs are important in mediating the effects of cadaverine. **(A)** 4T1 cells were treated with, 100 nM cadaverine (48 hours), or 100 nM cadaverine (48 hours) in combination with 5 µM NF449 G protein inhibitor, cells were stained with Texas Red-X Phalloidin- and DAPI then cells were assessed by confocal microscopy (n=2 in triplicates). **(B)** MDA-MB-231 cells were transfected with control si RNA or TAAR si RNA. The silencing efficacy was measured by Western blot. (n=2). **(C-D)** MDA-MB-231 cells were treated with vehicle or 0.3 µM cadaverine and transfected with control si RNA or TAAR si RNA. After 48 hours of incubation **(C)** TexasRed-X Phalloidin immunocytochemistry (n=1 in triplicates), and **(D)** MMP9 immunocytochemistry (n=1 in triplicates) were performed.

We assessed the available databases to collect data on TAAR1, TAAR8 and TAAR9. TAAR1 and TAAR9 expression did not show any major association with carcinogenesis or BC subtypes in contrast to TAAR8. TAAR8 expression decreased in pre-cancerous lesions, such as hyperplastic enlarged lobular units (HELUs) as compared to normal terminal ductal lobular units (TDLUs) [160]. In line with that, TAAR8 expression decreased in BC [161]. Decreases in TAAR8 expression was different between the histological subtypes of BC. TAAR8 expression

was lower in triple negative BCs as compared to non-triple negative BCs. There was a trend for lower TAAR8 expression in DCIS when compared to healthy tissue [162], TAAR8 expression was lower in ductal invasive BC as compared to healthy ducts [163] and there was a trend for lower TAAR8 expression in lobular invasive BC as compared to healthy lobes. Taken together, apparently, in early stage of BC TAAR8 expression decreases that is more pronounced in triple negative BCs.

6.2.2. Cadaverine biosynthesis is suppressed in BC

To get an insight whether intestinal cadaverine biosynthesis is altered in BC patients, we measured the abundance of the DNA coding for LdcC and CadA in human fecal DNA from the experimental cohort described in [11]. We designed primers for known CadA and LdcC genes in different bacteria. When comparing healthy individuals and BC patients we observed trends for lower abundance of *E.coli* CadA and also *E. coli*, *Enterobacter cloacae* and *Hafnia alvei* LdcC DNA in BC patients, although, these changes were not significant. Reduced CadA and LdcC abundance was more pronounced in clinical stage 0 patients as compared to the pool of all patients (Figure 25).

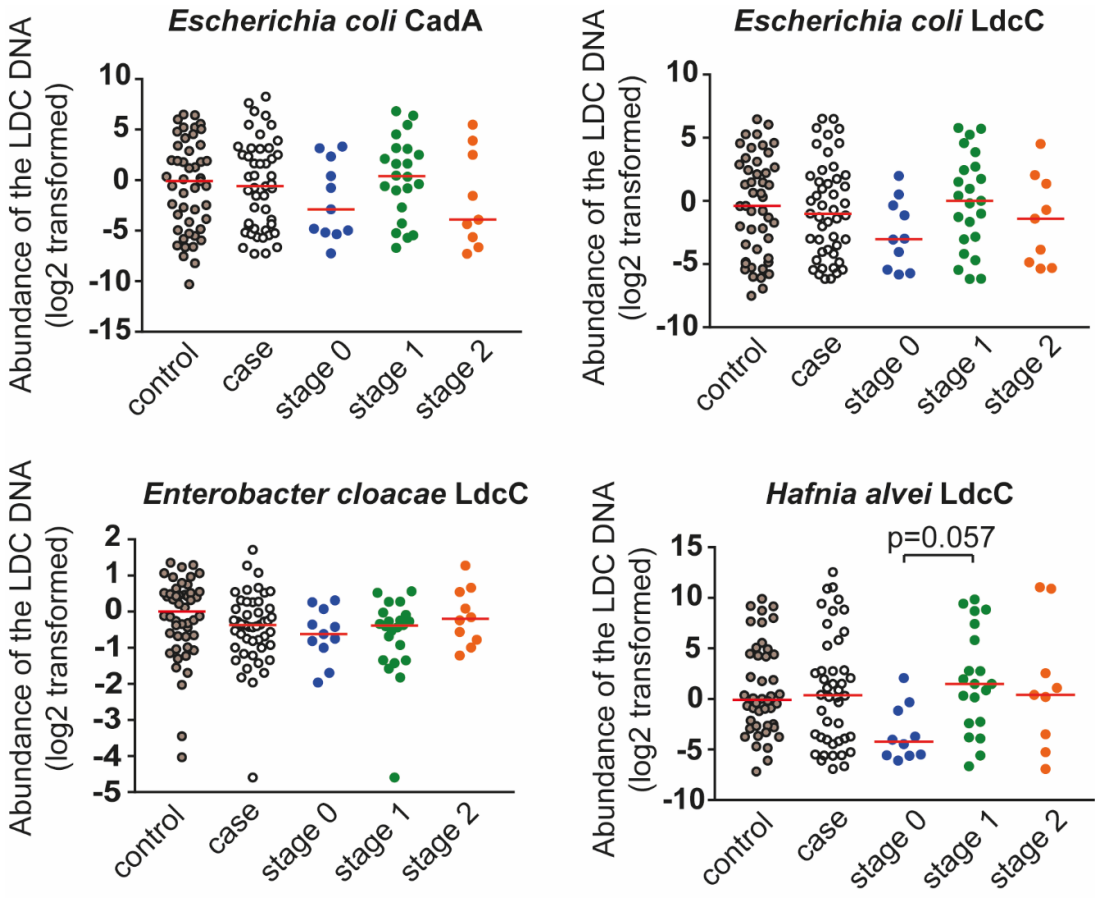

Figure 25. Cadaverine biosynthesis is suppressed in early stages of BC. Human fecal DNA samples were collected from 48 patients with different stages of BC, and from 46 healthy patients. The

abundance of DNA coding for CadA and LdcC of the indicated bacterial species were determined in the fecal DNA samples by qPCR. Median values are indicated by red line.

Subsequently, we assessed the protein levels of *E. coli* LdcC protein in feces by Western blotting. In the feces of stage 1 patients LdcC protein levels were markedly lower than the levels in the feces of healthy subjects (Figure 26B), in line with the lower fecal DNA abundances.

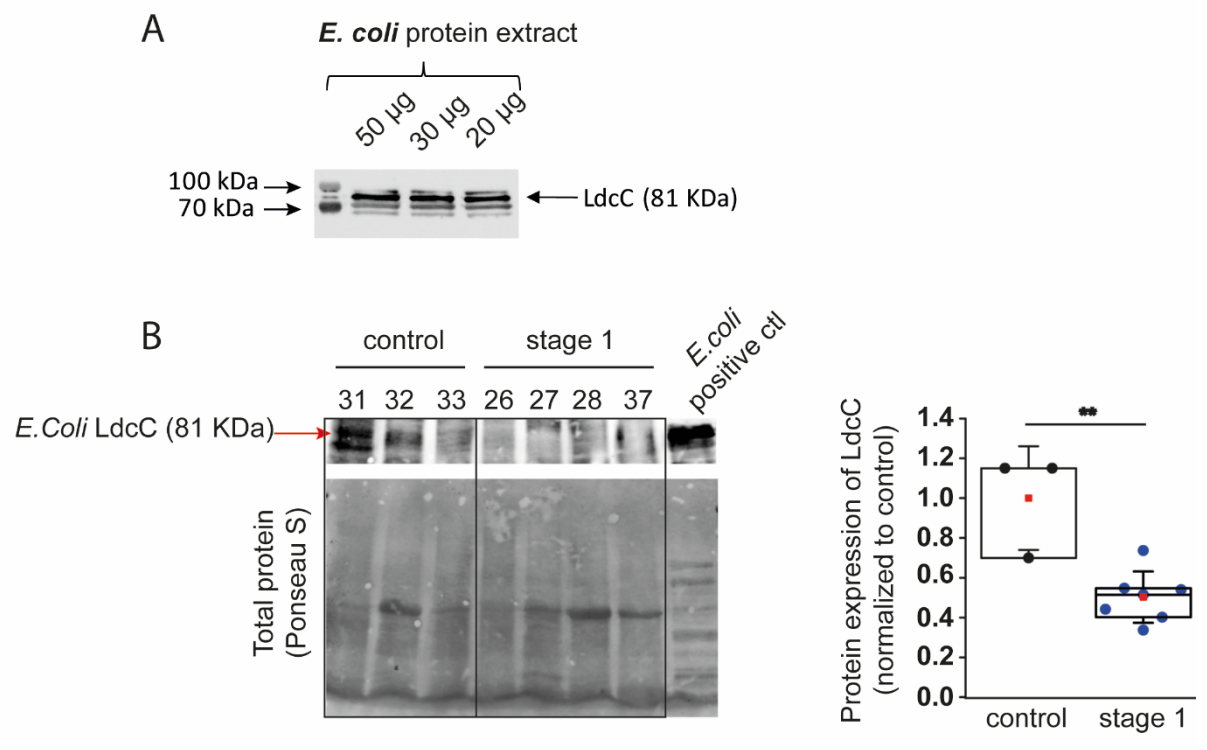

Figure 26. (A) Validation of E.coli LDC. (B) Protein expression of LDC decreased in stage 1 BC. **(A)** DH5α *E. coli* cells were grown in LB. After incubation overnight cells were collected and lysed in RIPA buffer. Samples were separated using SDS-PAGE (20, 30 and 50 µg protein extract were loaded) followed by Western blotting. Membranes were blocked with 5 % BSA and LdcC antibody (Abcam) was applied overnight on the membranes, for visualization HRP-linked secondary antibody (Cell Signaling Technology) was used. Blots were routinely cut as on the sample image. **(B)** Human fecal samples were collected from stage 1 BC patients (n=7) and from healthy (control) subjects (n=3). The *E. coli* LdcC protein level was determined using Western blot. Hereby we show a representative image. Band intensity was normalized to total protein content assessed by ponceau-S staining of whole blots. Box chart of LDC protein expression from fecal samples. Data was normalized to the mean of control samples. Blots were routinely cut as the representative blot.

We assessed the GEO database to study LDC expression in human BC. There was no difference in LDC mRNA expression between control and BC cases [164-166] or in LDC expression of the normal breast epithelium and cancer epithelium in patients [167]. Rather as an exception, LDC expression was lower in basal-like BC as compared to control (normal) breast epithelium of non-diseased individuals [168].

Finally, we assessed how expression of LDC in humans affects the outcome of BC using the kmplot.com database (the acquired data is represented in Figure 27; Table 12). Although,

differences in LDC expression did affect overall survival of the patients, in grade 1 patients higher expression of LDC was associated with significantly longer survival than lower expression of LDC. Interestingly, while LDC expression did not affect survival in ER- PR- patients, higher LDC expression correlated with better survival in ER+ PR+ patients (Figure 27; Table 12).

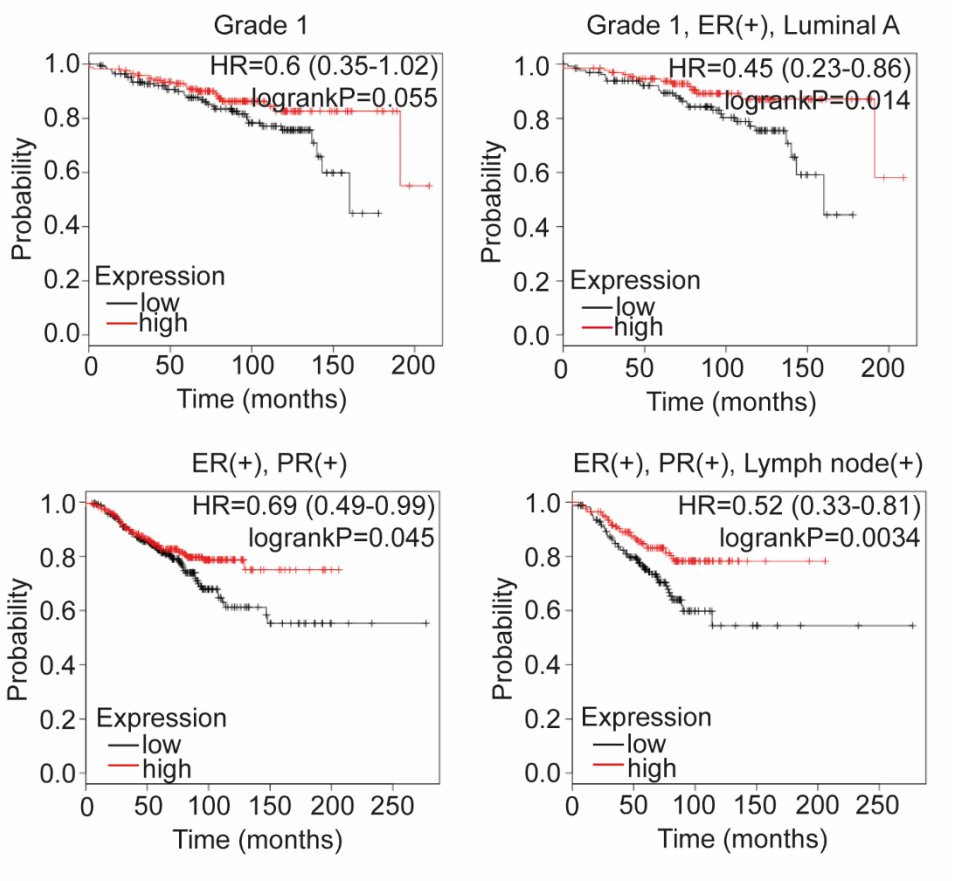

Figure 27. Representative plots of LDC related with different classes of BC. High expression of LDC is associated with significantly longer survival in low-grade BC. LDC expression do not affect survival in ER^- PR^-, but in ER^+ PR^+ patients. Kaplan-Meier plots, HR (with 95% confidency intervalls) and P values were exported directly from www.kmplot.com databese.

Table 12. BC survival and LDC. First column shows different breast cancer groups. Values were exported from www.kmplot.com database. Hazard Ratio (HR) indicates the probability of death in high LDC expression group, while P-values sign the difference between high and low expression groups.

LDC (201744_s_at)	HR (Hazard Ratio)	P-value (Log Rank Test)
All BCs, N=3951	1.07	0.23
ER(+), PR(+), N=577	0.69	**0.045**
ER(+), PR(+), Lymph node(+), N=344	0.52	**3.4×10^{-3}**
ER(+), PR(+), Lymph node(-), N=228	0.76	0.39
ER(-), PR(-), N=298	0.94	0.74
ER(-), PR(-), Lymph node(+), N=127	0.76	0.32
ER(-), PR(-), Lymph node(-), N=167	0.89	0.69
ER(-), PR(-), HER2(-), N=198	1.01	0.98
ER(+), Luminal A, N=1933	1.15	0.1
ER(+), Luminal A, Grade 1, N=267	0.45	**0.014**
ER(+), Luminal B, N=1149	1.11	0.27
ER(+), Luminal B, Grade 1, N=56	1.73	0.39
Grade 1, N=345	0.6	**0.055**
Grade 2, N=901	0.83	0.13
Grade 3, N=903	1.06	0.59
Basal subtype, N=618	1.18	0.19
Luminal A, N=1933	1.15	0.1
Luminal B, N=1149	1.11	0.27
ER(+), HER2(+), N=156	0.96	0.9
ER(-), HER2(+), N=96	1.57	0.16

6.3. LCA decrease the aggressiveness of BC in vivo

6.3.1. LCA attenuates the aggressiveness of BC in mice

We tested the effects of LCA in mice that were grafted with 4T1 cells and were treated with LCA (15 nmol LCA p.o. q.d.) or vehicle for 18 days. At the time of the sacrifice the infiltration capacity of the primary tumor to the surrounding tissues markedly decreased upon LCA treatment (Figure 28A). Furthermore, the number of the metastases was also lower in the LCA-treated group (Figure 28B).

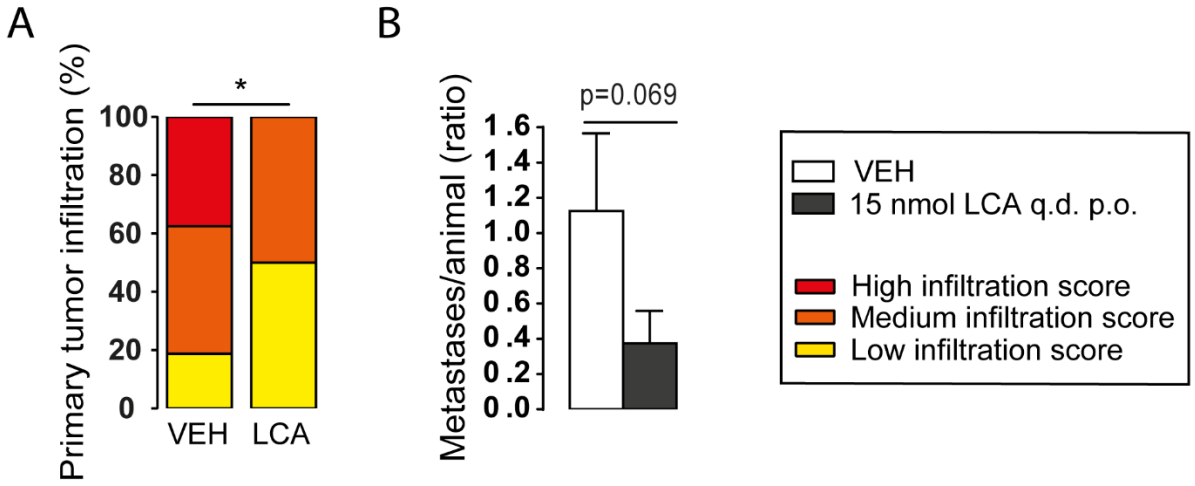

Figure 28. LCA inhibits the proliferation of BC cells and reduces cancer aggressiveness in vivo. **(A-B**) Female BALB/c mice were grafted with 4T1 cells as described and were treated with LCA (15 nmol q.d. p.o.) or vehicle (VEH) (n=8/8) for 18 days before sacrifice. Upon autopsy, mice **(A)** tumor infiltration and **(B)** the number of metastases were determined.

6.3.2. LCA Biosynthesis is suppressed in early phases of human BC

We next investigated how BA and LCA metabolism relates to BC in humans. LCA is produced through the deconjugation of chenodeoxycholic acid (CDCA) conjugates, followed by a dihydroxylation on carbon 7 by the action of the enzyme 7α/β hydroxysteroid dehydrogenase (7-HSDH) that is the rate-limiting step of LCA formation. The enzymes involved in the 7-dehydroxylation of BAs are organized into one operon called the BA-inducible (*bai*) operon wherein the *baiH* ORF codes for 7-HSDH in most bacterial species [169].

Total BA, CDCA and LCA levels were reduced in serum from BC patients as compared to age and sex matched healthy individuals (Figure 29A-C; Table 13), and we observed a similar trend in all other BAs we examined (Figure 29A; Table 13). Since both primary and secondary BA levels were lower in BC patients, we assessed the ratio between CDCA (the substrate for LCA synthesis) and LCA in human serum. We found a decrease in the LCA/CDCA ratio in BC patients compared to healthy individuals, and this decrease that was more marked when only

stage 1 patients were assessed (Figure 29D; Table 13). At later stages LCA/CDCA ratio normalized and even increased above the ratio of healthy individuals in stage 3 patients. These data are in good correlation with the data of Tang an co-workers [170] demonstrating that glycolithocholate sulphate levels were lower in BC patients compared to controls.

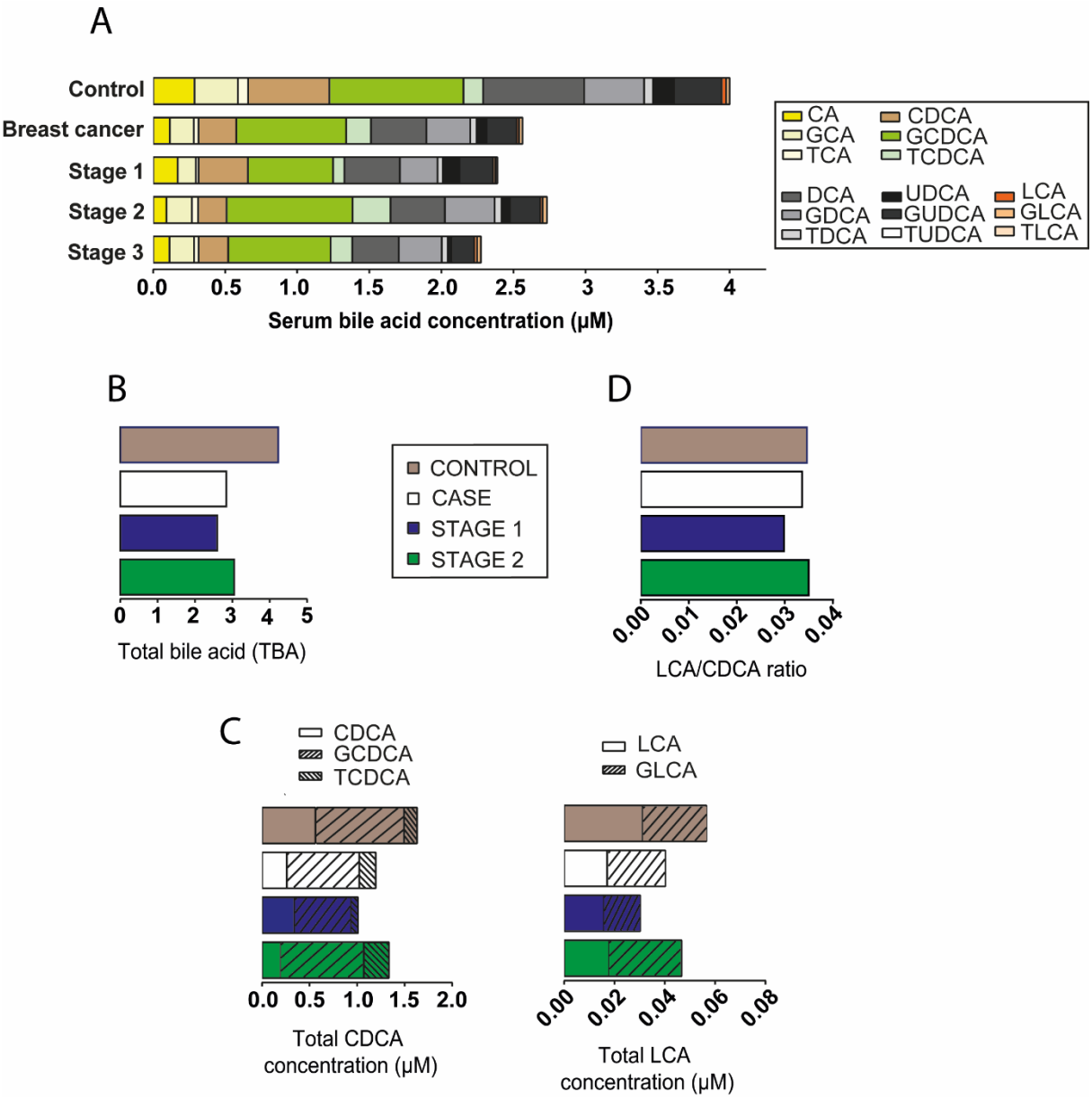

Figure 29. In early stages of BC LCA levels drop. Serum samples from the healthy controls and BC patients of *cohort 2* were pooled. **(A)** The BA composition of these pooled samples were determined. **(B)** By summing the different BA species total serum BA content was calculated. **(C)** Serum CDCA and LCA levels from the samples of healthy controls and BC patients are plotted. **(D)** LCA/CDCA ratio was calculated from the samples of healthy controls and BC patients. CA: cholic acid; GCA: glycocholic acid; TCA: taurocholic acid; CDCA: chenodeoxycholic acid; GCDCA: glycochenodeoxycholic acid; TCDCA: taurochenodeoxycholic acid; DCA: deoxycholic acid; GDCA: glycodeoxycholic acid; TDCA: taurodeoxycholic acid; UDCA: ursodeoxycholic acid; GUDCA: glycoursodeoxycholic acid; TUDCA: tauroursodeoxycholic acid; LCA: lithocholic acid; GLCA: glycolithocholic acid; TLCA: taurolithocholic acid.

Table 13. BA composition of the human serum samples (compare to Figure 29). Table shows the serum concentration of primary and secondary bile acids, as well as their glyco- and tauro-conjugated derivatives in serum samples of control and breast cancer patients. CA: cholic acid; GCA: glycocholic acid; TCA: taurocholic acid; CDCA: chenodeoxycholic acid; GCDCA: glycochenodeoxycholic acid; TCDCA: taurochenodeoxycholic acid; DCA: deoxycholic acid; GDCA: glycodeoxycholic acid; TDCA: taurodeoxycholic acid; UDCA: ursodeoxycholic acid; GUDCA: glycoursodeoxycholic acid; LCA: lithocholic acid; GLCA: glycolithocholic acid.

Primary BAs (µmol/L)						
	CA	***GCA***	***TCA***	***CDCA***	***GCDCA***	***TCDCA***
Control	0.287	0.301	0.071	0.563	0.931	0.137
BC	0.116	0.166	0.033	0.262	0.761	0.173
Stage 1	0.170	0.126	0.020	0.342	0.591	0.078
Stage 2	0.092	0.177	0.043	0.198	0.874	0.263
Stage 3	0.113	0.170	0.033	0.205	0.710	0.150

Secondary BAs (µmol/L)							
	DCA	***GDCA***	***TDCA***	***LCA***	***GLCA***	***UDCA***	***GUDCA***
Control	0.701	0.415	0.061	0.031	0.025	0.147	0.330
BC	0.384	0.304	0.045	0.017	0.023	0.069	0.209
Stage 1	0.385	0.261	0.038	0.016	0.014	0.114	0.233
Stage 2	0.377	0.345	0.049	0.018	0.029	0.058	0.209
Stage 3	0.323	0.297	0.043	0.020	0.026	0.027	0.157

To clarify how intestinal LCA biosynthesis is modified in BC, we assessed the abundance of the *baiH* (responsible for LCA production) ORF in human fecal DNA samples from the experimental *cohort 1* [11] (Table 7, *Cohort 1*). In order to do that we searched for bacterial species where the ORF for baiH was annotated. In our experiments we identified the baiH ORF of anaerobic, Gram positive and Gram-negative species and measured the abundance of the baiH ORF using qPCR assays. When all patients were compared to healthy controls, the abundance of baiH of *Clostridium sordelli, Staphylococcus haemolyticus, E. coli* and *Pseudomonas putida* was lower in BC patients, and the change was significant in the case of *Pseudomonas putida* (Figure 30A). These results correlate with the lower LCA levels and LCA/CDCA ratio of BC patients (Figure 29). A more pronounced decrease in the abundance of the baiH of *Bacteroides thetaiotaomicron, Clostridium sordelli, Staphylococcus haemolyticus, E. coli* and *Pseudomonas putida* were observed in stage 0 and stage 1 patients than in the pool of all patients (Figure 30B).

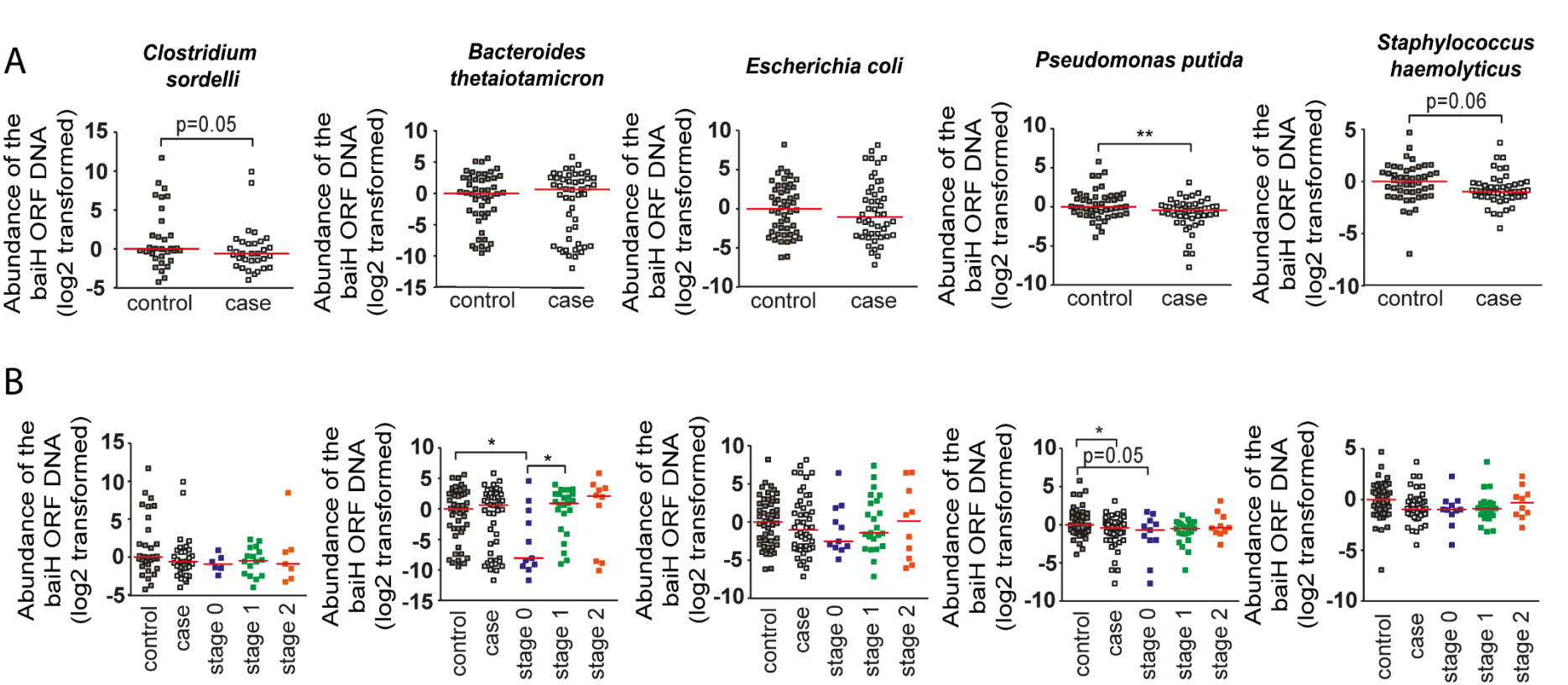

Figure 30. The abundance of baiH DNA is suppressed in early stages of human BC. The abundance of the baiH DNA was determined **(A-B)** in the fecal DNA sample of *cohort 1*. Median values indicated by red line. Values where c_t was lower than 45 were removed. Panel **A** depicts only the comparison of the control vs. cases, therefore on that panel Student's t-test was used to determine statistical significance.

Taken together, the bacterial LCA biosynthesis machinery in the intestine is downregulated in BC patients that is very pronounced in the early phase of the disease. Lower capacity to synthesize LCA then contributes to lower LCA levels. These finding together with the observation of Tang and co-workers [170] that glycolithocholate sulphate levels have a significant negative correlation with Ki67 (proliferation marker) positivity in human BC tumors, pointing towards the involvement of bacterial LCA metabolism in human BC pathogenesis.

7. DISCUSSION

To date no direct, casual relationship had been shown between BC and the microbiota, although several control-case studies highlight interconnections. Goedert and co-workers - comparing the fecal microbiota of BC patients with closely matched control women - found significantly altered microbiome composition and less diverse gut bacteria [11]. In addition, milk ducts in the breast are colonized by bacteria, and changes in the microbiome of BC tissue has also been observed [21, 22]. These finding suggest, that LCA and cadaverine may be produced by the breast's own microbiota, not only by the microbiome of the GI tract, however, share of the sources remain unclear. The relationship between BC and the microbiota is strengthened by the positive correlation between BC incidence/recurrence and antibiotic treatment [171-173], moreover, this association was also found in men [174]. These observations support our hypothesis of the relationship between microbial functions and BC.

7.1. The effects of cadaverine in BC

In contrast to other biogenic amines (spermine, spermidine, putrescine), cadaverine is ill-characterized. Based on the literature, serum level of diamines are higher in cancer patients than in healthy individuals and surgical removal of tumors normalize serum diamine levels [118, 119, 175]. Increased putrescine levels are in positive correlation with carcinogenesis, however, polyamine involvement is not proven in cancer development. Cadaverine levels are more variable: some studies report increases, others show trends for decrement [176] in different cancer diseases, nevertheless, BC patients still have not been evaluated.

In this study we characterized how cadaverine affects the behavior of BC cells. We characterized the cadaverine-driven effects in different (mouse and human) BC cell lines. Our data highlights that cadaverine has tumor suppressor role in BC in concentrations corresponding to the human reference serum concentrations [118, 119]. Cadaverine significantly inhibited EMT (Figure 17-19) by modifying the expression of genes participating in proliferation, adhesion and cell movement (Figure 20-21). Cadaverine also suppressed the ability of cells for invasion (Figure 20B), and the metastatic potential of 4T1 cells (Figure 14-15, 19C) *in vitro* and *in vivo* (BALB/c mice).

We also found significant changes in the OCR of cadaverine-treated cells, thereby, cadaverine may shift the metabolic profile of BC cells toward "reverse Warburg effect" by reducing stem-like characteristic of the cells (Figure 22) (Table 14).

Table 14. Significant changes after cadaverine/LCA treatment

Cadaverine experiments				
Measurement	**Indicating figure**	**Statistical test type**	**P-value**	**Between groups**
Primary tumor infiltration	***Figure 15A***	Fisher's exact test	$2*10^{-3}$	VEH and CAD-treated
Nuclear pleomorphism	***Figure 15B***	Fisher's exact test	$9*10^{-3}$	VEH and CAD-treated
Mitosis/hpf	***Figure 15C***	Two-Sample t-Test	***0.027***	VEH and CAD-treated
Mitosis	***Figure 15D***	Fisher's exact test	$3*10^{-3}$	VEH and CAD-treated
Normalized resistance	***Figure 17***	Two-Sample t-Test	***0.048***	CTL and 0.1 μM CAD
Actin morphology	***Figure 18A***	Chi-square test	$2.9*10^{-28}$ $1.*10^{-18}$ $3.9*10^{-10}$	CTL and 0.1 μM CAD CTL and 0.3 μM CAD CTL and 0.8 μM CAD
	Figure 24C	Chi-square test	***0.04*** $7*10^{-3}$ $3*10^{-3}$	CAD and TAAR1 CAD and TAAR8 CAD and TAAR9
MMP3 gene expression	***Figure 19A***	One-way ANOVA	***0.048*** ***0.033***	CTL and 0.3 μM CAD CTL and 0.8 μM CAD
	Figure 19C	Two-Sample t-Test	***0.027***	VEH and CAD-treated
MMP9 gene expression	***Figure 19A***	One-way ANOVA	$7*10^{-3}$ $9*10^{-3}$	CTL and 0.1 μM CAD CTL and 0.3 μM CAD
Tgfb3 gene expression	***Figure 19A***	One-way ANOVA	$9*10^{-3}$ $9.4*10^{-5}$ $1.9*10^{-5}$	CTL and 0.1 μM CAD CTL and 0.3 μM CAD CTL and 0.8 μM CAD
FgFbp1 gene expression	***Figure 19A***	One-way ANOVA	$1*10^{-3}$ $1.2*10^{-4}$	CTL and 0.3 μM CAD CTL and 0.8 μM CAD
Erbb3 gene expression	***Figure 19A***	One-way ANOVA	***0.037***	CTL and 0.8 μM CAD
Er1 gene expression	***Figure 19A***	One-way ANOVA	***0.035***	CTL and 0.3 μM CAD
Notch1 gene expression	***Figure 19A***	One-way ANOVA	$4*10^{-3}$ $1*10^{-3}$	CTL and 0.3 μM CAD CTL and 0.8 μM CAD
lgFbp4 gene expression	***Figure 19A***	One-way ANOVA	$9.4*10^{-5}$ $2.2*10^{-4}$ $6.8*10^{-6}$	CTL and 0.1 μM CAD CTL and 0.3 μM CAD CTL and 0.8 μM CAD
Spp1 gene expression	***Figure 19A***	One-way ANOVA	***0.024*** ***0.032***	CTL and 0.3 μM CAD CTL and 0.8 μM CAD
CDH1 gene expression	***Figure 19C***	Two-Sample t-Test	***0.041***	VEH and CAD-treated
DSC2 gene expression	***Figure 19C***	Two-Sample t-Test	***0.046***	VEH and CAD-treated
Invasion index	***Figure 20***	One-way ANOVA	$3*10^{-3}$ $3*10^{-3}$ $4.1*10^{-4}$	CTL and 0.1 μM CAD CTL and 0.3 μM CAD CTL and 0.8 μM CAD
MMP9 protein expression	***Figure 21A***	One-way ANOVA	10^{-3} 10^{-3}	CTL and 0.3 μM CAD CTL and 0.8 μM CAD
	Figure 21B	Kruskal–Wallis ANOVA	$<10^{-6}$ $<10^{-6}$	CTL and 0.3 μM CAD CTL and 0.8 μM CAD
	Figure 21C	Kruskal–Wallis ANOVA	$<10^{-4}$ $<10^{-4}$ $<10^{-4}$	CTL and 0.1 μM CAD CTL and 0.3 μM CAD CTL and 0.8 μM CAD
	Figure 24D	One-way ANOVA	$6*10^{-3}$ 10^{-3} $4*10^{-3}$	CTL and TAAR1 CAD and TAAR8 CAD and TAAR9
Oxygen consumption rate	***Figure 22A***	One-way ANOVA	$6*10^{-3}$ $1.1*10^{-6}$ $1.8*10^{-5}$	CTL and 0.1 μM CAD CTL and 0.3 μM CAD CTL and 0.8 μM CAD

ALDH positive cell number	***Figure 22B***	One-way ANOVA	***0.035***	CTL and 0.3 μM CAD
	Figure 22C	Two-Sample t-Test	***0.018***	CTL and 0.3 μM CAD
LdcC protein expression	***Figure 26B***	Two-Sample t-Test	$***3*10^{-3}***$	CTL and stage 1
LCA experiments				
Measurement	**Indicating figure**	**Statistical test type**	**P-value**	**Between groups**
Primary tumor infiltration	***Figure 28A***	Fisher's exact test	***0.012***	VEH and LCA-treated
Abundance of baiH ORF	***Figure 30A***	Two-Sample t-Test	$***3.4*10^{-3}***$	CTL and CASE
	Figure 30B	One-way ANOVA	***0.048*** ***0.042*** ***0.027***	CTL and stage 1 Stage 0 and stage 1 CTL and CASE

The applied concentrations (0.1 – 0.8 μM) are much lower than the ones used in previous studies (10 – 100 μM) [177, 178]. Our results indicating the possible involvement of TAARs (TAAR1, TAAR2, TAAR5, TAAR8 and TAAR9) in the anticancer effect of cadaverine, in line with the study about TAAR1 and better BC survival [136]. Elevated expression of these receptors correlates with better BC survival (Figure 23; Table 11). To validate these findings, we tested TAAR1, TAAR8 and TAAR9 involvement in cadaverine-evoked effects. All three measured receptors seem to participate in regulating MET, however, only TAAR8 and TAAR9 influenced MMP9 protein expression (Figure 24). Available metadata highlights that TAAR8 is reduced in precancerous stages and downregulated together with worsened disease. Due to the limited availability of reagents, we cannot exclude that – besides the ones we examined - other TAARs could be equally involved in regulating cadaverine effects (Figure 31).

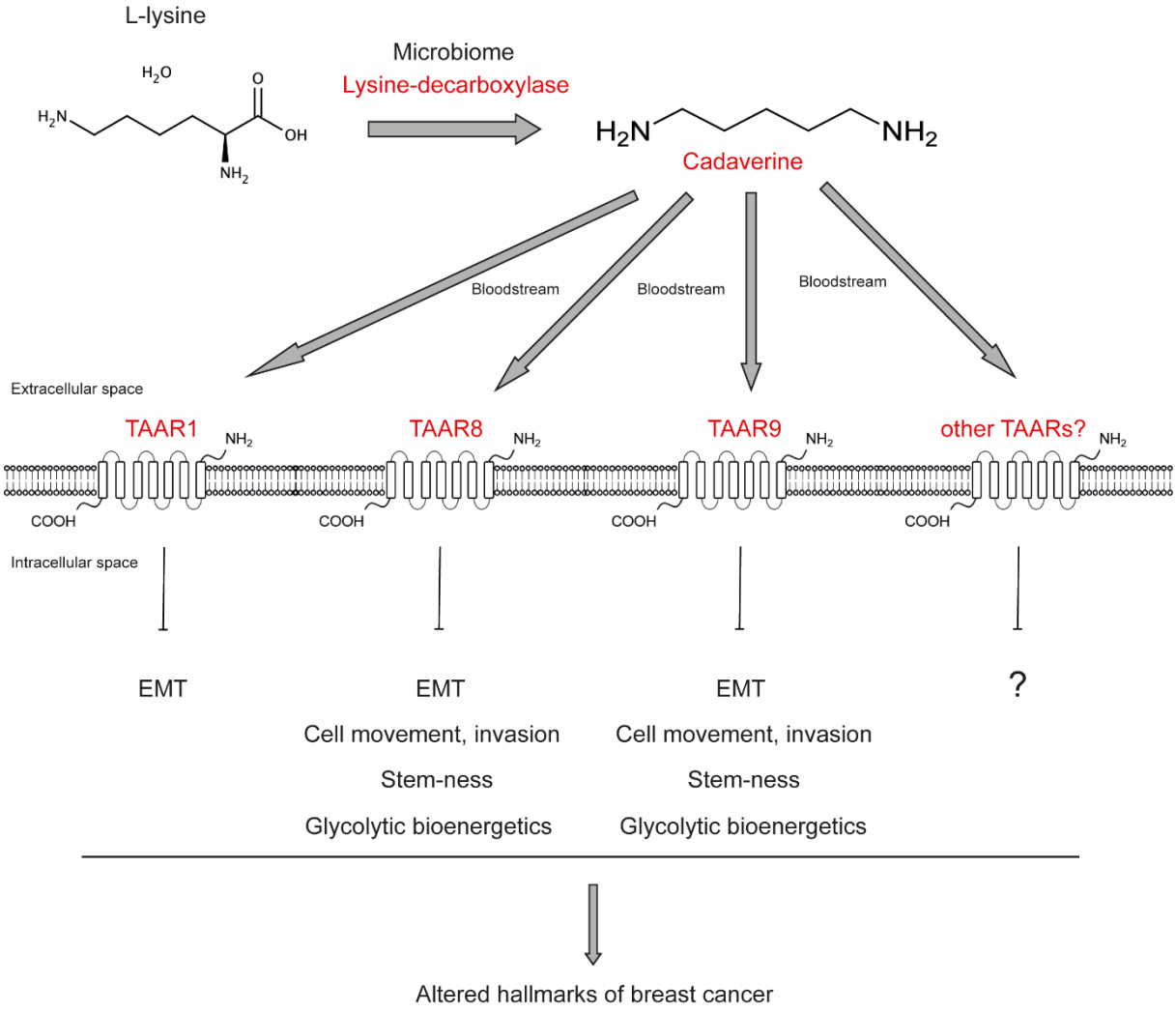

Figure 31. Schematic figure shows the effects of cadaverine on BC. Cadaverine is produced by LDC by the gut microbiota, and through the circulatory system, it reaches cancer cells located in a separate compartment than the GI tract. Through different TAARs, cadaverine influence EMT, cell movements, alter the bioenergetics and stem cell-ness of tumor cells, and thus alter several hallmarks of BC.

Our experiments show that bacterial cadaverine biosynthesis is suppressed in early stage BC (Figure 25). This observation suggests that the simplification of gut microbiome in early stage BC [11, 112, 114] leads to a decreased production of antiproliferative bacterial metabolites like cadaverine. Most drastic changes of the microbiota were associated with stage 1 carcinoma, in later stages cadaverine production restored and reached levels similar to levels of the controls (Figure 25). The *in silico* data we gathered for TAAR8 suggest that in parallel to the simplification or dysbiosis of the microbiome in tumors, the expression of cadaverine-sensing apparatus is probably also downregulated.

Bacteria on breast duct surfaces and human cells can also synthesize cadaverine. However, the share of these sources (breast tissue vs. tumor vs. gut vs. host) in cadaverine

production is largely unknown, high human expression of LDC prolongs survival in early stage BC patients (Figure 26-27; Table 12). These data further validate the potential anti-cancer properties of cadaverine.

7.2. The effects of LCA in BC

LCA, a metabolite of the microbiome, is synthesized in the gut and transferred to the breast through the circulatory system, where it might play an important role in bringing about an anti-tumor microenvironment. LCA is known to induce cell death in neuroblastoma, prostate cancer and MCF7 BC cells [179, 180]. As we noted earlier, 1 μM LCA concentration, used in our *in vivo* study, stands close to the LCA concentrations reported in the breast [148]. LCA may be produced by the breast's own microbiota and not only by the gut microbiome, nevertheless, the share of the two sources in not known. Our *in vivo* experiments demonstrated that LCA – similarly to cadaverine - significantly reduces the infiltration rate of primary tumors, as well as the metastatic potential of the tumor (Figure 28).

In my dissertation we also tried to partly answer the question: which bacteria species are important in LCA-mediated modulation of BC. Goedert and co-workers[181] have found [11] that compared with control patients, BC patients have significantly altered microbial composition (both α and β diversity change), while Ridlon and co-workers' research [169] shows, that anaerobic microbes are important in the production of secondary BAs, among them LCA. Our study highlights decrement in both the aerobic and the anaerobic microbial populations with early stage BC (Figure 30; Table 14). Our study confirmed, that both primary and secondary BA levels are suppressed in BC patients (Figure 29). We also measured the ratio between CDCA and LCA. LCA/CDCA ratio diminished in BC patients compared to control, and the decrement was the marked in stage 1 (Figure 29; Table 13), that normalized at later stages of BC. These data are in good correlation with Tang an co-workers' findings, that demonstrate reduced glycolithocholate sulphate levels in BC patients [170]. These results suggest the involvement of both aerobic and anaerobic flora in secondary BA production, and propound widespread suppression of the microbiome in BC.

8. SUMMARY

There is a strong connection between the microbiome and the host. The bacteria – living in different cavities of the human body – produces numerous bacterial metabolites (among cadaverine and LCA), that can alter the metabolism and energy homeostasis of the host. Through internal and external factors (diet, personal hygiene, genetics, age) the host can also influence the composition and function of the microbiome. Alterations in the composition or function of the microbiome is associated with BC, among other diseases.

Cadaverine - a biologically active diamine - is produced by the enzyme LDC by the gut microbiota from the amino acid L-lysine. Through the bloodstream cadaverine reaches BC cells at distant locations of the body. Although, cadaverine slightly reduced the proliferation and colony formation of 4T1 cells, it could convert mesenchymal-like cells to epithelial-like cells. To gain epithelial-like features, cancer cells undergo MET by suppressing the expression of genes play important role in cell proliferation, movement and invasion. Cadaverine treatment also decreased the “stem cell-ness” of 4T1 cells. Moreover, cadaverine increased the cell-cell and cell-surface connections, thereby, obstructing migration. These data were further supported by the observation, that cadaverine supplementation to mice grafted with 4T1 BC cells resulted in reduced infiltration of primary tumors to surrounding tissues, reduced tumor mass as well as the number of metastases. Histological examination of primary tumors revealed that cadaverine supplementation decreased the rate of mitosis and the nuclear pleomorphism. Our results show that members of the TAAR family (TAAR1, TAAR8 and TAAR9) could be responsible for the cadaverine-evoked effects. Silencing of these receptors prevented the cadaverine-elicited EMT and the cadaverine-induced decrement in MMP9 expression. Metadata analysis shows that TAAR8 is reduced in early stage of BC and were further downregulated together as the disease progressed. We also assessed human LDC expression using kmpolt.com database and found, that in grade 1 patients higher LDC expression correlated with significantly longer survival. To verify these findings, we compared the abundance and expression of LDC in samples from healthy individuals and BC patients. Both the abundance of LDC DNA and the protein levels were suppressed in early stages of BC compared to the controls.

We also assessed how the level of LCA – another bacterial metabolite, a secondary BA – differ in the serum of control vs. BC patients, and which bacterial species play important role in LCA production. In contrast to other studies it seems that both aerobic and anaerobic flora participate in LCA production. The abundance of baiH ORF (responsible for LCA production) decreased significantly in early stage BC samples compared to matched control samples. BA composition of human serum samples highlight, that total BA levels, as well as

LCA levels and LCA/CDCA ratio were reduced in serum from BC patients as compared to healthy individuals, the decrement was the more pronounced in stage 1 BC.

This study confirms that cadaverine and LCA can suppress hallmarks of BC cells, thereby, puts cadaverine and LCA on the list of bacterial metabolites that control carcinogenesis. These observations support the hypothesis that bacterial metabolites influence carcinogenesis in organs far from the gut, however, this field requires more research to understand the connection between microbes and distantly located tumors.

9. ÖSSZEFOGLALÁS

A mikrobiom és a gazdaszervezet között erős kapcsolat áll fenn. A baktériumok – melyek az emberi szervezet különböző testüregeiben élnek – számos metabolitot termelnek (közöttük kadaverint és litokólsavat), amelyek hatással vannak a gazdaszervezet anyagcseréjére és energia háztartására. Külső és belső tényezők (étrend, személyes higiénia, genetika, kor) segítségével a gazdaszervezet is befolyásolja a mikrobiom összetételét és működését. Számos betegség, köztük az emlődaganat is összefüggésbe hozható a mikrobiom összetételében és működésében bekövetkező változásokkal.

A kadaverin – egy biológiailag aktív diamin – L-lizin aminosavból keletkezik a mikrobiom lizin dekarboxiláz nevű enzimje által. A véráramon keresztül a kadaverin eljut a test különböző részeiben elhelyezkedő tumorsejtekhez. Habár kísérleteinkben a kadaverin csak kissé csökkentette a 4T1 sejtek proliferációját és kolónia formáló képességét, képes volt a mezenchimális jellegű sejteket epiteliális jellegűvé alakítani. Hogy a sejtek elnyerjék epitheliális jellegüket, mezenchimális-epiteliális tranzíción (MET) esnek át csökkentve azon gének kifejeződését, melyek szerepet játszanak a sejtproliferációban, sejtmozgásban és invázióban. A kadaverin kezelés a 4T1 sejtek “őssejt szerűségét” is csökkentette. Mi több, a kadaverin erősítette a sejt-sejt közötti, illetve a sejt-felszín közötti kapcsolatokat, ezáltal gátolva a migrációt. Ezek az eredmények további megerősítést nyertek azáltal, hogy 4T1 emlőtumorral beoltott egerekben kadaverin etetés hatására csökkent az elsődleges tumor beszűrődése a környező szövetekbe, csökkent a tumorok tömege és az áttétek száma is. Az elsődleges tumorok hisztológiai elemzése rávilágított, hogy a kadaverin csökkenti a tumoros sejtek osztódásának ütemét, illetve a sejtmagok heterogenitását. Eredményeink azt mutatják, hogy a trace amin-kapcsolt receptorok (TAAR1, TAAR8, TAAR9) lehetnek a felelősek a kadaverin hatásáért. Ezen receptorok genetikai csendesítése kivédte a kadaverinnek mind az epiteliális-mezenchimális tranzícióban (EMT), mind a matrix-metalloproteináz-9 (MMP9) kifejeződésben bekövetkezett hatását. Metaadat-analízis azt mutatta, hogy a TAAR8 csökkent szintjét mutatja korai emlődaganatban, ami a betegség előrehaladtával tovább csökken. Továbbá kmplot.com adatbázisban kerestük a human lizin-dekarboxiláz (LDC) és az emlődaganat összefüggéseit. Azt találtuk, hogy 1-es grádusú emlődaganatban a magasabb LDC szint hosszabb túléléssel korrelál. Hogy megerősítsük ezen összefüggéseket, megvizsgáltuk az LDC szintjét emlődaganatos páciensek és egészséges önkéntesek székletmintáiban. Az enzim DNS és fehérje szintje is csökkenést mutatott korai emlődaganatos mintákban, összehasonlítva az egészséges önkéntesek mintáival.

Megvizsgáltuk továbbá, hogy egy másik bakteriális metabolit, a litokólsav (LCA, másodlagos epesav) szintje hogyan változik egészséges önkéntesek és emlődaganatos

páciensek szérum mintáiban. Szerettünk volna választ kapni arra a kérdésre is, hogy mely baktériumfajok vesznek részt az LCA termelésében. Más tanulmányokkal ellentétben úgy tűnik, hogy mind az aerob, mind az anaerob flóra részt vesz az LCA szintézisben. Méréseink azt mutatják, hogy a baiH ORF (mely az LCA termelésért felelős) korai stádiumú emlőrákban szignifikáns csökkenést mutat, összehasonlítva kontroll mintákkal. A vizsgált human szérum minták epesav összetétele rávilágított, hogy az LCA szintjén kívül a teljes epesav szint és az LCA/CDCA arány is csökkent tumoros betegekben, valamint a csökkenés az 1-es stádiumú betegekben volt a legszembetűnőbb.

Jelen disszertáció megerősíti a felvetést, hogy a kadaverin és az LCA képes megváltoztatni az emlőtumor sejtek tulajdonságait, ezáltal a kadaverin és az LCA felkerül az olyan bakteriális metabolitok listájára, melyek képesek befolyásolni a tumorképződést. Mindezen megfigyelések alátámasztják a feltevést, miszerint a bakteriális metabolitok képesek befolyásolni a tumorképződést/növekedést olyan szervekben is, melyek az emésztőrendszertől távol helyezkednek el, habár ez a terület további kutatásokat igényel, hogy teljességében megértsük a kapcsolatot a mikrobiom és az emésztőrendszeren kívül elhelyezkedő tumorok között.

10. REFERENCES

1. Hanahan, D. and R.A. Weinberg, *Hallmarks of cancer: the next generation.* Cell, 2011. **144**(5): p. 646-74.
2. Lynch, S.V. and O. Pedersen, *The Human Intestinal Microbiome in Health and Disease.* N Engl J Med, 2016. **375**(24): p. 2369-2379.
3. Smits, L.P., et al., *Therapeutic potential of fecal microbiota transplantation.* Gastroenterology, 2013. **145**(5): p. 946-53.
4. Garrett, W.S., *Cancer and the microbiota.* Science, 2015. **348**(6230): p. 80-6.
5. Krishnan, S., N. Alden, and K. Lee, *Pathways and functions of gut microbiota metabolism impacting host physiology.* Curr Opin Biotechnol, 2015. **36**: p. 137-45.
6. Reijnders, D., et al., *Effects of Gut Microbiota Manipulation by Antibiotics on Host Metabolism in Obese Humans: A Randomized Double-Blind Placebo-Controlled Trial.* Cell Metab, 2016. **24**(1): p. 63-74.
7. Macfabe, D., *Autism: metabolism, mitochondria, and the microbiome.* Glob Adv Health Med, 2013. **2**(6): p. 52-66.
8. Fulbright, L.E., M. Ellermann, and J.C. Arthur, *The microbiome and the hallmarks of cancer.* PLoS Pathog, 2017. **13**(9): p. e1006480.
9. Kundu, P., et al., *Our Gut Microbiome: The Evolving Inner Self.* Cell, 2017. **171**(7): p. 1481-1493.
10. Maruvada, P., et al., *The Human Microbiome and Obesity: Moving beyond Associations.* Cell Host Microbe, 2017. **22**(5): p. 589-599.
11. Goedert, J.J., et al., *Investigation of the association between the fecal microbiota and breast cancer in postmenopausal women: a population-based case-control pilot study.* J Natl Cancer Inst, 2015. **107**(8).
12. Yu, Y., et al., *The role of the cutaneous microbiome in skin cancer: lessons learned from the gut.* J Drugs Dermatol, 2015. **14**(5): p. 461-5.
13. Yu, H., et al., *Urinary microbiota in patients with prostate cancer and benign prostatic hyperplasia.* Arch Med Sci, 2015. **11**(2): p. 385-94.
14. Chase, D., et al., *The vaginal and gastrointestinal microbiomes in gynecologic cancers: a review of applications in etiology, symptoms and treatment.* Gynecol Oncol, 2015. **138**(1): p. 190-200.
15. Gui, Q.F., et al., *Well-balanced commensal microbiota contributes to anti-cancer response in a lung cancer mouse model.* Genet Mol Res, 2015. **14**(2): p. 5642-51.
16. Yamamoto, M.L. and R.H. Schiestl, *Lymphoma caused by intestinal microbiota.* Int J Environ Res Public Health, 2014. **11**(9): p. 9038-49.
17. Yamamoto, M.L. and R.H. Schiestl, *Intestinal microbiome and lymphoma development.* Cancer J, 2014. **20**(3): p. 190-4.
18. Flores, R., et al., *Fecal microbial determinants of fecal and systemic estrogens and estrogen metabolites: a cross-sectional study.* J Transl Med, 2012. **10**: p. 253.
19. Fuhrman, B.J., et al., *Associations of the fecal microbiome with urinary estrogens and estrogen metabolites in postmenopausal women.* J Clin Endocrinol Metab, 2014. **99**(12): p. 4632-40.
20. Xuan, C., et al., *Microbial dysbiosis is associated with human breast cancer.* PLoS One, 2014. **9**(1): p. e83744.
21. Hieken, T.J., et al., *The Microbiome of Aseptically Collected Human Breast Tissue in Benign and Malignant Disease.* Sci Rep, 2016. **6**: p. 30751.
22. Urbaniak, C., et al., *The Microbiota of Breast Tissue and Its Association with Breast Cancer.* Appl Environ Microbiol, 2016. **82**(16): p. 5039-48.

23. Goedert, J.J., et al., *Postmenopausal breast cancer and oestrogen associations with the IgA-coated and IgA-noncoated faecal microbiota.* Br J Cancer, 2018. **118**(4): p. 471-479.
24. Kahn, S.E., M.E. Cooper, and S. Del Prato, *Pathophysiology and treatment of type 2 diabetes: perspectives on the past, present, and future.* Lancet, 2014. **383**(9922): p. 1068-83.
25. Sundaram, S., A.R. Johnson, and L. Makowski, *Obesity, metabolism and the microenvironment: Links to cancer.* J Carcinog, 2013. **12**: p. 19.
26. Dapito, D.H., et al., *Promotion of hepatocellular carcinoma by the intestinal microbiota and TLR4.* Cancer Cell, 2012. **21**(4): p. 504-16.
27. Rowland, I.R., *Role of the gut flora in toxicity and cancer*. 1988, London ; San Diego: Academic Press. x, 517 p.
28. Yoshimoto, S., et al., *Obesity-induced gut microbial metabolite promotes liver cancer through senescence secretome.* Nature, 2013. **499**(7456): p. 97-101.
29. Xie, G., et al., *Dysregulated hepatic bile acids collaboratively promote liver carcinogenesis.* Int J Cancer, 2016. **139**(8): p. 1764-75.
30. Shellman, Z., et al., *Bile acids: a potential role in the pathogenesis of pharyngeal malignancy.* Clin Otolaryngol, 2017. **42**(5): p. 969-973.
31. Luu, T.H., et al., *Lithocholic bile acid inhibits lipogenesis and induces apoptosis in breast cancer cells.* Cell Oncol (Dordr), 2018. **41**(1): p. 13-24.
32. Bindels, L.B., et al., *Gut microbiota-derived propionate reduces cancer cell proliferation in the liver.* Br J Cancer, 2012. **107**(8): p. 1337-44.
33. Darbre, P.D. and M.F. Fernandez, *Environmental oestrogens and breast cancer: long-term low-dose effects of mixtures of various chemical combinations.* J Epidemiol Community Health, 2013. **67**(3): p. 203-5.
34. Ferlay, J., et al., *Cancer incidence and mortality worldwide: sources, methods and major patterns in GLOBOCAN 2012.* Int J Cancer, 2015. **136**(5): p. E359-86.
35. Torre, L.A., et al., *Global cancer statistics, 2012.* CA Cancer J Clin, 2015. **65**(2): p. 87-108.
36. Oh, H., et al., *Breast cancer risk factors in relation to estrogen receptor, progesterone receptor, insulin-like growth factor-1 receptor, and Ki67 expression in normal breast tissue.* NPJ Breast Cancer, 2017. **3**: p. 39.
37. Fernandez, M.F., et al., *Breast Cancer and Its Relationship with the Microbiota.* Int J Environ Res Public Health, 2018. **15**(8).
38. Schatten, H., *Cell and molecular biology of breast cancer*. viii, 383 pages.
39. Cserni, G., et al., *The new TNM-based staging of breast cancer.* Virchows Arch, 2018. **472**(5): p. 697-703.
40. Sotiriou, C. and L. Pusztai, *Gene-expression signatures in breast cancer.* N Engl J Med, 2009. **360**(8): p. 790-800.
41. Davies, M.A. and Y. Samuels, *Analysis of the genome to personalize therapy for melanoma.* Oncogene, 2010. **29**(41): p. 5545-55.
42. Yuan, T.L. and L.C. Cantley, *PI3K pathway alterations in cancer: variations on a theme.* Oncogene, 2008. **27**(41): p. 5497-510.
43. Jiang, B.H. and L.Z. Liu, *PI3K/PTEN signaling in angiogenesis and tumorigenesis.* Adv Cancer Res, 2009. **102**: p. 19-65.
44. Sudarsanam, S. and D.E. Johnson, *Functional consequences of mTOR inhibition.* Curr Opin Drug Discov Devel, 2010. **13**(1): p. 31-40.
45. Deshpande, A., P. Sicinski, and P.W. Hinds, *Cyclins and cdks in development and cancer: a perspective.* Oncogene, 2005. **24**(17): p. 2909-15.
46. Burkhart, D.L. and J. Sage, *Cellular mechanisms of tumour suppression by the retinoblastoma gene.* Nat Rev Cancer, 2008. **8**(9): p. 671-82.
47. Hanahan, D. and J. Folkman, *Patterns and emerging mechanisms of the angiogenic switch during tumorigenesis.* Cell, 1996. **86**(3): p. 353-64.
48. Cavallaro, U. and G. Christofori, *Cell adhesion and signalling by cadherins and Ig-CAMs in cancer.* Nat Rev Cancer, 2004. **4**(2): p. 118-32.

49. Berx, G. and F. van Roy, *Involvement of members of the cadherin superfamily in cancer.* Cold Spring Harb Perspect Biol, 2009. **1**(6): p. a003129.
50. Negrini, S., V.G. Gorgoulis, and T.D. Halazonetis, *Genomic instability--an evolving hallmark of cancer.* Nat Rev Mol Cell Biol, 2010. **11**(3): p. 220-8.
51. Salk, J.J., E.J. Fox, and L.A. Loeb, *Mutational heterogeneity in human cancers: origin and consequences.* Annu Rev Pathol, 2010. **5**: p. 51-75.
52. DeNardo, D.G., P. Andreu, and L.M. Coussens, *Interactions between lymphocytes and myeloid cells regulate pro- versus anti-tumor immunity.* Cancer Metastasis Rev, 2010. **29**(2): p. 309-16.
53. Grivennikov, S.I., F.R. Greten, and M. Karin, *Immunity, inflammation, and cancer.* Cell, 2010. **140**(6): p. 883-99.
54. Qian, B.Z. and J.W. Pollard, *Macrophage diversity enhances tumor progression and metastasis.* Cell, 2010. **141**(1): p. 39-51.
55. Warburg, O., F. Wind, and E. Negelein, *The Metabolism of Tumors in the Body.* J Gen Physiol, 1927. **8**(6): p. 519-30.
56. Clark, W.H., *Tumour progression and the nature of cancer.* Br J Cancer, 1991. **64**(4): p. 631-44.
57. Reya, T., et al., *Stem cells, cancer, and cancer stem cells.* Nature, 2001. **414**(6859): p. 105-11.
58. Al-Hajj, M., et al., *Prospective identification of tumorigenic breast cancer cells.* Proc Natl Acad Sci U S A, 2003. **100**(7): p. 3983-8.
59. Buck, E., et al., *Loss of homotypic cell adhesion by epithelial-mesenchymal transition or mutation limits sensitivity to epidermal growth factor receptor inhibition.* Mol Cancer Ther, 2007. **6**(2): p. 532-41.
60. Creighton, C.J., et al., *Residual breast cancers after conventional therapy display mesenchymal as well as tumor-initiating features.* Proc Natl Acad Sci U S A, 2009. **106**(33): p. 13820-5.
61. Singh, A. and J. Settleman, *EMT, cancer stem cells and drug resistance: an emerging axis of evil in the war on cancer.* Oncogene, 2010. **29**(34): p. 4741-51.
62. Dirat, B., et al., *Unraveling the obesity and breast cancer links: a role for cancer-associated adipocytes?* Endocr Dev, 2010. **19**: p. 45-52.
63. Pietras, K. and A. Ostman, *Hallmarks of cancer: interactions with the tumor stroma.* Exp Cell Res, 2010. **316**(8): p. 1324-31.
64. Rasanen, K. and A. Vaheri, *Activation of fibroblasts in cancer stroma.* Exp Cell Res, 2010. **316**(17): p. 2713-22.
65. Shimoda, M., K.T. Mellody, and A. Orimo, *Carcinoma-associated fibroblasts are a rate-limiting determinant for tumour progression.* Semin Cell Dev Biol, 2010. **21**(1): p. 19-25.
66. Pavlides, S., et al., *The reverse Warburg effect: aerobic glycolysis in cancer associated fibroblasts and the tumor stroma.* Cell Cycle, 2009. **8**(23): p. 3984-4001.
67. Nagy, J.A., et al., *Heterogeneity of the tumor vasculature.* Semin Thromb Hemost, 2010. **36**(3): p. 321-31.
68. Ruoslahti, E., *Specialization of tumour vasculature.* Nat Rev Cancer, 2002. **2**(2): p. 83-90.
69. Ruoslahti, E., S.N. Bhatia, and M.J. Sailor, *Targeting of drugs and nanoparticles to tumors.* J Cell Biol, 2010. **188**(6): p. 759-68.
70. Gaengel, K., et al., *Endothelial-mural cell signaling in vascular development and angiogenesis.* Arterioscler Thromb Vasc Biol, 2009. **29**(5): p. 630-8.
71. Coffelt, S.B., et al., *Elusive identities and overlapping phenotypes of proangiogenic myeloid cells in tumors.* Am J Pathol, 2010. **176**(4): p. 1564-76.
72. Egeblad, M., E.S. Nakasone, and Z. Werb, *Tumors as organs: complex tissues that interface with the entire organism.* Dev Cell, 2010. **18**(6): p. 884-901.
73. Murdoch, C., et al., *The role of myeloid cells in the promotion of tumour angiogenesis.* Nat Rev Cancer, 2008. **8**(8): p. 618-31.

74. Yuen, G.J., E. Demissie, and S. Pillai, *B lymphocytes and cancer: a love-hate relationship.* Trends Cancer, 2016. **2**(12): p. 747-757.
75. Uribe-Querol, E. and C. Rosales, *Neutrophils in Cancer: Two Sides of the Same Coin.* J Immunol Res, 2015. **2015**: p. 983698.
76. De Palma, M., et al., *Tie2-expressing monocytes: regulation of tumor angiogenesis and therapeutic implications.* Trends Immunol, 2007. **28**(12): p. 519-24.
77. Mantovani, A., *Molecular pathways linking inflammation and cancer.* Curr Mol Med, 2010. **10**(4): p. 369-73.
78. Bergfeld, S.A. and Y.A. DeClerck, *Bone marrow-derived mesenchymal stem cells and the tumor microenvironment.* Cancer Metastasis Rev, 2010. **29**(2): p. 249-61.
79. Kalluri, R. and R.A. Weinberg, *The basics of epithelial-mesenchymal transition.* J Clin Invest, 2009. **119**(6): p. 1420-8.
80. Hay, E.D. and A. Zuk, *Transformations between epithelium and mesenchyme: normal, pathological, and experimentally induced.* Am J Kidney Dis, 1995. **26**(4): p. 678-90.
81. Parsons, J.T., A.R. Horwitz, and M.A. Schwartz, *Cell adhesion: integrating cytoskeletal dynamics and cellular tension.* Nat Rev Mol Cell Biol, 2010. **11**(9): p. 633-43.
82. Hazan, R.B., et al., *N-cadherin promotes adhesion between invasive breast cancer cells and the stroma.* Cell Adhes Commun, 1997. **4**(6): p. 399-411.
83. Zeisberg, M. and E.G. Neilson, *Biomarkers for epithelial-mesenchymal transitions.* J Clin Invest, 2009. **119**(6): p. 1429-37.
84. Hugo, H., et al., *Epithelial--mesenchymal and mesenchymal--epithelial transitions in carcinoma progression.* J Cell Physiol, 2007. **213**(2): p. 374-83.
85. Lee, J.M., et al., *The epithelial-mesenchymal transition: new insights in signaling, development, and disease.* J Cell Biol, 2006. **172**(7): p. 973-81.
86. Brabletz, T., *To differentiate or not--routes towards metastasis.* Nat Rev Cancer, 2012. **12**(6): p. 425-36.
87. Chao, Y.L., C.R. Shepard, and A. Wells, *Breast carcinoma cells re-express E-cadherin during mesenchymal to epithelial reverting transition.* Mol Cancer, 2010. **9**: p. 179.
88. Asiedu, M.K., et al., *TGFbeta/TNF(alpha)-mediated epithelial-mesenchymal transition generates breast cancer stem cells with a claudin-low phenotype.* Cancer Res, 2011. **71**(13): p. 4707-19.
89. Aslakson, C.J. and F.R. Miller, *Selective events in the metastatic process defined by analysis of the sequential dissemination of subpopulations of a mouse mammary tumor.* Cancer Res, 1992. **52**(6): p. 1399-405.
90. Dykxhoorn, D.M., et al., *miR-200 enhances mouse breast cancer cell colonization to form distant metastases.* PLoS One, 2009. **4**(9): p. e7181.
91. Takebe, N., R.Q. Warren, and S.P. Ivy, *Breast cancer growth and metastasis: interplay between cancer stem cells, embryonic signaling pathways and epithelial-to-mesenchymal transition.* Breast Cancer Res, 2011. **13**(3): p. 211.
92. Liu, H., et al., *Cancer stem cells from human breast tumors are involved in spontaneous metastases in orthotopic mouse models.* Proc Natl Acad Sci U S A, 2010. **107**(42): p. 18115-20.
93. Peiris-Pages, M., et al., *Cancer stem cell metabolism.* Breast Cancer Res, 2016. **18**(1): p. 55.
94. De Francesco, E.M., F. Sotgia, and M.P. Lisanti, *Cancer stem cells (CSCs): metabolic strategies for their identification and eradication.* Biochem J, 2018. **475**(9): p. 1611-1634.
95. Ginestier, C., et al., *ALDH1 is a marker of normal and malignant human mammary stem cells and a predictor of poor clinical outcome.* Cell Stem Cell, 2007. **1**(5): p. 555-67.
96. Graff, J.R., et al., *E-cadherin expression is silenced by DNA hypermethylation in human breast and prostate carcinomas.* Cancer Res, 1995. **55**(22): p. 5195-9.
97. Lombaerts, M., et al., *E-cadherin transcriptional downregulation by promoter methylation but not mutation is related to epithelial-to-mesenchymal transition in breast cancer cell lines.* Br J Cancer, 2006. **94**(5): p. 661-71.

98. Bartel, D.P., *MicroRNAs: target recognition and regulatory functions.* Cell, 2009. **136**(2): p. 215-33.
99. Valastyan, S. and R.A. Weinberg, *MicroRNAs: Crucial multi-tasking components in the complex circuitry of tumor metastasis.* Cell Cycle, 2009. **8**(21): p. 3506-12.
100. Mani, S.A., et al., *The epithelial-mesenchymal transition generates cells with properties of stem cells.* Cell, 2008. **133**(4): p. 704-15.
101. Drasin, D.J., T.P. Robin, and H.L. Ford, *Breast cancer epithelial-to-mesenchymal transition: examining the functional consequences of plasticity.* Breast Cancer Res, 2011. **13**(6): p. 226.
102. Zhang, D., et al., *Epidermal growth factor receptor tyrosine kinase inhibitor reverses mesenchymal to epithelial phenotype and inhibits metastasis in inflammatory breast cancer.* Clin Cancer Res, 2009. **15**(21): p. 6639-48.
103. Orlichenko, L.S. and D.C. Radisky, *Matrix metalloproteinases stimulate epithelial-mesenchymal transition during tumor development.* Clin Exp Metastasis, 2008. **25**(6): p. 593-600.
104. Schlaeppi, K. and D. Bulgarelli, *The plant microbiome at work.* Mol Plant Microbe Interact, 2015. **28**(3): p. 212-7.
105. Human Microbiome Project, C., *Structure, function and diversity of the healthy human microbiome.* Nature, 2012. **486**(7402): p. 207-14.
106. Li, J., et al., *An integrated catalog of reference genes in the human gut microbiome.* Nat Biotechnol, 2014. **32**(8): p. 834-41.
107. Rea, D., et al., *Microbiota effects on cancer: from risks to therapies.* Oncotarget, 2018. **9**(25): p. 17915-17927.
108. Pugin, B., et al., *A wide diversity of bacteria from the human gut produces and degrades biogenic amines.* Microb Ecol Health Dis, 2017. **28**(1): p. 1353881.
109. Ridlon, J.M., et al., *Consequences of bile salt biotransformations by intestinal bacteria.* Gut Microbes, 2016. **7**(1): p. 22-39.
110. Robinson, K., *Helicobacter pylori-Mediated Protection against Extra-Gastric Immune and Inflammatory Disorders: The Evidence and Controversies.* Diseases, 2015. **3**(2): p. 34-55.
111. Ye, W., et al., *Helicobacter pylori infection and gastric atrophy: risk of adenocarcinoma and squamous-cell carcinoma of the esophagus and adenocarcinoma of the gastric cardia.* J Natl Cancer Inst, 2004. **96**(5): p. 388-96.
112. Luu, T.H., et al., *Intestinal Proportion of Blautia sp. is Associated with Clinical Stage and Histoprognostic Grade in Patients with Early-Stage Breast Cancer.* Nutr Cancer, 2017. **69**(2): p. 267-275.
113. Backhed, F., et al., *The gut microbiota as an environmental factor that regulates fat storage.* Proc Natl Acad Sci U S A, 2004. **101**(44): p. 15718-23.
114. Bard, J.-M., et al., *Relationship Between Intestinal Microbiota and Clinical Characteristics of Patients with Early Stage Breast Cancer.* The FASEB Journal, 2015. **29**(1_supplement): p. 914.2.
115. Rhee, H.J., E.J. Kim, and J.K. Lee, *Physiological polyamines: simple primordial stress molecules.* J Cell Mol Med, 2007. **11**(4): p. 685-703.
116. Kusano, T., et al., *Polyamines: essential factors for growth and survival.* Planta, 2008. **228**(3): p. 367-81.
117. Shah, P. and E. Swiatlo, *A multifaceted role for polyamines in bacterial pathogens.* Mol Microbiol, 2008. **68**(1): p. 4-16.
118. Loser, C., et al., *Polyamine concentrations in pancreatic tissue, serum, and urine of patients with pancreatic cancer.* Pancreas, 1990. **5**(2): p. 119-27.
119. Loser, C., et al., *Polyamines in colorectal cancer. Evaluation of polyamine concentrations in the colon tissue, serum, and urine of 50 patients with colorectal cancer.* Cancer, 1990. **65**(4): p. 958-66.
120. Samartzidou, H., et al., *Cadaverine inhibition of porin plays a role in cell survival at acidic pH.* J Bacteriol, 2003. **185**(1): p. 13-9.

121. Andersson, A.C., S. Henningsson, and E. Rosengren, *Formation of cadaverine in the pregnant rat.* Acta Physiol Scand, 1979. **105**(4): p. 508-12.
122. Wang, Q., et al., *Comparison of the effects of Mylabris and Acanthopanax senticosus on promising cancer marker polyamines in plasma of a Hepatoma-22 mouse model using HPLC-ESI-MS.* Biomed Chromatogr, 2013. **27**(2): p. 208-15.
123. Miller-Fleming, L., et al., *Remaining Mysteries of Molecular Biology: The Role of Polyamines in the Cell.* J Mol Biol, 2015. **427**(21): p. 3389-406.
124. Kojima, S. and Y. Kamio, *Molecular basis for the maintenance of envelope integrity in Selenomonas ruminantium: cadaverine biosynthesis and covalent modification into the peptidoglycan play a major role.* J Nutr Sci Vitaminol (Tokyo), 2012. **58**(3): p. 153-60.
125. Kikuchi, Y., et al., *Characterization of a second lysine decarboxylase isolated from Escherichia coli.* J Bacteriol, 1997. **179**(14): p. 4486-92.
126. Yamamoto, Y., et al., *The Escherichia coli ldcC gene encodes another lysine decarboxylase, probably a constitutive enzyme.* Genes Genet Syst, 1997. **72**(3): p. 167-72.
127. Haneburger, I., et al., *New insights into the signaling mechanism of the pH-responsive, membrane-integrated transcriptional activator CadC of Escherichia coli.* J Biol Chem, 2011. **286**(12): p. 10681-9.
128. Brameyer, S., et al., *DNA-binding directs the localization of a membrane-integrated receptor of the ToxR family.* Commun Biol, 2019. **2**: p. 4.
129. Hussain, A., et al., *High-affinity olfactory receptor for the death-associated odor cadaverine.* Proc Natl Acad Sci U S A, 2013. **110**(48): p. 19579-84.
130. Izquierdo, C., et al., *Identifying human diamine sensors for death related putrescine and cadaverine molecules.* PLoS Comput Biol, 2018. **14**(1): p. e1005945.
131. Li, Q., et al., *Non-classical amine recognition evolved in a large clade of olfactory receptors.* Elife, 2015. **4**: p. e10441.
132. Babusyte, A., et al., *Biogenic amines activate blood leukocytes via trace amine-associated receptors TAAR1 and TAAR2.* J Leukoc Biol, 2013. **93**(3): p. 387-94.
133. Vladimirov, V.I., et al., *The trace amine associated receptor (TAAR6) gene is not associated with schizophrenia in the Irish Case-Control Study of Schizophrenia (ICCSS) sample.* Schizophr Res, 2009. **107**(2-3): p. 249-54.
134. Muhlhaus, J., et al., *Analysis of human TAAR8 and murine Taar8b mediated signaling pathways and expression profile.* Int J Mol Sci, 2014. **15**(11): p. 20638-55.
135. Farooqui, T., *Trace Amine-Mediated Olfactory Learning and Memory in Mammals and Insects: A Brief Comparative Review.* Trace Amines and Neurological Disorders: Potential Mechanisms and Risk Factors, 2016: p. 181-202.
136. Vattai, A., et al., *Increased trace amine-associated receptor 1 (TAAR1) expression is associated with a positive survival rate in patients with breast cancer.* J Cancer Res Clin Oncol, 2017. **143**(9): p. 1637-1647.
137. Hofmann, A.F., *The continuing importance of bile acids in liver and intestinal disease.* Arch Intern Med, 1999. **159**(22): p. 2647-58.
138. Gerard, P., *Metabolism of cholesterol and bile acids by the gut microbiota.* Pathogens, 2013. **3**(1): p. 14-24.
139. Sherrod, J.A. and P.B. Hylemon, *Partial purification and characterization of NAD-dependent 7alpha-hydroxysteroid dehydrogenase from Bacteroides thetaiotaomicron.* Biochim Biophys Acta, 1977. **486**(2): p. 351-8.
140. White, B.A., R.J. Fricke, and P.B. Hylemon, *7 beta-Dehydroxylation of ursodeoxycholic acid by whole cells and cell extracts of the intestinal anaerobic bacterium, Eubacterium species V.P.I. 12708.* J Lipid Res, 1982. **23**(1): p. 145-53.
141. Ridlon, J.M., D.J. Kang, and P.B. Hylemon, *Isolation and characterization of a bile acid inducible 7alpha-dehydroxylating operon in Clostridium hylemonae TN271.* Anaerobe, 2010. **16**(2): p. 137-46.

142. Ishizawa, M., D. Akagi, and M. Makishima, *Lithocholic Acid Is a Vitamin D Receptor Ligand That Acts Preferentially in the Ileum.* Int J Mol Sci, 2018. **19**(7).
143. Beilke, L.D., et al., *Constitutive androstane receptor-mediated changes in bile acid composition contributes to hepatoprotection from lithocholic acid-induced liver injury in mice.* Drug Metab Dispos, 2009. **37**(5): p. 1035-45.
144. Staudinger, J.L., et al., *The nuclear receptor PXR is a lithocholic acid sensor that protects against liver toxicity.* Proc Natl Acad Sci U S A, 2001. **98**(6): p. 3369-74.
145. Zwicker, B.L. and L.B. Agellon, *Transport and biological activities of bile acids.* Int J Biochem Cell Biol, 2013. **45**(7): p. 1389-98.
146. Duboc, H., et al., *Connecting dysbiosis, bile-acid dysmetabolism and gut inflammation in inflammatory bowel diseases.* Gut, 2013. **62**(4): p. 531-9.
147. McGarr, S.E., J.M. Ridlon, and P.B. Hylemon, *Diet, anaerobic bacterial metabolism, and colon cancer: a review of the literature.* J Clin Gastroenterol, 2005. **39**(2): p. 98-109.
148. Raju, U., M. Levitz, and N.B. Javitt, *Bile acids in human breast cyst fluid: the identification of lithocholic acid.* J Clin Endocrinol Metab, 1990. **70**(4): p. 1030-4.
149. Kovacs, T., et al., *Cadaverine, a metabolite of the microbiome, reduces breast cancer aggressiveness through trace amino acid receptors.* Sci Rep, 2019. **9**(1): p. 1300.
150. Miko, E., et al., *Lithocholic acid, a bacterial metabolite reduces breast cancer cell proliferation and aggressiveness.* Biochim Biophys Acta Bioenerg, 2018. **1859**(9): p. 958-974.
151. Hohenegger, M., et al., *Gsalpha-selective G protein antagonists.* Proc Natl Acad Sci U S A, 1998. **95**(1): p. 346-51.
152. Sun, Q., et al., *Aldehyde reactivity with 2-thiobarbituric acid and TBARS in freeze-dried beef during accelerated storage.* Meat Sci, 2001. **57**(1): p. 55-60.
153. Kilkenny, C., et al., *Improving bioscience research reporting: The ARRIVE guidelines for reporting animal research.* J Pharmacol Pharmacother, 2010. **1**(2): p. 94-9.
154. McGrath, J.C. and E. Lilley, *Implementing guidelines on reporting research using animals (ARRIVE etc.): new requirements for publication in BJP.* Br J Pharmacol, 2015. **172**(13): p. 3189-93.
155. Howlader, N., et al., *Overview of breast cancer collaborative stage data items--their definitions, quality, usage, and clinical implications: a review of SEER data for 2004-2010.* Cancer, 2014. **120 Suppl 23**: p. 3771-80.
156. Nagy, G.G., et al., *[Detailed methodological recommendations for the treatment of Clostridium difficile-associated diarrhea with faecal transplantation].* Orv Hetil, 2013. **154**(1): p. 10-9.
157. Watanabe, M., et al., *Bile acids induce energy expenditure by promoting intracellular thyroid hormone activation.* Nature, 2006. **439**(7075): p. 484-9.
158. Sakakura, H., et al., *Simultaneous determination of bile acids in rat bile and serum by high-performance liquid chromatography.* J Chromatogr, 1993. **621**(2): p. 123-31.
159. Liberles, S.D., *Trace amine-associated receptors: ligands, neural circuits, and behaviors.* Curr Opin Neurobiol, 2015. **34**: p. 1-7.
160. NCBI_GEO_Profiles, *TAAR8 expression in hyperplastic enlarged lubular units (HELUs) versus normal terminal ductal lobular units (TDLUs)*. 2018: https://www.ncbi.nlm.nih.gov/geoprofiles/39407988.
161. Gent_Database, *TAAR8 expression in cancers (search term: TAAR8)*. 2018: http://medicalgenome.kribb.re.kr/GENT/
162. NCBI_GEO_Profiles, *TAAR8 expression in DCIS vs. healthy breast tissue*. 2018: https://www.ncbi.nlm.nih.gov/geo/tools/profileGraph.cgi?ID=GDS3853:1553552_at.
163. NCBI_GEO_Profiles, *TAAR8 - Invasive ductal and lobular breast carcinomas*. 2018: https://www.ncbi.nlm.nih.gov/geoprofiles/36691448.
164. NCBI_GEO_Profiles. *LDC expression in control, DCIS, ICS*. 2018 [cited 2018 04 06 2018].
165. NCBI_GEO_Profiles. *LDC expression in epithelium and stroma of normal breast and invasive breast cancer*. 2018 [cited 2018 04 06 2018].

166. NCBI_GEO_Profiles. *LDC expression in ER- and ER+ breast cancer patients, prophylactic mastectomy patients, and normal breast epithelia from reduction mammoplasty patients.* 2018 [cited 2018 04 06 2018].
167. NCBI_GEO_Profiles. *Normal epithelium vs. breast cancer epithelium in patients*. 2018 04 06 2018].
168. NCBI_GEO_Profiles. *LDC expression in control vs. non-basal vs. basal-like breast cancer*. 2018 [cited 2018 04 06 2018].
169. Ridlon, J.M., D.J. Kang, and P.B. Hylemon, *Bile salt biotransformations by human intestinal bacteria.* J Lipid Res, 2006. **47**(2): p. 241-59.
170. Tang, X., et al., *A joint analysis of metabolomics and genetics of breast cancer.* Breast Cancer Res, 2014. **16**(4): p. 415.
171. Velicer, C.M., et al., *Antibiotic use in relation to the risk of breast cancer.* JAMA, 2004. **291**(7): p. 827-35.
172. Tamim, H.M., et al., *Risk of breast cancer in relation to antibiotic use.* Pharmacoepidemiol Drug Saf, 2008. **17**(2): p. 144-50.
173. Wirtz, H.S., et al., *Frequent antibiotic use and second breast cancer events.* Cancer Epidemiol Biomarkers Prev, 2013. **22**(9): p. 1588-99.
174. Satram-Hoang, S., et al., *A pilot study of male breast cancer in the Veterans Affairs healthcare system.* J Environ Pathol Toxicol Oncol, 2010. **29**(3): p. 235-44.
175. Elitsur, Y., et al., *Polyamine levels, ornithine decarboxylase (ODC) activity, and ODC-mRNA expression in normal and cancerous human colonocytes.* Life Sci, 1992. **50**(19): p. 1417-24.
176. Liu, R., et al., *Determination of polyamine metabolome in plasma and urine by ultrahigh performance liquid chromatography-tandem mass spectrometry method: application to identify potential markers for human hepatic cancer.* Anal Chim Acta, 2013. **791**: p. 36-45.
177. Aizencang, G., et al., *Antiproliferative effects of N1,N4-dibenzylputrescine in human and rodent tumor cells.* Cell Mol Biol (Noisy-le-grand), 1998. **44**(4): p. 615-25.
178. Olaya, J., V. Neopikhanov, and A. Uribe, *Lipopolysaccharide of Escherichia coli, polyamines, and acetic acid stimulate cell proliferation in intestinal epithelial cells.* In Vitro Cell Dev Biol Anim, 1999. **35**(1): p. 43-8.
179. Goldberg, A.A., et al., *Bile acids induce apoptosis selectively in androgen-dependent and -independent prostate cancer cells.* PeerJ, 2013. **1**: p. e122.
180. Goldberg, A.A., et al., *Lithocholic bile acid selectively kills neuroblastoma cells, while sparing normal neuronal cells.* Oncotarget, 2011. **2**(10): p. 761-82.
181. Chakraborty, S., et al., *Correlation between lipid peroxidation-induced TBARS level and disease severity in obsessive-compulsive disorder.* Prog Neuropsychopharmacol Biol Psychiatry, 2009. **33**(2): p. 363-6.

11. PUBLICATION LIST (APPROVED BY THE KENÉZY LIFE SCIENCE LIBRARY)

UNIVERSITY of DEBRECEN

UNIVERSITY AND NATIONAL LIBRAY
UNIVERSITY OF DEBRECEN
H-4002 Egyetem tér 1, Debrecen
Phone: +3652/410-443, email: publikaciok@lib.unideb.hu

Registry number: DEENK/36/2019.PL
Subject: PhD Publikációs Lista

Candidate: Tünde Kovács
Neptun ID: V3U2C8
Doctoral School: Doctoral School of Molecular Medicine

List of publications related to the dissertation

1. **Kovács, T.**, Mikó, E., Vida, A., Sebő, É., Tóth, J., Csonka, T., Boratkó, A., Ujlaki, G., Lente, G., Kovács, P., Tóth, D., Árkossy, P., Kiss, B. K., Méhes, G., Goedert, J. J., Bai, P.: Cadaverine, a metabolite of the microbiome, reduces breast cancer aggressiveness through trace amino acid receptors.
   Sci Rep. 9 (1), 1-14, 2019.
   DOI: http://dx.doi.org/10.1038/s41598-018-37664-7
   IF: 4.122 (2017)

2. Mikó, E., Vida, A., **Kovács, T.**, Ujlaki, G., Trencsényi, G., Márton, J., Sári, Z., Kovács, P., Boratkó, A., Hujber, Z., Csonka, T., Antal-Szalmás, P., Watanabe, M., Gombos, I., Csóka, B., Kiss, B. K., Vígh, L., Szabó, J., Méhes, G., Sebestyén, A., Goedert, J. J., Bai, P.: Lithocholic acid, a bacterial metabolite reduces breast cancer cell proliferation and aggressiveness.
   Biochim. Biophys. Acta Bioenerg. 1859 (9), 958-974, 2018.
   DOI: http://dx.doi.org/10.1016/j.bbabio.2018.04.002
   IF: 4.28 (2017)

List of other publications

3. Vida, A., Kardos, G., **Kovács, T.**, Bodrogi, B., Bai, P.: Deletion of poly(ADP?ribose) polymerase-1 changes the composition of the microbiome in the gut.
   Mol. Med. Rep. 18 (5), 4335-4341, 2018.
   DOI: http://dx.doi.org/10.3892/mmr.2018.9474
   IF: 1.922 (2017)

4. Trencsényi, G., Dénes, N., Nagy, G., Kis, A., Vida, A., Farkas, F., Péli-Szabó, J., **Kovács, T.**, Berényi, E., Garai, I., Bai, P., Hunyadi, J., Kertész, I.: Comparative preclinical evaluation of 68Ga-NODAGA and 68Ga-HBED-CC conjugated procainamide in melanoma imaging.
   J. Pharmaceut. Biomed. Anal. 139, 54-64, 2017.
   DOI: http://dx.doi.org/org/10.1016/j.jpba.2017.02.049
   IF: 2.831

UNIVERSITY AND NATIONAL LIBRAY
UNIVERSITY OF DEBRECEN
H-4002 Egyetem tér 1, Debrecen
Phone: +3652/410-443, email: publikaciok@lib.unideb.hu

5. Kertész, I., Vida, A., Nagy, G., Emri, M., Farkas, A., Kis, A., Angyal, J., Dénes, N., Péli-Szabó, J., **Kovács, T.**, Bai, P., Trencsényi, G.: In Vivo Imaging of Experimental Melanoma Tumors Using The Novel Radiotracer 68Ga-NODAGA-Procainamide (PCA).
J. Cancer. 8 (5), 774-785, 2017.
DOI: http://dx.doi.org/10.7150/jca.17550
IF: 3.249

6. Mikó, E., **Kovács, T.**, Fodor, T., Bai, P.: Methods to assess to role of poly(ADP-ribose) polymerases in regulating mitochondrial oxidation.
Methods Mol. Biol. 1608, 185-200, 2017.

Total IF of journals (all publications): 16,404
Total IF of journals (publications related to the dissertation): 8,402

The Candidate's publication data submitted to the iDEa Tudóstér have been validated by DEENK on the basis of the Journal Citation Report (Impact Factor) database.

19 February, 2019

DEBRECENI EGYETEM * Egyetemi és Nemzeti Könyvtár *

12. KEYWORDS

cadaverine, LCA, microbiome, breast cancer, stem cell, EMT, MET, invasion, metastasis, trace amine-associated receptor, lysine decarboxylase, baiH

TÁRGYSZAVAK

kadaverin, litokólsav, mikrobiom, emlőcarcinoma, őssejt, EMT, MET, inváz ió, metasztázis, trace amin-kapcsolt receptor, lizin dekarboxiláz, baiH

13. ACKNOWLEDGEMENT

First of all, I would like to thank my supervisor, Prof. Péter Bay for the patient guidance, encouragement, continuous support and motivation during my PhD study. I am grateful that he gave me the opportunity to learn and work in his research group.

I would also like to thank to Prof. László Virág, head of Department of Medical Chemistry, for giving me the opportunity to work at the department, to Dr. Beáta Lontay for enabling me the use of the JuLi Br real-time video microscope, and to Mitsuhiro Watanabe (Department of Internal Medicine, Keio University Endo, Japan), who provided LC/MS equipment for metabolite measurements.

Many thanks to my colleagues, Dr. Edit Mikó and Dr. András Vida for the valuable discussions and helpful advices, and - besides them - to Gyula Ujlaki, Patrik Kovács and Gréta Lente for their help in carrying out the experiments. I am thankful to Árpád Bálind and Csaba Molnár for their help in Cell Profiler and Advanced Cell Classifier softwares.

I am very grateful to Dr. Anita Boratkó for performing ECIS experiments, to Dr. Tamás Csonka and Dr. Gábor Méhes for the histological experiments.

We are grateful for James J. Goedert (NCI-NIH) and Dr. Jacques Ravel (University of Mariland Medical School) for transferring the human fecal DNA samples, to Dr. László Takács (BSI KFT. Debrecen) for the human serum specimens, and to Dr. Éva Sebő (Kenézy Gyula Country Hospital, Debrecen) and Dr. Judit Tóth for the collection of human fecal samples.

I am also thankful to László Finta for their excellent technical assistance, and at last but not least, I would like to thank to my loving family and to all my dear friends for their continuous encouragement during my PhD studies.

14. APPENDIX

The thesis is based on the following publications: